# JOURNAL OF
# MECHANICAL ENGINEERING

The Institution of Engineers, Bangladesh
Volume: ME 52, No. 1, July 2023

## MECHANICAL ENGINEERING DIVISION

ISSN: 0379-4318

JOURNAL OF

# MECHANICAL ENGINEERING

**Volume: ME 52, No. 1, July 2023**

**Published by :**

## MECHANICAL ENGINEERING DIVISION

**The Institution of Engineers, Bangladesh**

Head Quarters : Ramna, Dhaka-1000

Bangladesh

JOURNAL OF
# MECHANICAL ENGINEERING
**Volume: ME 52, No. 1, July 2023**

## EDITORIAL BOARD

# CONTENTS :

# A CONCEPTION OF FLOATING STADIUM FOR INDOOR GAMES IN THE CAPITAL CITY OF BANGLADESH

**Md Samiun Nur Islam[1], Mrinal Kanti Roy[1], Md. Mashiur Rahaman[1*] and Md. Moynul Hasan[1]**

[1]Department of Naval Architecture and Marine Engineering, Bangladesh University of Engineering and Technology, Dhaka-1000, Bangladesh

*Corresponding Email: mashiurrahaman@name.buet.ac.bd

***Abstract**: Dhaka, the capital of Bangladesh, is one of the fastest-growing megacities in the world, having a population of approximately 22.5 million and 23,789 active schools with approximately 224,141 regular students. To meet the housing demand for this overpopulated number of people, playgrounds and open fields are being used to create homes and commercial spaces while the children play with electronic devices at home, hampering their mental and physical growth. In developed and developing countries such as Australia, Belgium, Argentina, and India, there is an average of 10,000 to 20,000 playgrounds across all major cities with an average of 2,000 to 5,000 square kilometers. On the other hand, according to Dhaka Metropolitan Development Plan (DMDP) and Detailed Area Plan (DAP), there is a deficit of 152.80 acres of playgrounds and open fields in Dhaka city. In present, the Indoor Floating Stadium is conceptualized as an alternative to this problem without occupying any land territory within a city. Instead, the Indoor Floating Stadium will be built on calm water (Hatirjheel, Dhanmondi Lake, Purbachal Ecopark lake, Nikunja Lake, Ramna Lake, Diabari Lake, Chandrima Udyan), providing an open space for children to play as well as for adults to spend quality time.*

***Keywords:** Dhaka city, playground, open field, overpopulation, floating indoor stadium.*

## INTRODUCTION

Dhaka is one of the most densely populated cities worldwide, with a population of approximately 22.5 million, which is higher than any other country in the world. Among the 22.5 million people, around 9-10 million are youth which is almost half of the population of this mega city. Nevertheless, the alarming fact is that the authority seems to need to be more concerned about this significant population's physical and mental well-being. Youngsters can only play indoors with the scarcity of playgrounds. On the other hand, the government and the city corporation do not care about the situation. The improperly planned and uncontrolled expansion of Bangladesh's metropolitan areas has contributed significantly to the scarcity of playgrounds or vacant places. Existing playgrounds have been occupied to carry out commercial and industrial operations, deterring youngsters from using them. Additionally, the growth of the urban population has led to a significant increase in demand for housing, industrial and commercial property, public buildings, and infrastructure, all of which have reduced the availability of playgrounds. The Dhaka Metropolitan Development Plan (DMDP) suggests that Dhaka City had 0.5 square meters of green space per capita in 1995. In 2009, a critical review of the Detailed Area Plan (DAP) suggested that there were only 0.052 square meters of green space per capita.

In another context, Dhaka has some noteworthy lakes in crucial positions, including residential and commercial areas, schools, and small neighborhoods. The fertile flood plains of Dhaka City have approximately 30-35 khals or natural drainage, summarizing up almost 437 km in length[2] together with the four major rivers like-the, Buriganga River, the Turag River, the Balu River, and the Tongi River.

Sports have been a part of human life since the very beginning of human civilization. Though it was initially intended for preparing warriors for battle, or hunting and training, sports gained worldwide popularity after the organization of the first Olympic Games in 776 BC by the Greeks, even though the exact timeline of the origin of sports is unknown to ordinary people. People, especially youngsters, have traditionally raced and wrestled for fun, which later became a regular social event when people would assemble in specific vacant spots or playgrounds and engage in recreational physical games. A community used to meet at the playground to play games, which was more of a social gathering than just playing games. It is a significant societal phenomenon with several physical, mental, and social benefits. Unfortunately, these social gatherings are rare in cities due to a lack of opportunities and vacant spots. Youths are the foundational stones and the future of a country, as well as the future of humanity. They are expected to be energetic and appearances to be filled with vitality. This generation will be the

future leaders of the country and the world. They are expected to be innovative and can think outside of the box in their minds. However, in recent decades, it has appeared that youthful generations in the Dhaka city area are undergoing plenty of physical problems, mental fatigue, and depression due to the inadequacy of playgrounds, which resulted in less to almost no physical activity outside of their homes. Therefore, they are unable to provide the finest possible output as required. To cope with this depression, they seek out drugs and illegal methamphetamine and engage in gang culture instead of sports because they neither have enough space to play nor access to the playgrounds next to their homes and neighborhood. Besides that, the playgrounds where their predecessors used to play have been abolished for good. They suffer from physical and mental ailments because of excessive stress, physical problems, and mental fatigue on their shoulders. A variety of factors, ranging from familial and cultural expectations to a more significant standard of living, have forced them to engage in activities that have the potential to disrupt their mental health, resulting in the city dealing with a generation growing up with significantly less physical activity. As a result, this has become a global problem among adolescents. Because of this, it has always been a topic of significant interest to mental fatigue, the effects of physical infirmity, and stress-related researchers and professionals. The impact of physical activity on well-being was analyzed in Mental Health Foundation's report[7]. A review of the research which is suggestive, linking children's physical activities to many elements of their learning and development was mentioned by Whitebread et. al[1].

Though dedicated floating stadium does not exist yet, most of the first world country have sufficient green space per capita. New York city authorities formed public playgrounds to keep children safe from the streets and bad influences. Surprisingly only 20 percent of the targeted children were paying attention in these playgrounds. The reason is children preferred to play nearby to family, friends and neighbors rather than in isolated playgrounds. In Japan number of sport park is 834 excluding other types of city park, in USA there are approximately 20,000 individual parks and more than 10,000 playgrounds, in UK more than 16,000 playgrounds provided by district council and in Canada, Toronto transforms it's 858 playgrounds in modern play spaces. In Australia, authorities have a good focus on how they can keep a playground safe for a child and present lucratively to them. They even focusing on building smart playground for children. Likewise, Bangladesh there is no adequate playgrounds for 25 children in India and Pakistan. These neighboring countries children also facing problem to go to the few existing playgrounds because of security and other issues.

This study intends to propose an alternate solution to the expanding Dhaka city's playground dilemma. Furthermore, make a new dimension through the water-body named Floating Indoor stadium. The Indoor Floating Stadium is designed as an alternative to this problem without occupying any land territory within a city. Instead, the Indoor Floating Stadium will be built on calm water (Hatirjheel, Dhanmondi Lake, Purbachal Ecopark lake, Nikunja Lake, Ramna Lake, Diabari Lake, Crescent Lake, Chandrima Udyan), providing an open space for children to play as well as for adults to spend quality time. This adaptable and mobile stadium may host various sporting events and serve as a practice space for neighborhood or school-based sports teams. A floating stadium has advantages for athletes, the younger generation, and the neighborhood.

In the present study, extensive data were accumulated using various means, including literature reviews and potential consumer analysis. The primary data were generated by a detailed questionnaire survey to the target user, the youth, namely school and college-going students. As for secondary data, the present situation of parks and the availability of open fields were sorted through existing information. Furthermore, the importance of playgrounds and the secure place was taken from detailed literature and article reviews. A professional attitude was ensured in collecting data through the methods mentioned earlier. After analyzing the current situation and intensive data, this paper presents a conceptual overview of the Floating Stadium for Indoor Games.

## RESULTS AND DISCUSSIONS

People are asked various questions to find out if the market is ready to accept this new idea of floating indoor stadium in the Dhaka city. The participated age group is mostly from 21-25 years old from different kinds of occupation have shown interest to this project. Maximum percentage is from student and non-government employees. Almost all the areas of Dhaka have participated and shown interest to this survey and 95% individuals will be happy to get such an alternative option for playground crisis shown in **Fig.-1**.

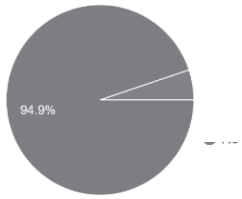


**Fig. 1**: Interested in sports of the respondents

Availability of playground available near their locality were also asked. 40% of them said there are no playground at all and among rest of the 60% people who said that they have playground nearby they replied there just a little space available for playing.

The situations of available playgrounds are summarized in **Fig.-2** and **Fig.-3**. It is seen from **Fig.-2** and **Fig.-3** that available playgrounds are mostly busy and overcrowded in both holidays and working days. It is also seen that during holidays, the waiting time too high.

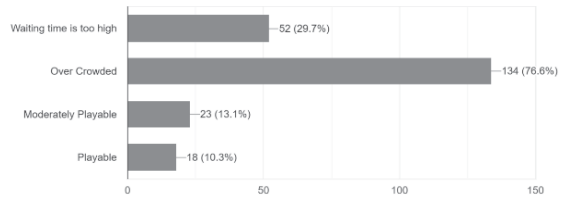


**Fig.-2:** Playground situation in holidays

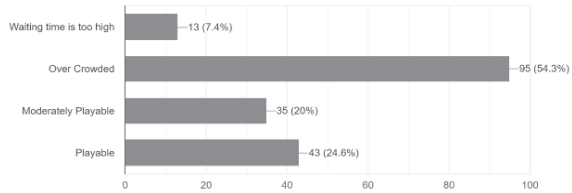


**Fig.-3:** Playground situation in normal working days

But respondents are in few cases not interested to go to playgrounds shown in **Fig.-4.** From Fig.-4 it is noticed that more than half of the respondents of the survey is not interested to use the existing conventional playgrounds due to lack of security; uneven field condition; absence of lighting facilities; not properly and regularly maintained; lack of first aid facilities and unhygienic washrooms.

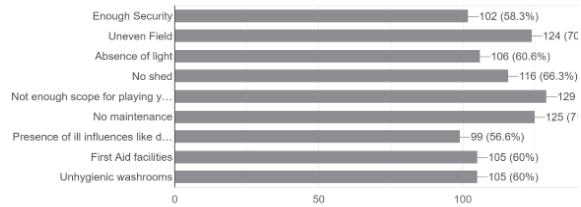


**Fig.-4:** Scenario of visit to conventional existing playgrounds

People are also asked about opinion to accept new ideas like floating indoor stadium which will solve all their problems regarding playgrounds. The responses are mentioned in **Fig.-5**. It is noticed from **Fig.-5** that around 70% of the respondents show their interest about the floating indoor stadium.

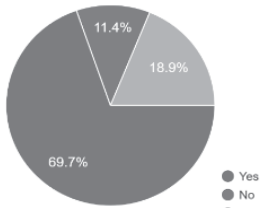


**Fig.-5:** Opinion of the respondents about the floating stadium

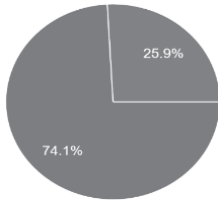


**Fig.-6:** Willingness of paying

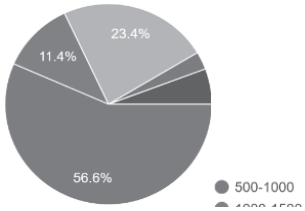


**Fig.-7:** Range of monthly payment

**Fig.-6** and **Fig.-7** show the willingness of payment and the preferable range is 500-2000 BDT monthly respectively. From **Fig.-6** and **Fig.-7**, around 74 % of the respondents are ready to pay for using the facilities and the amount is about BDT 500 – 1000. Statistics of the respondents about the other facilities in the floating indoor stadium is given in **Fig.-8**. It is seen from **Fig.-8**, the additional facilities such as canteen, gymnasium and restroom are more priority.

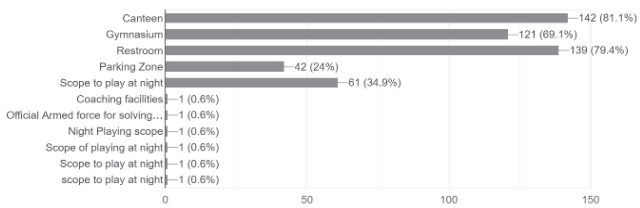


**Fig.-8:** Additional facilities requirements

## SELECTION OF LOCATION

According to Tran[3], the following points should be kept in mind for the selection of the suitable location for the floating indoor stadium.

- Sites should be nearby residential area
- Playground is far from the floating stadium

- High transportation facilities
- Easy access
- Near to school, colleges, or universities

Based on the Tran[3] study, the locations of the floating indoor stadium for the Dhaka city is identified in the present study, which are Hatirjheel Lake, Gulshan Lake, Dhanmondi Lake and Diabari, Uttara. These areas were selected because they are easily accessible and close to residential areas. Better transportation facilities make it easier for people to come. Floating stadiums will not hinder water transport of lakes and will not negatively impact the environment because waste management will be better in these locations.

Hatirjheel Lake is very close to residential area "Mahanagar Project" and near to AUST (Ahsanullah University of Engineering and Technology) and BUTex (Bangladesh University of Engineering and Technology) shown in **Fig.-9**.


**Fig.-9:** Location of Hatirjheel Lake

Gulshan Lake located near to Scholastica School and Gulshan Club shown in **Fig.-10**.

Diabari, Uttara located at Diabari, near Metrorail station; a growing residential area in Uttara. Also close to DPS STS School and Uttara CFC Club. The location is shown in **Fig.-12**.

**Fig.-10:** Location of Gulshan Lake

Location of Dhanmondi Lake is beside Rabindra Sarobar, Lt. Seikh Jamal Dhanmondi Club and close to Dhanmondi residential area shown in **Fig.-11**.

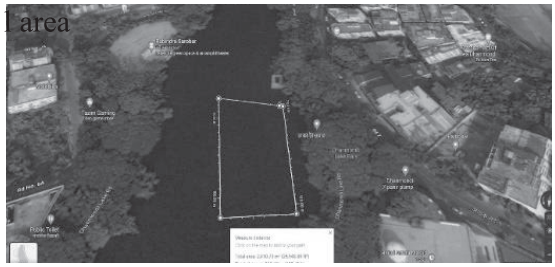

**Fig.-11:** Location of Dhanmondi Lake

**Fig.-12:** Location of Diabari

## CONCEPTUAL GENERAL ARRANGEMENT PLAN

A preliminary General Arrangement (GA) Plan of the vessel is developed, which is shown in **Fig.-13**. **Table-[1]** shows the principal particulars of the vessel.

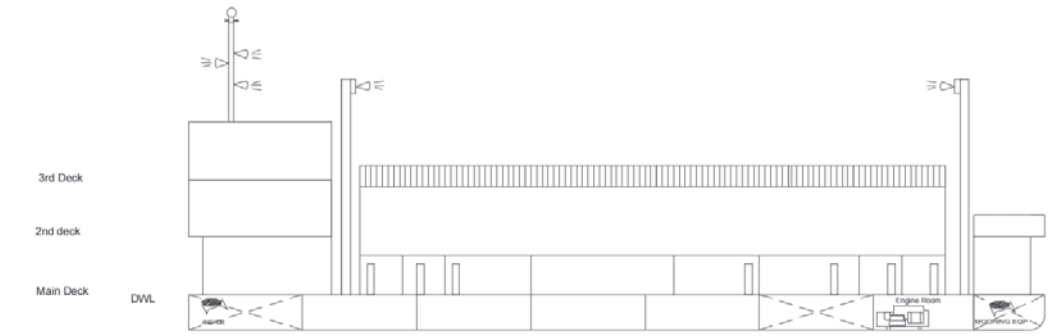


Elevation

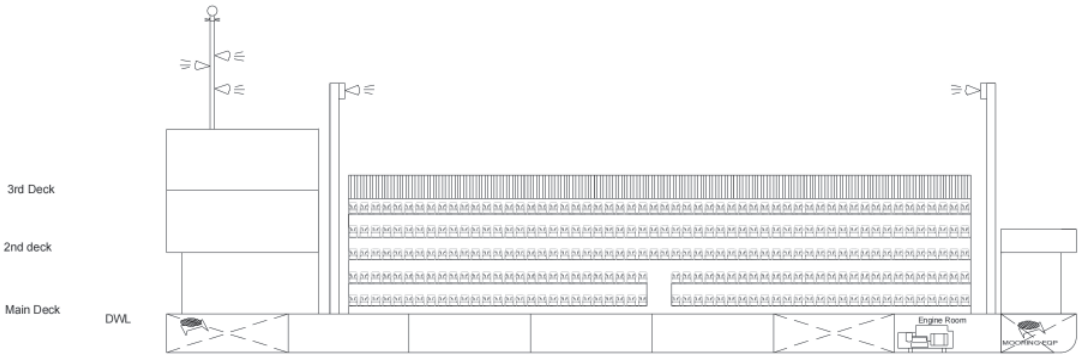


Side View

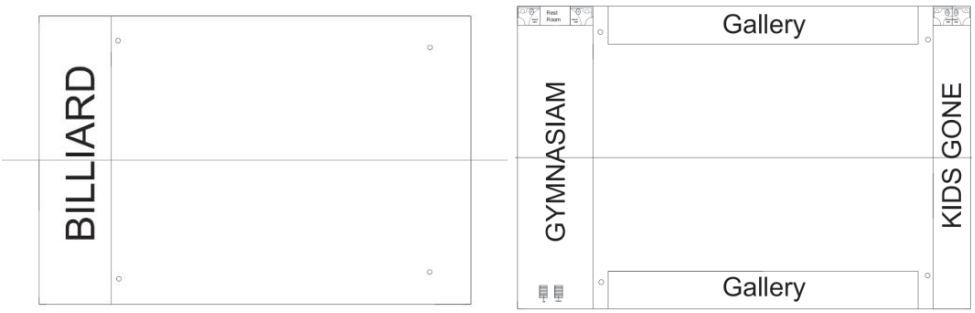


3rd Deck 2nd Deck

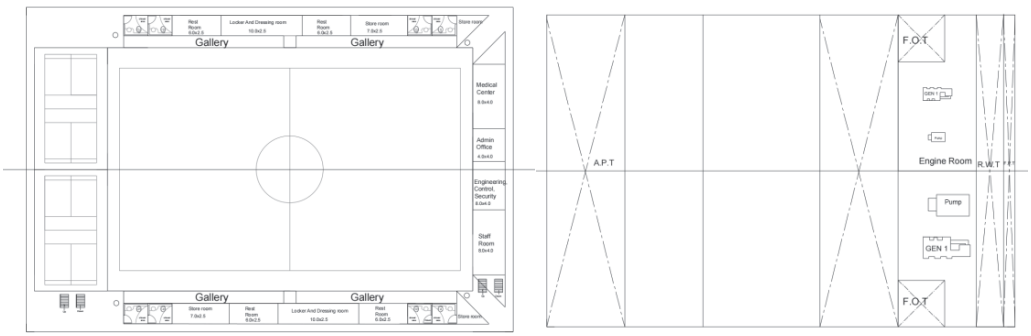


Main Deck Under Deck

**Fig.-12:** Preliminary General Arrangement Plan of the stadium

**Table-1:** Principal particulars of the Floating Indoor Stadium

| Item | Symbol | Value | Unit |
|---|---|---|---|
| Length Overall | $L_{OA}$ | 60.00 | [meter] |
| Length Between Perpendiculars | $L_{BP}$ | 60.00 | [meter] |
| Breadth Moulded | $B_{MLD}$ | 40.00 | [meter] |
| Depth Moulded | $D_{MLD}$ | 2.50 | [meter] |
| Draft Design | T | 2.20 | [meter] |
| Block co-efficient | $C_B$ | 0.94 | -- |

## CHALLENGES

### Cost:

In every situation, cost is a significant consideration when making a crucial decision to serve the customers. It does not matter how luxurious the amenities are, unless the cost exceeds the customer's budget, service won't be availed. A same thing goes when estimating the price of Floating Stadium for Indoor Games. In order to achieve a very satisfying experience, the pricing package should not be too high. It is paramount that the service provider is able to earn substantial revenue, one that will offset their incurred costs, and two, that won't burden their customers. Eventually, a continuous revenue stream and customers will eventually lead to a successful business.

### Disposal of Black Water:

As the indoor stadium will be located in lakes so the environment contamination is a matter of concerning factor. And disposal of black water should not be flashed in the water of lakes directly.

## CONCLUSION

This adaptable and mobile stadium may host a variety of sporting events and serve as a practice space for neighborhood or school-based sports teams. A floating stadium has advantages for athletes as well as for the younger generation and the neighborhood. People who look up to sports idols are more inclined to be active themselves. Sports are a good thing that can inspire, educate, and connect people. Sports have the power to unite a city like Dhaka, which is a melting pot of ethnicities and backgrounds. This magnificent edifice will be a source of pride for the inhabitants of the surrounding area. Residents from the same school who support the same team will form bonds. Team sports may have the effect of bringing together individuals of different races and beliefs.

## RECOMMENDATION

After the detailed design of the stadium, the entire business venture must be analyzed rigorously from economical and financial standpoint.

## REFERENCES

1. Whitebread, David & Neale, Dave & Jensen, Hanne & Liu, Claire & Solis, Lynneth & Hopkins, Emily & Hirsh-Pasek, Kathy & Zosh, Jennifer. (2017). The role of play in children's development: a review of the evidence. Doi: 10.13140/RG.2.2.18500.73606.

2. Marju Ben Sayed and Shigeko Haruyama, "Flood Risk Measuring under the Flood Protection Embankment Construction in Dhaka Metropolitan Zone," *Journal of Geosciences and Geomatics*, Vol. 5, No. 2, pp. 46–58, 2017, Doi: 10.12691/jgg-5-2-1.

3. My Tran, "Future Floating Stadiums Case Study: Honolulu Hawaii", Doctoral Thesis, The University of Hawaii.

# Influence of Vegetable Oil-Based MQL on Surface Roughness and Chip-Thickness Ratio of Monel 400

**Mahjabin Moon [1*], Sheak Salman [1], Khalid Ibn Muneer [1], AKM Nurul Amin [2], and Mohammad Morshed[1]**

[1] Department of Mechanical and Production Engineering, Ahsanullah University of Science and Technology, Dhaka, Bangladesh

[2] Department of Industrial and Production Engineering, Military Institute of Science & Technology (MIST), Dhaka, Bangladesh

*Corresponding Email: mahjabin.mpe@aust.edu

***Abstract:*** *This study highlights the impact of minimum quantity lubrication (MQL) using vegetable oil in turning of Monel 400, a Ni-Cu alloy which falls under the class of materials that are difficult to cut. In this experiment, two vegetable oils (Soybean and Palm oil) have been used and their effectiveness has been examined in respect of surface roughness and chip-thickness ratio. This research also includes an overall comparison between the dry and MQL assisted machining processes. Soft computation frameworks such as Response surface methodology (RSM) and Artificial neural network (ANN) are being developed to obtain optimized parameter settings as well as predict changes in output corresponding to any variation in the input. The results confirmed that MQL assisted machining provides better results than those in machining under dry conditions whereas Soybean offers superior performance compared to Palm oil.*

***Keyword:*** *MQL, Vegetable oil, Surface roughness, Chip thickness ratio, ANN, RSM.*

## 1. INTRODUCTION

Monel 400 is well known for its excellent corrosion resistance along with its superior strength and toughness. It has wide range of applications which include the refining of uranium, isotope separation in the production of nuclear fuel, propellers, valves, nozzles, pump shafts and heat exchangers in oil refineries, sulfuric acid and hydrofluoric acid alkylation plants, submarines, chemical industries, etc. [1]. Like other nickel-based alloys, Monel 400 normally hardens rapidly, as a result, high pressures produced during machining that causes a hardening effect on Monel which in turns slows down subsequent machining [2]. As the performance of the final product depends largely on the surface quality, achieving good surface finish is a must. But due to its poor machinability, the conventional machining process of Monel is very challenging [3]. One of the problems of conventional machining of these "difficult to machine" Nickel-based alloys is that the tool-workpiece contact produces excessive heat because of friction which directly affects surface quality of the final product [4], [5]. Intense heat is generated during machining at the following zones- a) the principal deformation zone, b) the chip-tool interface, and c) the work-tool interface [6]. This high heat results in a blunt cutting tool with a built-up edge which requires more cutting force and ends up with high surface roughness. To overcome this phenomenon, flood coolant has been used in large amounts for decades. But with time, different problems associated with the usage of conventional cutting fluid came to light. Though it reduces the heat generated at the tool-work contact, it has an undesirable environmental impact, including soil and water contamination [7]. Besides, the usage of cutting fluid based on mineral oil is also related to worker's health issues like respiratory disorders, skin diseases, lung cancer, and hereditary diseases are just some examples [8]. In addition, the cost of coolants accounts for nearly 7 to 17 percent of the total cost of machining, which is a substantial amount [7], [9]. Considering the cost and other problems related to flood coolant, Jiang et al. (2015) went for the hot turning operation of Monel 400 using coated carbide inserts and found that with the increase of temperature, roughness also increases [10].

Technologies like MQL, dry or near dry machining is nowadays considered as a great choice in this regard, which minimizes or even eliminates the need of using cutting fluids leading to the reduction of cost and ecological impact, usage and removal of fluid cutting [10]. In MQL, minute amount of high-quality lubricant (5 ml/hr-600 ml/hr) is used as a mist and is aimed at the precise tool-workpiece contact instead of employing typical flood coolants [2]. As a result the usage of fluid reduces significantly and at the same time, it eliminates the need for coolant treatment and disposal which in turn minimizes environmental impact [10]. It improves machinability characteristics as the coolant is applied directly at the heat source which in turns eliminates the need for cleaning up after each operation by providing neat and clean work areas and saves time. It also helps to avoid health risks due to fumes, smoke, and gas. To reduce the cost and make the process more environment friendly, Devillez et al. (2011) used coated carbide inserts in turning Inconel 718 in CNC lathe which is

suitable for both dry and wet environments where surface roughness value for dry conditions reduced surprisingly [11]. In order to achieve the desired result, it is needed to compensate for the need for coolant. The tool material and coating of the tool should be selected in a way so that it can withstand high temperature [12]. According to Dhar et al. (2006); Varadarajan, Philip, and Ramamoorthy (2002) MQL offers better performance in comparison with the dry conditions in respect of cutting temperature, cutting forces, surface finish and tool life [13], [14].

To reduce the usage of cutting fluids, after completing an experiment with coated carbide ball end mill cutters, Thepsonthi, Hamdi, and Mitsui (2009) proposed a minimum cutting fluid approach in machining hardened steel, concluding that it enhances surface roughness when compared to conventional methods and flood coolant [15]. With cemented cutting tools and a MQL approach, Ho et al. (2015) achieved less tool wear and improved surface quality while milling high strength steel [16]. Using 100% disposable fluids made from renewable plant-based oils, the advantages of near-dry machining can be further enhanced. Vegetable oil molecules are long, heavy and dipolar and have homogeneous density which provide a strong and thin lubricating film that can absorb high pressure. Vegetable oils are well known for their exceptionally high viscosity index (VI). When exposed to high temperatures, the oil viscosity does not decrease much, and when exposed to low temperatures, it does not increase as much as petroleum oils. Having higher flash points is another essential attribute of vegetable oils (Soybean oil-326°C). Investigations run by Heisel et al. (1994) and Dhar et al. (2006) have shown that MQL, coupled with vegetable oils, is appropriate for machining materials with a high degree of difficulty in cutting [13], [17]. Many scholars opted for vegetable oils serving as MQL's base oil. Zhang et al. (2015) analyzed grinding performance using soybean, rapeseed, and palm oils as base oils [18]. In this work the lubricating capabilities of MQL with nanoparticles added were examined and they found that palm oil-based fluid showed optimal lubricating property under the influence of $MoS_2$ nanoparticles. They further observed the vegetable oils' cooling performances and analyzed their mechanism [19]. Rahim and Sasahara (2011) drilled Inconel 718 with AlTiN coated carbide drill bit under MQL condition using palm oil and synthetic ester concluding that the higher viscosity of palm oil provided better surface finish [20]. Lawal et al. (2014) evaluated the effectiveness of inorganic and vegetable oil-based coolants in machining AISI 4340 steel using cemented carbide tools while implementing the Taguchi method [21]. Cottonseed and palm oil-based cutting fluids outperformed other oils in terms of heat conductivity and environmental friendliness in that study.

Thus, by reviewing the existing literature on machining using different oil based MQL, it can be concluded that vegetable oil is a cost-effective and environmentally sustainable cutting fluid that can be used for machining tough and challenging materials. A small number of studies have been conducted on near dry and vegetable oil-based MQL assisted turning processes of Monel 400 metals. This study's objectives were to evaluate the effects of vegetable oil based MQL on the machinability of Monel 400 during dry machining and to compare the performances of two oils. The prediction models are also developed using RSM and ANN.

## 2. MATERIALS AND METHOD

A high-speed engine lathe (Model CS6266B) equipped with MQL setup was used for turning Monel 400 (Ni 63.7%, Cu 31%, Fe 2.5%). The workpiece was in the shape of a round bar (Ø60×200mm), with a hardness of 65 Rockwell B. Coated carbide inserts (SNMG 432E) were used with a PSBNR-2525 M12 tool holder. The tools had a -6º inclination angle, rake angle that is orthogonal of -6º, 6º angle of orthogonal clearance, nose radius 0.8 mm and 75º auxiliary cutting-edge angle. Investigational requirements are presented in Table 1.

Table 1: Experimental condition

| | |
|---|---|
| Machine tool | Lathe Machine (Model No CS6266B) |
| Workpiece | Monel 400 (Ni=63.7%, Cu=31%, Fe=2.5%, Mn=2%, Si=0.5, S=0.02%, C=0.3%) |
| Size (mm) | Ø60×200mm |
| Cutting insert | Coated Carbide, SNMG 432E (P-30 ISO specification), Drillco |
| Tool holder | PSBNR-2525 M12 (ISO specification), Drillco |
| Tool Geometry | −6, −6, 6, 6, 15, 75, 0.8 (mm) |
| Cutting velocity, $V_c$ | 75 m/min, 94 m/min, 119 m/min |
| Feed rate, $S_0$ | 0.2 mm/rev and 0.3 mm/rev |
| Depth of cut, $t$ | 1.0 mm |
| MQL supply (through external nozzle) | Air: 8.0 bar, lubricant: 12 ml/h |
| Environment | Dry and MQL |

The experiments were carried out using two vegetable oils (soybean and palm oil) & also under dry condition.

Two discrete feed rates (f), 0.2 mm/rev, 0.3 mm/rev, and three discrete cutting speeds (Vc), 75 m/min, 94 m/min, 119 m/min were chosen as input variables whereas surface roughness, (Ra) and chip-thickness ratio (r) were chosen as output variables. A total of 18 runs were designed. The cutters and cutting states (cutting speed, feed rate) were chosen in accordance with the Nickel Development Institute Reference Book guidelines (Series no. 11008) [22]. Vegetable oils were used due to their high lubricating and cooling characteristics. Table 2 shows the physical properties of soybean and palm oils.

Table 2: Physical properties of Palm & Soybean Oil

| Parameter | Palm | Soybean |
|---|---|---|
| Density | 890.1 kg/m3 | 913.8 kg/m3 |
| Heat Capacity | 1.848 Kj/kg.k | 1.973 Kj/kg.k |
| Thermal Conductivity | 0.1726 w/m.k | 0.1700 w/m.k |
| Dynamic Viscosity | 77.19 mPas | 59-62 mPas |
| Kinematic Viscosity | 39.6 mm2/s | 32.6 mm2/s |
| Smoke Point | 2350C | 2380C |
| Flash Point | 2670C | 3170C |

MQL setup (**Fig. 1**) developed by Rahman et al. (2019) was used here consisting of a specially designed nozzle (1.5 mm hole whereas the inner part consists of 4 0.5 mm holes) to achieve better mix [23]. Surface roughness and chip-thickness ratio were used to assess the efficiency of vegetable oil-based MQL on Monel 400. The value of surface roughness was determined using a Phase II SRG-4500 roughness tester where a diamond tip stylus was used to trace across the sample making the data highly reliable. As the inserts were altered after each cut, the wear of tools was less. Vernier calliper was used to measure the chip-thickness ratio. A prediction model was developed using an artificial neural network (ANN), which was then compared to the findings obtained using response surface methods (RSM).

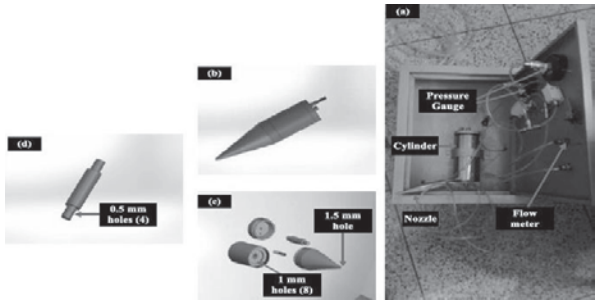


**Fig. 1:** The photographic view of the (a) MQL system with (b) schematic representation of the nozzle, (c) exploded view of the nozzle and (d) Inner part with four 0.5 mm holes for fluid supply.

## 3. RESULTS AND DISCUSSIONS

### 3.1 Experimental Results

A contact type profilometer named Phase II SRG-4500 roughness tester was used to calculate the machined surface's surface roughness values where a diamond tip stylus traces across the surface and this process is repeated three times for each run to obtain more reliable results.

To measure the chip thickness ratio, a Vernier calliper was used. Chip thickness ratio (r) is the proportion of uncut chip thickness ($a_1$) to chip thickness ($a_2$). Chip thickness ratio was measured using the following formula:

$$r = a_1/a_2 \qquad (1)$$

#### 3.1.1 Effect of factors on surface roughness

Significant heat is generated during dry machining, which increases surface roughness [23]. When compared to wet conditions, MQL created a better surface finish. The improvement in machined surface induced by MQL is highly dependent on both the material of the workpiece and the tool [24]. In this study, new inserts were used for each operation so tool wear was negligible. For various cutting speeds, increasing the feed rate will result in a rougher surface. This occurred as the feed rate increased during machining, which increased cutting forces because of significant frictional forces on the tool's rake face [25]. The connection of cutting speed and surface roughness can be found to be inversely proportional. The surface roughness normally decreases as the cutting speed is raised. The correlation between feed rate and surface roughness is comparative as well. Typically, when the feed rate rises, surface roughness also raises. By increasing cutting speed and decreasing feed rate, surface roughness values can be reduced (**Fig. 2**). Cutting speed 119 m/min, feed rate 0.2mm/rev, and

soybean oil yielded the lowest surface roughness of 1.678 m.

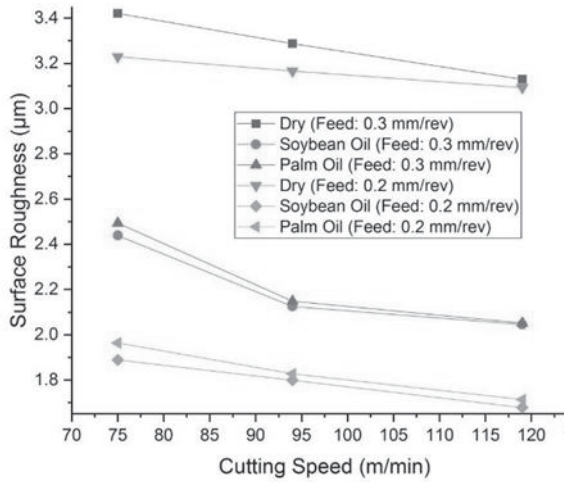


**Fig. 2:** Surface roughness vs. Cutting speed

3.1.2 Effect of factors on chip thickness ratio

Any ductile material generates heat in its primary deformation zone during machining because of plastic deformation and shear, secondary deformation zone (chip-tool interface) because of gliding & flank surface (tool-workpiece interface) because of friction and the chip-tool interaction produces the highest temperature of all [23]. Since the conventional flood coolant can only penetrate slightly in the chip-tool edge by capillary action because flowing chips make mass contact with tool rake face, the temperature can't be reduced effectively [23]. The authors of this study measured the chip thickness ratio in respect of dry and MQL assisted machining. The nozzle of MQL setup provides easy access to the maximum heat produced zone which wasn't possible using conventional flood coolant. Noticeably improved result has been found using vegetable oil based MQL in comparison to dry machining.

Though coated carbide provided solid lubrication during dry machining, it didn't reduce the impact of friction that much. Due to very little or no ambient air, higher temperature was produced in the chip tool interface. Mechanical energy converted into heat energy and influenced this rise in temperature [26]. This conversion occurs because of the cutting force generated on the workpiece by the tool [27].

Cutting speed is another major component in the making of heat in the chip tool contact. Increased cutting speed increases the temperature. Increased cutting speed achieves a better material removal rate, but it also causes more friction, which raises the temperature [28]. Higher cutting speed reduces machining time. Short duration in machining does not provide the tool enough time for cooling down and results in high temperature in the chip tool interface which in turns lead to low chip thickness ratio [29], [30]. Experimental results are shown in (**Fig. 3**).

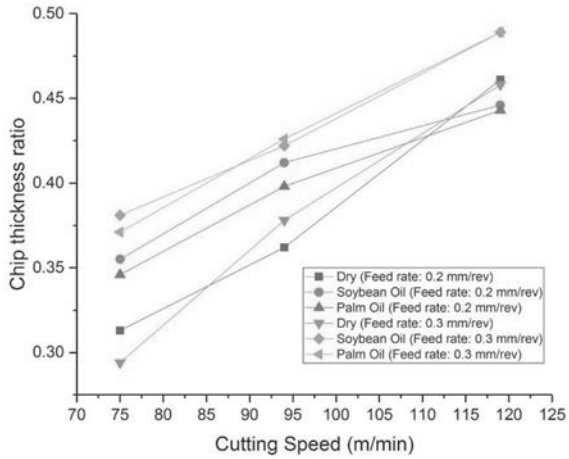


**Fig. 3:** Chip thickness ratio vs. Cutting speeds

With the increase of cutting speed and feed rate, the chip thickness ratio began to increase. The highest value was found 0.489 for cutting rate of 119 m/min, feed rate 0.3 mm/rev where soybean oil was the MQL fluid whereas the lowest value was 0.294 for the cutting speed (75 m/min) and feed rate (0.3 mm/min) in a dry cutting environment.

3.2 Numerical Results

3.2.1 Response Surface Methodology

The response surface methodology is employed in this study to build a connection between dependent (surface roughness, chip thickness ratio) and independent factors (feed rate, cutting velocity and environment). Two of the input variables are numeric (feed rate and cutting velocity) and the other is categorical (cutting environment) (Table 3). Design summaries of the responses are presented in Table 4.

Table 3: Machining process parameters values

| Factor | Name | Units | Type | Level 1 | Level 2 | Level 3 |
|---|---|---|---|---|---|---|
| A | Cutting Speed | m/min | Numeric | 75 | 94 | 119 |

| | | | | | | |
|---|---|---|---|---|---|---|
| **B** | Feed Rate | mm/rev | Numeric | 0.2 | 0.3 | - |
| **C** | Environment | | Categoric | Soybean oil | Palm oil | Dry |

Table 4: Design summary of the responses

| Response | Name | Min. | Max | Mean | Std. Dev. | Ratio | Transform | Model |
|---|---|---|---|---|---|---|---|---|
| R1 | Surface Roughness (μm) | 1.678 | 3.421 | 2.42 | 0.618 | 2.04 | None | 2FI |
| R2 | Chip Thickness Ratio | 0.294 | 0.489 | 0.4024 | 0.0568 | 1.66 | None | 2FI |

The most common second order mathematical form used in RSM is shown in Eqn. 2. In this case, Y is the dependent variable (output parameters like surface irregularity and ratio of chip thickness), $X_{i/j}$ is a set of controllable variables (input factors like cutting velocity, cutting depth, feed rate and environment); bo, $b_i$ and $b_{ij}$ are the regression coefficients for the linear, quadratic, and cross-product terms respectively.

$$Y\ (Response\ of\ interest) = b_o + \sum_{i=1}^{n} b_i x_i + \sum_{i=1}^{n} b_i x_{ii^2} + \sum_{i=1}^{n}\sum_{j=1}^{n} b_{ij} x_i x_j \quad (2)$$

In this investigation, Design Expert version 12 was used to develop mathematical equations and further analysis of the measured response values.

3.2.2 Analysis of variance (Classical sum of squares – Type II)

ANOVA is conducted to identify whether the experimental outcomes are statistically significant. In the ANOVA tables, the SS (sum of squares), MS (mean square), df (degree of freedom), Prob>F, and F-value for each factor will be displayed where the sum of average squared deviations is denoted by SS and the difference between individual samples is referred to as MS, which can be calculated by dividing the SS value by the df. Higher F-value shows greater probability that mean differences are occurred by the real effects not by the chances alone. The probability of F value is calculated using F value and degree of freedom. The F value of probability indicates whether the model is meaningful. The term is counted as important to the model if its value is lower than 0.05. If the value is higher than 0.10, it signifies that The term seems to have no effect on the evolution of the model. Models with larger R2 values can make more accurate predictions.

3.2.2.1 Surface roughness

Statistical analysis of experimental data was performed using ANOVA to investigate the parameters' relative importance in respect of the dependent variable (Table 5).

Table 5: ANOVA for Surface Roughness [Sum of squares Type-II]

| Source | Sum of Squares | df | Mean Square | F-value | p-value | |
|---|---|---|---|---|---|---|
| Model | 6.46 | 9 | 0.7173 | 155.85 | < 0.0001 | significant |
| A-Cutting speed | 0.2085 | 1 | 0.2085 | 45.3 | 0.0001 | |
| B-Feed rate | 0.3955 | 1 | 0.3955 | 85.92 | < 0.0001 | |
| C-Environment | 5.74 | 2 | 2.87 | 623.56 | < 0.0001 | |
| AB | 0.0326 | 1 | 0.0326 | 7.08 | 0.0287 | |
| AC | 0.0038 | 2 | 0.0019 | 0.4157 | 0.6734 | |
| BC | 0.0753 | 2 | 0.0377 | 8.18 | 0.0116 | |
| Residual | 0.0368 | 8 | 0.0046 | | | |
| Cor Total | 6.49 | 17 | | | | |

The F-value of 155.85 for this model suggests that it is noteworthy. When the P-values of the model terms are below 0.0500, it is found important. As a result, the important model terms here are A, B, C, AB, and BC. The P-values of model terms higher than 0.1000 are regarded as non-significant. Table 6 demonstrates that the Projected $R^2$ of 0.9726 is in fair understanding with the Adjusted $R^2$ of 0.9879; i.e., there is a difference of less than 0.2 between them.

Table 6: Model summary for Surface Roughness

| Source | Sequential p-value | Std. Dev. | $R^2$ | Adjusted $R^2$ | Predicted $R^2$ | PRESS | |
|---|---|---|---|---|---|---|---|
| Linear | < 0.0001 | 0.1069 | 0.9771 | 0.9701 | 0.9549 | 0.293 | |
| 2FI | 0.0245 | 0.0678 | 0.9943 | 0.9879 | 0.9726 | 0.178 | Suggested |
| Quadratic | 0.0475 | 0.0537 | 0.9969 | 0.9924 | 0.9799 | 0.1304 | Aliased |

As we can see from the F-value of the model in the ANOVA for Surface Roughness, the 2FI model is significant for 155.85 with probability greater than F which is lower than 0.0001. As a result, the factors A, B, C, AB, AC, and BC are shown to be noteworthy. Highest F –value of 623.56 was found for C – Environment followed by B- feed rate, A- cutting velocity with F-value of 85.92 and 45.30 respectively. The Adjusted $R^2$ and the Predicted $R^2$ are maximized in the model summary. Fig. 4, represents the 3D surface plot generated by RSM of surface roughness. Surface roughness vs. feed rate and cutting speed for dry, palm, and soybean oil are shown in **Fig. 4** (a), (b), and (c) respectively Surface roughness is observed to increase

as cutting speed and feed rate are increased.

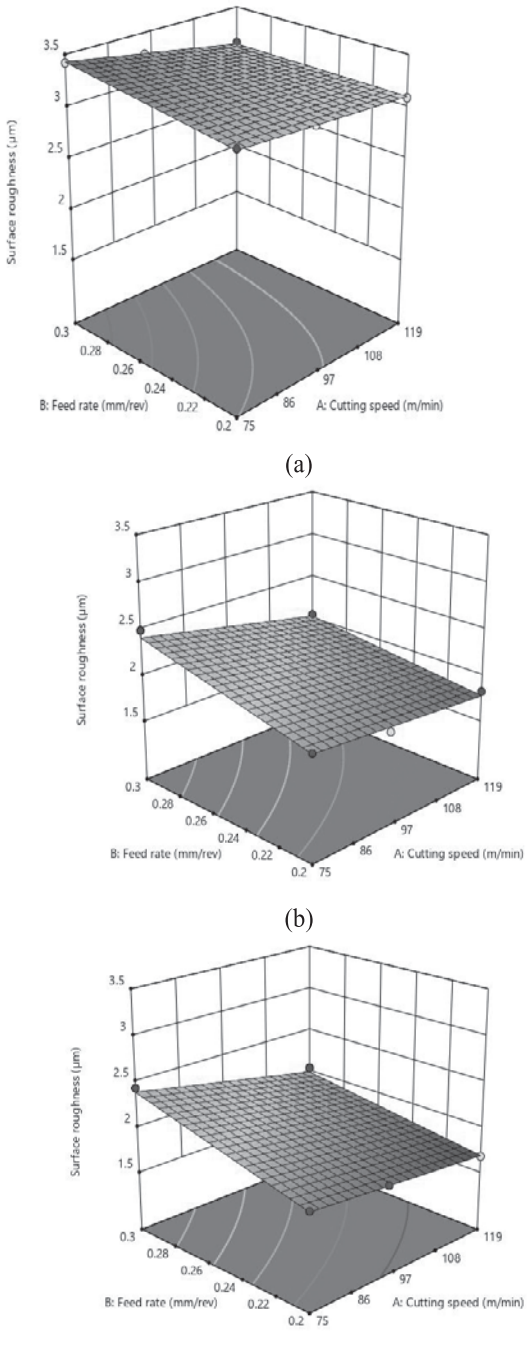


**Fig. 4**: Effects of various parameters on surface roughness generated by RSM (a) dry (b) palm (c) soybean

The established equations for surface roughness are shown below.

$$R_{a_{dry}} = 2.26191 + 0.006959 \times V_c + 5.69853 \times f - 0.047242 \times V_c \times f$$

$$R_{a_{soyabean}} = 0.472131 + 0.005082 \times V_c + 8.67853 \times f - 0.047242 \times V_c \times f \quad (4)$$

$$R_{a_{palm}} = 0.630208 + 0.005470 \times V_c + 8.12186 \times f - 0.047242 \times V_c \times f \quad (5)$$

3.2.2.2 Chip thickness ratio

ANOVA for experimental data of chip thickness ratio with related statistical terms is shown in Table 7. According to Table 7, A-cutting speed appears to have the most influence on F value. Next on the rank is C-environment and B- feed rate. The model has an F-value of 83.21, indicating that it is important. By chance, an F-value of this magnitude might occur only 0.01 percent of the time due to noise.

Table 7: ANOVA for Chip Thickness Ratio [Sum of squares Type-II]

| Source | Sum of Squares | df | Mean Square | F-value | p-value | |
|---|---|---|---|---|---|---|
| Model | 0.0542 | 9 | 0.006 | 83.21 | < 0.0001 | significant |
| A-Cutting Speed | 0.0438 | 1 | 0.0438 | 604.99 | < 0.0001 | |
| B-Feed Rate | 0.0016 | 1 | 0.0016 | 22.44 | 0.0015 | |
| C-Environment | 0.0056 | 2 | 0.0028 | 38.62 | < 0.0001 | |
| AB | 0.0002 | 1 | 0.0002 | 3.26 | 0.1085 | |
| AC | 0.0019 | 2 | 0.001 | 13.41 | 0.0028 | |
| BC | 0.001 | 2 | 0.0005 | 7.06 | 0.0171 | |
| Residual | 0.0006 | 8 | 0.0001 | | | |
| Cor Total | 0.0548 | 17 | | | | |

Considered notable are model terms with P-values lower than 0.0500. A and C are important model terms here. The model terms that have a value larger than 0.1000 are not relevant. In many models that are not relevant (unless in support of hierarchy), the reduction in the model frequently improves the model. According to Table 8 it has been noted that, the Adjusted $R^2$ value of 0.9775 is reasonably close to the predicted value of $R^2$ of 0.9514; i.e., there is a discrepancy of less than 0.2.

Table 8: Model Summary of the Chip Thickness ratio model

| Source | Sequential p-value | Std. Dev. | $R^2$ | Adjusted $R^2$ | Predicted $R^2$ | PRESS | |
|---|---|---|---|---|---|---|---|
| Linear | < 0.0001 | 0.0171 | 0.931 | 0.9098 | 0.8581 | 0.0078 | |
| 2FI | 0.0041 | 0.0085 | 0.9894 | 0.9775 | 0.9514 | 0.0027 | Suggested |
| Quadratic | 0.3643 | 0.0085 | 0.9907 | 0.9774 | 0.9456 | 0.003 | Aliased |

The three-dimensional image of chip thickness ratio obtained by RSM is shown in **Fig. 5**. **Fig.5** (a), (b) and (c) highlights ratio of chip thickness vs. feed rate and for dry cutting speed, palm, and soybean oil respectively.

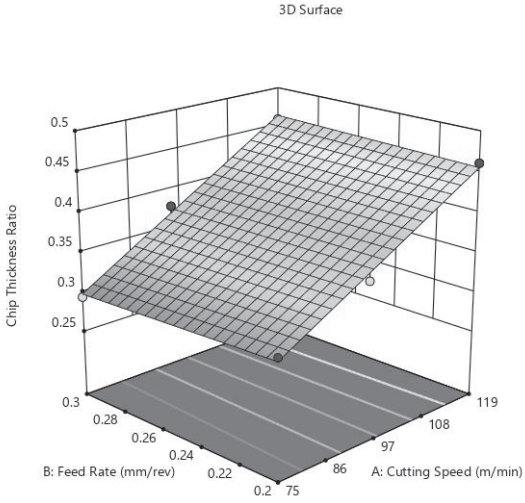


(a)

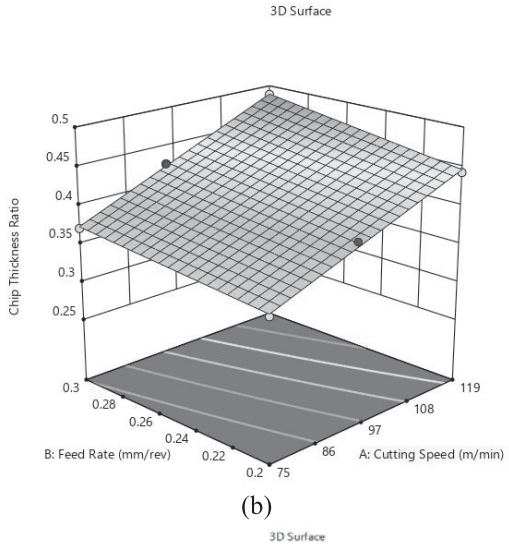


(b)

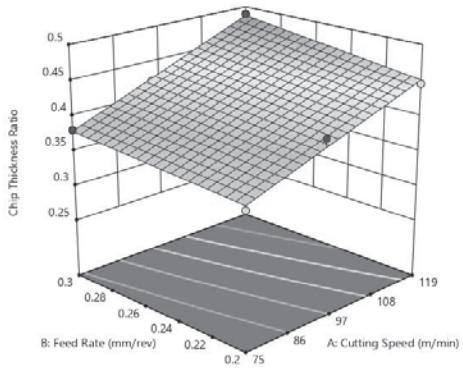


(c)

**Fig. 5**: Effects of various parameters on chip thickness ratio generated by RSM (a) dry (b) palm (c) soybean

With increasing cutting speed and decreasing feed rate, surface roughness is observed to increase. The following are the derived formulas for chip thickness ratio.

$$r_{dry} = 0.138642 + 0.00254192 \times V_c - 0.406037 \times f + 0.00402122 \times V_c \times f \quad (6)$$

$$r_{soyabean} = 0.232274 + 0.00124367 \times V_c - 0.122704 \times f + 0.00402122 \times V_c \times f \quad (7)$$

$$r_{palm} = 0.194826 + 0.00141153 \times V_c - 0.0593703 \times f + 0.00402122 \times V_c \times f \quad (8)$$

3.2.3 Artificial neural network

As illustrated in **Fig.6**, a feed-forward back-propagation neural network (BP-NN) was created for this study, two '3-n-1' structures were adopted, with two numerical input neurons positioned at the network's input layer are representing cutting speed (m/min), feed (mm/rev) and one categorical factor is representing cutting environment and output neurons at the output layer are delineating each of the two responses, namely: (a) Surface roughness (μm) and (b) Chip thickness ratio.

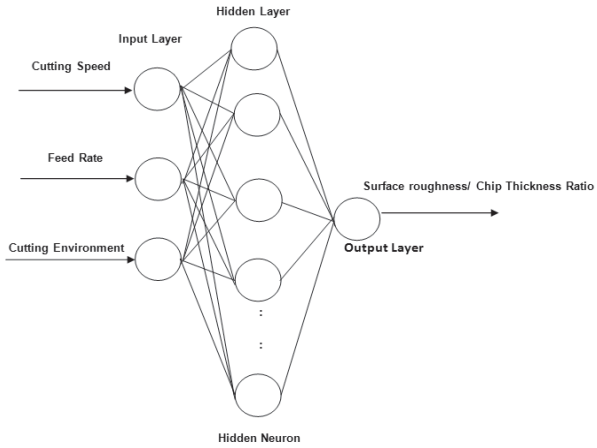


**Fig.6**: 3-n-1 ANN architecture

In total 18 data sets under dry and MQL, machining state is divided into two parts: 15 data sets for training and validation and 3 data sets to test the prediction accuracy. The Bayesian regularization algorithm was used to train the network. The ANN model was built, trained, and tested using the MATLAB R2016b Neural Network Toolbox. Neural network toolbox estimates weights and bias values at the beginning of each training phase so results may vary for the same network architecture. Mean absolute percentage error was calculated for the training, testing and overall performance using the following equation.

$$MAPE = \frac{1}{N}\sum_{n=1}^{N}\left(\frac{|Actual - Predicted|}{Actual}\right)X100 \qquad (9)$$

3.2.3.1 Surface roughness

20 neurons were used in the middle layer for predicting surface roughness. The correlation coefficient (R-value) between the output values (predicted) and the target values is used to assess the performance of the constructed network (experimental). It is a measure of how well the difference in output is clarified by targets ranging from 0 to 1. For1, it shows that the target and output values are perfectly correlated. A correlation coefficient of 0.96459 was obtained, indicating a strong association (**Fig. 7**). Through ANN, training MAPE was 6.83 and Testing MAPE was found to be 7.38 for surface roughness (**Fig. 11**).

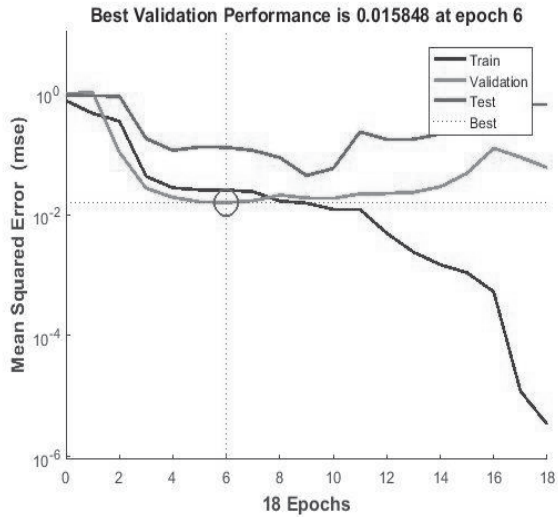


**Fig. 8**: Performance curves of Surface roughness

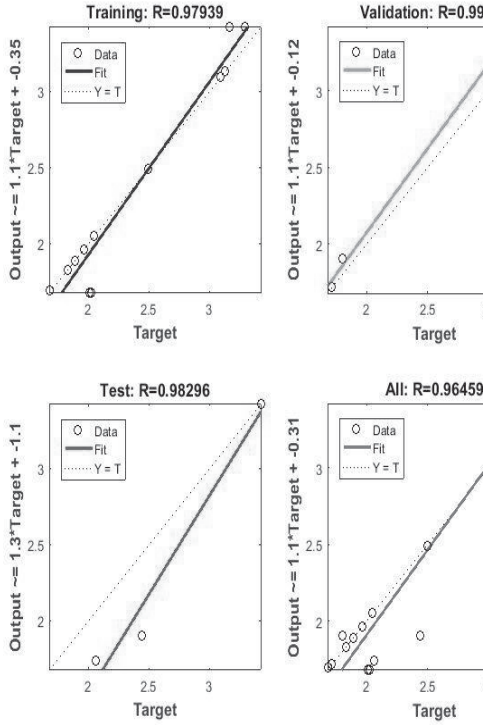


**Fig. 7**: Regression curve between predicted and experimental values of Surface roughness

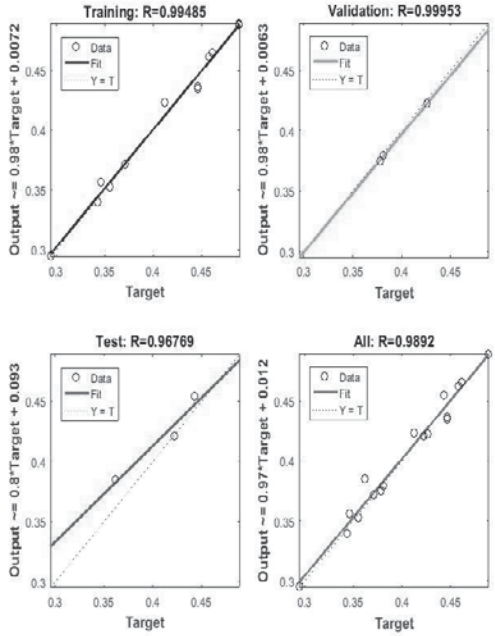


**Fig. 9**: Regression curve showing relationship between the predicted and experimental values of Chip thickness

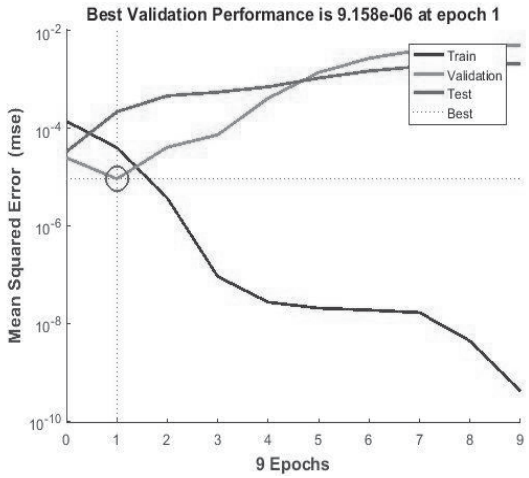


**Fig. 10**: Performance curves of chip thickness ratio

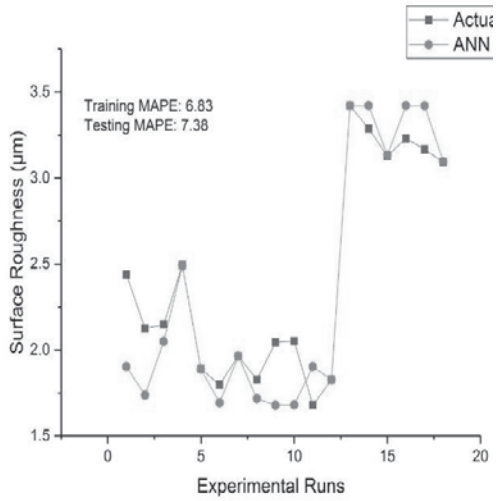


**Fig. 11**: Comparison of Surface roughness values obtained by experiment and ANN

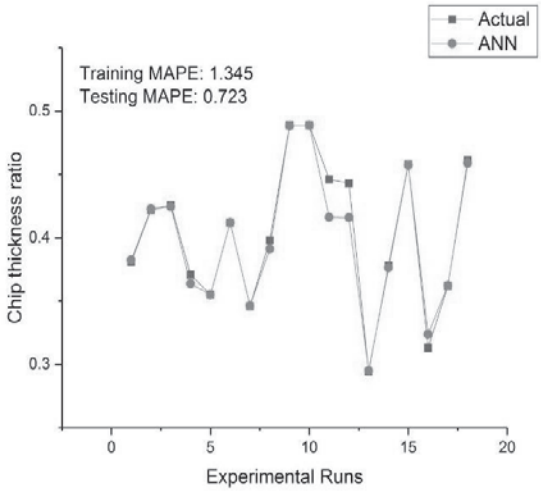


**Fig. 12**: Comparison of chip-thickness ratio values obtained from experiments and generated by ANN

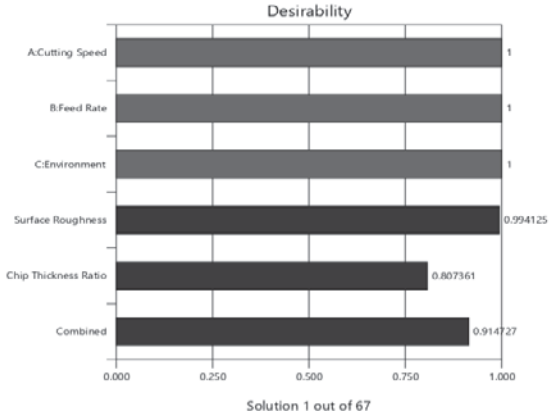


**Fig. 13**: Desirability curve for combinations of categorical factor levels

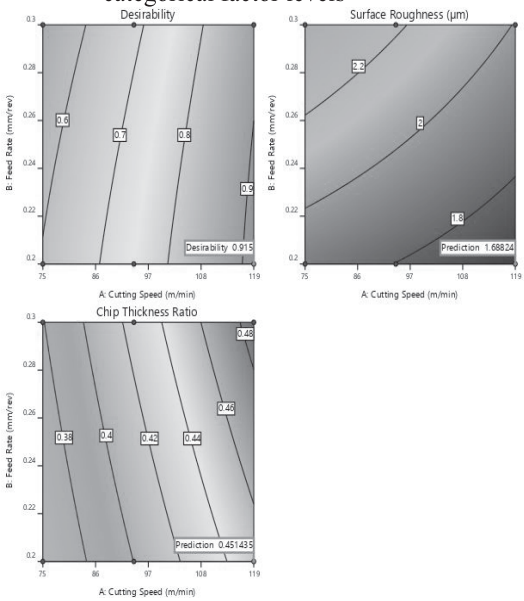

**Fig. 14**: Contour plots using desirability value for each individual factors and responses.

3.2.3.2 Chip-thickness ratio

15 neurons were deployed to construct the neural network for predicting chip thickness ratio. The correlation coefficient is 0.9892 (**Fig. 9**). MAPE for training was 1.345 and MAPE for testing was 0.723 (**Fig. 12**).

**Fig. 8** and **Fig. 10** show the performance plots of surface roughness and chip-thickness ratio respectively where with the epochs, the MSE (Mean Square Error) of ANN have decreased. For all cases, low value of MSE was found at the end of the training phase which indicates well trained ANN i.e., the outputs for the training sets have become very close to each other.

**Fig. 11** and **Fig. 12** were created by comparing experimental data with data obtained using ANN for surface finish and chip-thickness ratio, respectively. The data reveal that in most studies, the error percentage is less than 1%.

3.2.4 Multi-objective optimization

By building mathematical models, a desire-based multi-objective optimization function is utilized to enhance the parameters of the process. An objective function D is used to convert the output responses into desirability di, the value of which ranges from 0 (least) to 1 (most) [32]. To achieve all the goals as well as attain high desirability (di=1), the objective function, D identifies a point by weighting the factors based on their importance and satisfying the constraint limits (Table 9).

Table 9: Constraints of the multi objective optimization

| Name | Goal | Lower Limit | Upper Limit | Lower Weight | Upper Weight | Importance |
|---|---|---|---|---|---|---|
| A: Cutting Speed | is in range | 75 | 119 | 1 | 1 | 3 |
| B: Feed Rate | is in range | 0.2 | 0.3 | 1 | 1 | 3 |
| C: Environment | is in range | Soybean oil | Dry | 1 | 1 | 3 |
| Surface Roughness | mini mize | 1.678 | 3.421 | 1 | 1 | 3 |
| Chip Thickness Ratio | maxi mize | 0.294 | 0.489 | 1 | 1 | 3 |

The current optimization method aimed to find the optimal amounts of factor settings that would result in the lowest surface roughness and highest chip-thickness ratio. In desirability function (Eqn. 10), n specifies the measurement's response range; if any of the responses or components fall beyond their desirability range, the total function becomes zero. Particular desirability function of each goal can be adjusted by assigning weights. The "priority" of a certain target in relation to the other objectives might be modified, affecting the optimization process (Eqn. 11). The factors and responses are given the same weight values in this case. The factors and the roughness of the response surface and the other response are indicated as a priority of 3 out of 5. The ratio of chip thickness with an important factor of 2 has been included.

$$D = (d_1 \times d_2 \times \cdots \times d_n)^{\frac{1}{n}} = \left(\prod_{i=1}^{n} d_i\right)^{\frac{1}{n}} \quad (10)$$

$$D = ({d_1}^{r_1} \times {d_2}^{r_2} \times \cdots \times {d_n}^{r_n})^{\frac{1}{n}} = \left(\prod_{i=1}^{n} {d_i}^{r_i}\right)^{\frac{1}{\sum r_i}} \quad (11)$$

$$\begin{aligned}
d_i &= 0, && Response_i \le Low_i \\
d_i &= \left[\frac{Response_i - Low_i}{Target_i - Low_i}\right]^{wt_i}, && Low_i < Response_i < Target_i \\
d_i &= 1, && Response_i = Target_i \\
d_i &= \left[\frac{High_i - Response_i}{High_i - Target_i}\right]^{wt_i}, && Target_i < Response_i < High_i \\
d_i &= 0, && Response_i \ge High_i
\end{aligned}$$

For goal ‘within range (a constraint)’, desirability will be defined by the following formulas:

$$\begin{aligned}
d_i &= 0, && Response_i \le Low_i \\
d_i &= 1, && Low_i < Response_i < High_i \\
d_i &= 0, && Response_i \ge High_i
\end{aligned}$$

By solving the regression model with the limit criterion of decreasing surface roughness and maximizing chip thickness ratio, the optimal machining conditions were calculated. Table 10 shows that For Soybean oil with a desirability of0.915, an ideal cutting speed of 119 m/min and a feed rate of 0.2 mm/rev is estimated (**Fig. 13**).

Table 10: Solutions

| No. | Cutting Speed | Feed Rate | Environment | Surface Roughness | Chip Thickness Ratio | Desirability | |
|---|---|---|---|---|---|---|---|
| 1 | 119 | 0.2 | Soybean oil | 1.688 | 0.451 | 0.915 | Selected |

| | | | | | | |
|---|---|---|---|---|---|---|
| 2 | 119 | 0.204 | Soybean oil | 1.701 | 0.453 | 0.914 |
| 3 | 118.842 | 0.2 | Soybean oil | 1.689 | 0.451 | 0.914 |
| 4 | 119 | 0.208 | Soybean oil | 1.711 | 0.454 | 0.914 |
| 5 | 119 | 0.208 | Soybean oil | 1.713 | 0.454 | 0.913 |

For optimum cutting conditions, surface roughness is 1.688 µm and chip thickness ratio is 0.451. **Fig. 14** represents the contour plots which are generated using desirability value.

## 4. CONCLUSION

The investigation came to the following conclusions:

1. Over a dry environment, vegetable oil based MQL aided machining is better for turning Monel 400.
2. Soybean oil offers better cutting responses (improved surface roughness and higher chip thickness ratio) over palm oil during MQL assisted machining.
3. From the multi parameter optimization solution, the optimum cutting conditions were found to be a cutting speed of 119 m/min, feed rate of 0.2 mm/rev and Soybean oil as MQL medium.
4. Surface roughness of Monel 400 is most significantly influenced by cutting environment, which is after that feed rate and cutting speed.
5. Cutting velocity is the most crucial aspect impacting chip thickness ratio, after that environment and feed rate.
6. The ANN formulated prediction model for Surface roughness and Chip thickness showed respectively 93.17% and 98.655% accuracy in training and 92.62% and 99.277% accuracy in testing respectively.

## References

[1] L. E. Shoemaker and G. D. Smith, "Nickel: A Century of Innovation A Century of Monel Metal : 1906 – 2006," no. September, 2006.

[2] A. Kulandaivel and S. Kumar, "Effect of magneto rheological minimum quantity lubrication on machinability, wettability and tribological behavior in turning of Monel K500 alloy," Mach. Sci. Technol., vol. 24, no. 5, pp. 810–836, Sep. 2020, doi: 10.1080/10910344.2020.1765179

[3] R. Arunachalam and M. A. Mannan, "MACHINABILITY OF NICKEL-BASED HIGH TEMPERATURE ALLOYS," Mach. Sci. Technol., vol. 4, no. 1, pp. 127–168, Jan. 2000, doi: 10.1080/10940340008945703.

[4] A. R. Motorcu, Y. Isik, A. Kus, and M. C. Cakir, "Analysis of the cutting temperature and surface roughness during the orthogonal machining of AISI 4140 alloy steel via the taguchi method," Mater. Tehnol., vol. 50, no. 3, pp. 343–351, 2016, doi: 10.17222/mit.2015.021.

[5] Y. Matsumoto, F. Hashimoto, and G. Lahoti, "Surface integrity generated by precision hard turning," CIRP Ann. - Manuf. Technol., vol. 48, no. 1, pp. 59–62, 1999, doi: 10.1016/S0007-8506(07)63131-X.

[6] L. B. Abhang and M. Hameedullah, "Chip-tool interface temperature prediction model for turning process," Int. J. Eng. Sci. Technol., vol. 2, no. 4, pp. 382–393, 2010.

[7] A. Adler et al., "Catheter-associated bloodstream infections in pediatric hematology-oncology patients: Factors associated with catheter removal and recurrence," J. Pediatr. Hematol. Oncol., vol. 28, no. 1, pp. 23–28, 2006, doi: 10.1080/10910340500534282.

[8] N. Takeshi, "NII-Electronic Library Service," Chem. Pharm. Bull., vol. 57, no. 534, pp. 364–370, 1977, [Online]. Available: http://www.mendeley.com/research/geology-volcanic-history-eruptive-style-yakedake-volcano-group-central-japan/.

[9] E. . Klocke.F, "Keynote on Dry Cutting," CIRP Ann., vol. 46, no. 2, pp. 519–526, 1997.

[10] Z. Jiang, F. Zhou, H. Zhang, Y. Wang, and J. W. Sutherland, "Optimization of machining parameters considering minimum cutting fluid consumption," J. Clean. Prod., vol. 108, pp. 183–191, 2015, doi: 10.1016/j.jclepro.2015.06.007.

[11] A. Devillez, G. Le Coz, S. Dominiak, and D. Dudzinski, "Dry machining of Inconel 718, workpiece surface integrity," J. Mater. Process. Technol., vol. 211, no. 10, pp. 1590–1598, 2011, doi: 10.1016/j.jmatprotec.2011.04.011.

[12] M. Mosleh, K. A. Shirvani, S. T. Smith, J. H. Belk, and G. Lipczynski, "A study of minimum quantity lubrication (MQL) by nanofluids in orbital drilling and tribological testing," J. Manuf. Mater. Process., vol. 3, no. 1, 2019, doi: 10.3390/jmmp3010005.

[13] N. R. Dhar, M. W. Islam, S. Islam, and M. A. H. Mithu, "The influence of minimum quantity of lubrication (MQL) on cutting temperature, chip and dimensional accuracy in turning AISI-1040 steel," J. Mater. Process. Technol., vol. 171, no. 1, pp. 93–99, 2006, doi: 10.1016/j.jmatprotec.2005.06.047.

[14] A. S. Varadarajan, P. K. Philip, and B. Ramamoorthy, "Investigations on hard turning with minimal cutting fluid application (HTMF) and its comparison with dry and wet turning," Int. J. Mach. Tools Manuf., vol. 42, no. 2, pp. 193–200, 2002, doi: 10.1016/S0890-6955(01)00119-5.

[15] T. Thepsonthi, M. Hamdi, and K. Mitsui, "Investigation into minimal-cutting-fluid application in high-speed milling of hardened steel using carbide mills," Int. J. Mach. Tools Manuf., vol. 49, no. 2, pp. 156–162, 2009, doi: 10.1016/j.ijmachtools.2008.09.007.

[16] J. K. Ho, C. H. Tsai, M. Y. Tsai, M. X. Tu, and J. C. Sung, "Development of a novel cooling system-assisted minimum quantity lubrication method for improvement of milling performance," J. Chinese Inst. Eng., vol. 38, no. 3, pp. 322–331, Apr. 2015, doi: 10.1080/02533839.2014.970387.

[17] U. Heisel et al., "Application of minimum quantity cooling lubrication technology in cutting processes," Prod. Eng., vol. II, no. 1, pp. 49–54, 1994, [Online]. Available: http://elib.uni-stuttgart.de/opus/volltexte/2010/5072.

[18] Y. Zhang, C. Li, D. Jia, D. Zhang, and X. Zhang, "Experimental evaluation of MoS2 nanoparticles in jet MQL grinding with different types of vegetable oil as base oil," J. Clean. Prod., vol. 87, no. C, pp. 930–940, 2015, doi: 10.1016/j.jclepro.2014.10.027.

[19] Y. Zhang et al., Experimental evaluation of cooling performance by friction coefficient and specific friction energy in nanofluid minimum quantity lubrication grinding with different types of vegetable oil, vol. 139. Elsevier Ltd, 2016.

[20] E. A. Rahim and H. Sasahara, "AN ANALYSIS OF SURFACE INTEGRITY WHEN DRILLING INCONEL 718 USING PALM OIL AND SYNTHETIC ESTER UNDER MQL CONDITION," Mach. Sci. Technol., vol. 15, no. 1, pp. 76–90, Apr. 2011. Doi: 10.1080/10910344.2011.557967.

[21] S. A. Lawal, I. A. Choudhury, and Y. Nukman, "Evaluation of vegetable and mineral oil-in-water emulsion cutting fluids in turning AISI 4340 steel with coated carbide tools," J. Clean. Prod., vol. 66, pp. 610–618, 2014, doi: 10.1016/j.jclepro.2013.11.066.

[22] Nickel Development Institute, "Machining Nickel Alloys," A Nickel Dev. Inst. Ref. B., pp. 2–6, 1995.

[23] S. S. Rahman, M. Z. I. Ashraf, A. N. Amin, M. S. Bashar, M. F. K. Ashik, and M. Kamruzzaman, "Tuning nanofluids for improved lubrication performance in turning biomedical grade titanium alloy," J. Clean. Prod., vol. 206, pp. 180–196, 2019, doi: 10.1016/j.jclepro.2018.09.150.

[24] N. R. Dhar, M. Kamruzzaman, and M. Ahmed, "Effect of minimum quantity lubrication (MQL) on tool wear and surface roughness in turning AISI-4340 steel," J. Mater. Process. Technol., vol. 172, no. 2, pp. 299–304, 2006, doi: 10.1016/j.jmatprotec.2005.09.022.

[25] T. H. Sayed and M. M. Koura, "Modeling and Prediction of Surface Roughness During Dry Turning Process," vol. 3, no. 7, pp. 694–699, 2014.

[26] M. B. Da Silva and J. Wallbank, "Cutting temperature: prediction and measurement methods - a review," J. Mater. Process. Technol., vol. 88, no. 1, pp. 195–202, 1999, doi: 10.1016/S0924-0136(98)00395-1.

[27] R. R. Moura, M. B. da Silva, Á. R. Machado, and W. F. Sales, "The effect of application of cutting fluid with solid lubricant in suspension during cutting of Ti-6Al-4V alloy," Wear, vol. 332–333, pp. 762–771, 2015, doi: 10.1016/j.wear.2015.02.051.

[28] F. Koné, C. Czarnota, B. Haddag, and M. Nouari, "Modeling of velocity-dependent chip flow angle and experimental analysis when machining 304L austenitic stainless steel with groove coated-carbide tools," J. Mater. Process. Technol., vol. 213, no. 7, pp. 1166–1178, 2013, doi: 10.1016/j.jmatprotec.2013.01.015.

[29] A. Molinari and M. Nouari, "Modeling of tool wear by diffusion in metal cutting," Wear, vol. 252, no. 1–2, pp. 135–149, 2002, doi: 10.1016/S0043-1648(01)00858-4.

[30] S. K. Ali, S.M., Dhar, N.R., Dey, "Effect of Minimum Quantity Lubrication (Mql) on Cutting Performance in Turning Medium Carbon Steel By Uncoated Carbide Insert At Different Speed-Feed Combinations," Adv. Prod. Eng. Manag., vol. 6, no. 3, pp. 185–196, 2011, [Online]. Available: http://maja.uni-mb.si/files/apem/APEM6-3_185-196.pdf.

# MACHINING PARAMETERS OPTIMIZATION FOR TURNING OPERATION FOR AL ALLOY 4343 ON VERTICAL CNC MILLING MACHINE USING TAGUCHI ANALYSIS AND GENETIC ALGORITHM

**Zahid Hasan*, Mahjabin Moon, Morshed Ahmed, Md. Wasiur Rahman, Ashfaq Ebna Millat, Mehedi Hasan Sourov**

Department of Mechanical and Production Engineering (MPE)
Ahsanullah University of Science and Technology (AUST), Tejgaon Industrial Area, Bangladesh
*Corresponding Email: zhshuvo.ipe@aust.edu

***Abstract:*** *Aluminum alloy is unique for different industrial applications when compared to other materials; it has a high strength-to-weight ratio. Its good electrical and thermal conductivity, reflectivity, and recyclability make it useful in a variety of applications. A vertical CNC milling machine will be used as a machine tool in this research. This research will find out whether it is possible to achieve the specified surface roughness value through turning operation in a vertical CNC milling machine. In this study, a CNC milling machine will be used for the Turning operation of Aluminum 4343 alloys using a square nose and cobalt steel mill cutter. Taguchi method and the genetic algorithm will be used to identify optimal cutting variables for achieving surface roughness as low as possible. The optimum variables will be determined utilizing various combinations of feed rate ($F_r$), depth of cut ($D_c$), number of passes (P), and spindle speed (N). After machining, the value of the surface roughness will be determined for each combination. One of the most important criteria for this study is surface roughness. The results of this research will be based on its quality. Taguchi Method Analysis will be used to create various combination sets of cutting parameters. Following that, the genetic algorithm will be used to analyze the result of surface roughness. The most important objective of this research is to measure the effect of different parameter combinations on the surface roughness of Aluminum 4343 material through turning operation using a square nose and mill cutter in a vertical CNC milling machine. By using various analyses, best machining variables for decreasing surface roughness will be determined. Analyzing experimental and expected data results in the formulation of process parameters. Surface roughness is measured in relation to machining parameters, and the optimal combination of cutting parameters for minimizing surface roughness is assessed. Machining has an impact on machined surface roughness is measured and the optimum machining state is calculated to minimize the roughness of the surface. By using validation experiments, the predicted values are confirmed comparing with experimental value shaving some negligible errors.*

***Keywords:*** *Vertical CNC milling machine, Turning operation, Parameter optimization, AA 4343.*

## INTRODUCTION

Raw resources are transformed into worthwhile products through the manufacturing process. Manufacturing procedures can be divided into two categories: primary manufacturing processes and secondary manufacturing processes. Traditional and contemporary machining are both a part of secondary production. Some of the current operations that are referred to as primary manufacturing processes include welding, casting, and forging. A workpiece can be given the proper shape and surplus metal is removed from it through the process of machining. More people are currently using modern machining than any other type of machining. Modern machining includes CNC machining. A CNC machine can perform a wide range of precision operations. It must first need the coding for this. Additionally, any complicated task can be completed quickly.

Different machining procedures fall under various categories. Taking milling, turning, drilling, grinding, boring, etc. as examples. It is a form of micro-threading machining to turn between them. A cutting tool with a single point is used to create tiny threads from a cylindrical workpiece that is rotating. Turning is typically done on lathes. Compared to lathe machines, milling machines offer significantly wider variety of machining techniques. Almost any machining operation can be carried out using a milling machine. It is easy to see that, with the exception of a few, almost all product parts can be manufactured in a milling machine. Then, for a few tasks like turning, you'll need to employ a lathe machine. It is a more costly and time-consuming treatment in terms of total cost and duration. Therefore, it is crucial to understand what results or challenges can be encountered when turning operations are performed on a milling machine as opposed to a lathe. Additionally, there are more CNC milling machines on the market than CNC lathes. CNC lathes are more expensive and need more room. Additionally, lathe machining involves a fair amount of vibration. Furthermore, the lathe is turned using a single-pointed cutting tool. On the other hand, milling

machines use multipoint cutting tools. As a result, turning operations at CNC milling will go more quickly. Due to this, a CNC milling machine rather than a CNC lathe will be employed in this study. The machining operation will make use of the Haas VF-2. It serves as both the company's flagship model and the foundation for the most well-known machines in the VF Series. Dimensions: 762 x 406 x 508 mm. Features: 20-station carousel tool changer, 30 HP vector drive, 8100 RPM direct drive, 42.3 cm/s rapids, 40 taper, power-failure detection module, and 1000 MB of program memory. It is a vertical machining center. The cutting tool will be an insert coated with carbide. To machine the metal, 4343-grade aluminum will be utilized. Its elements are 7.49% silicon and 92.51% aluminum. As an alloy, aluminum has a far wider variety of uses. The biggest advantage of aluminum is how light it is. Aluminum and aluminum alloys are joined together using the filler metal AL 4343. Corrosion resistance in AL 4343 is lower than in AL 718. The solution temperature during heat treatment must be lower than the solidus of the braze alloy in order to maintain joint integrity. One of the investigation's most important conclusions is whether aluminum alloy can be turned effectively in a milling machine.

In this instance, the output will be the surface roughness following milling. This procedure will include four parameters. The variables are: Feed Rate ($F_r$), Spindle Speed (N), Cut Depth ($D_c$) and Number of Passes (P). Operating different configurations of these variables will allow comparisons of surface roughness. The Taguchi method's L9 algorithm will be used for this. The Taguchi method is a useful design strategy. This can raise the level of the product's processing quality. It is also possible to minimize the number of experiments and processing modifications. The usage of a genetic algorithm will follow. This is a method of optimization. From a large pool of potential solutions, it is simple to quickly identify the best one.

## LITERATURE REVIEW

Vertical milling aluminum alloy methods are examined. Thus, many research publications are published on milling machines, vertical milling machines, Aluminum Alloys, machining parameters, lubrication, heat production in milling operations, and so on. These research publications were published worldwide between 1985 and 2020. These articles are summarized.

End milling uses Taguchi optimization to optimize cutting variables. An L-27 (313) orthogonal array was used for semi-finishing and finishing high-speed cutting using a TiN-coated Carbide inserted end-mill tool. S/N ratio and Pareto Analysis of Variance (ANOVA) were used to determine how milling parameters affect surface roughness. Hardened steel DIN GX40CRMOV5-1 could be cut at 0.5mm, 355 m/min, and 0.1mm per tooth[1].

Turning is best at 248.69 m/min. 0.3 mm/rev feed rate, 1.8 mm cut depth, and 0.8 mm nose radius. For AECM, 248.69 m/min cutting speed, 0.3 mm/rev feed rate, 1 mm depth of cut, and 1.2 mm nose radius are optimum. There is a 61.776 percent, 57.025 percent, and 7.49 percent improvement over tough turning conditions[2].

The Taguchi method of turning SCM 440 alloy steel yielded the lowest surface roughness to find optimal cutting settings. The Taguchi approach found that depth of cut and feed reduced surface roughness. Cutting speed only slightly affected surface roughness, according to studies[3].

The turning process is a focus of the optimization of machining parameters. The material is medium carbon, the turning tool is molybdenum high-speed steel (HSS), and (AISI 1045). The Box Behnken and analysis of variance (ANOVA) techniques are used to assess how machining parameters affect surface roughness. Utilizing linear regressions, mathematical models relating the impact of machining factors were created[4].

Research was done to find the best tuning parameters for milling aluminum alloy 6063 with carbon nitride. The studies used the Taguchi method L27 orthogonal array and evaluated it according to the lower is better rule. The main and dominant factor that affects the turning operation's reactions is revealed by this investigation. The results of the investigation showed that the feed rate, followed by the speed, had an impact on the reactions[5].

EN-8 steel was turned using a CNC. In order to forecast surface roughness, second-order mathematical models for machining parameters were developed using the response surface approach (RSM). The model that was employed for optimization was validated using the F-test. Through the use of Analysis of Variance, the models' suitability for surface roughness was determined (ANOVA). The surface roughness prediction model was improved using a genetic algorithm to determine the ideal cutting parameters[6].

Researchers enhanced the machining parameters for a CNC turning operation using a Taguchi L9 orthogonal array. The workpiece, which was manufactured of IS2062 E250 steel, was cut using a carbide cutting tool. Surface roughness and hardness are the experiment's outcome parameters, whereas speed feed and depth of cut are its input variables. Variability analysis was

utilized by the study team at the International Conference on Recent Trends in Nanomaterials for Power, Environmental, and Engineering Applications to decide what level of peer review was necessary[7].

This article discussed how to reduce surface roughness when machining mild steel by using the Taguchi method and the Genetic Algorithm. A 25 mm diameter face miller was fitted with three zinc-coated carbide tools. The machining parameters employed were spindle speed, passes, feed rate, and depth of cut. A FANUC CNC vertical machining center was used to conduct the experiment[8].

While reviewing these works, it became clear that publishers and scholars were omitting some fields. Some topics have not yet been thoroughly investigated. For instance, turning is frequently done on a lathe. However, no research has been done on how different cutting variables, such as the temperature created by the cutting fluid, affect the material's surface roughness in vertical CNC milling machines. In this experiment, aluminum 4343 will be utilized. To evaluate the impact of cutting parameters on surface roughness in conventional or CNC lathes, numerous studies have been carried out. Despite the fact that many different materials are employed in this situation, it is unknown how varied cutting conditions and parameters would affect the Aluminum 4343 material. One of the most popular materials in the industrial sector is aluminum. Therefore, it is crucial to investigate the effects of various cutting settings on it. In order to raise the level of living for individuals, these kinds of studies are required. With the development of technology, researchers and publishers are contributing to society in a variety of ways by gathering data through their studies, tests, and investigations.

This is why an unexplored subject has been chosen for exploration and study of its numerous facets. It has been chosen to test a CNC vertical milling machine by cutting an aluminum alloy with the specific grade 4343 utilizing a variety of cutting factors and cutting combinations. To achieve the least amount of surface roughness on the machined surface, it is determined to optimize the cutting factors. Additionally, it has been chosen to apply the Taguchi Method and Genetic Algorithm in this study.

Under the heading "Machining Parameters Optimization of Turning Operation for Al Alloy 4343 on Vertical CNC Milling Machine Using Taguchi Analysis and Genetic Algorithm," the research paper will address the subject.

In this study, the surface roughness of a machined surface made of aluminum alloy 4343 will be examined. To optimize the machining factors, the Taguchi approach and the genetic algorithm will be applied. By comparing the anticipated value with the experimental value, the percentage of error for the two methods discussed above can also be calculated.

## METHODOLOGY

For this investigation, CNC milling machines will be employed. There are two common milling machine kinds. These milling devices are both horizontal and vertical. Using multiple-point cutting tools, almost all procedures can be completed swiftly and precisely. In this study, the turning process will be carried out, and its optimal parameters will be identified. Additionally, this turning action is not suitable for the horizontal milling machine. As a result, a vertical milling machine will be used. This investigation will use aluminum alloy because of how much more widely it can be applied. Aluminum 4343-grade material will be employed in this study. It will be used for the turning operation, and its many properties will be examined. In this scenario, factors like cutting depth ($D_c$), spindle rpm (N), feed rate ($F_r$), and number of passes (P) would be taken into account during the machining process. Following the process, the surface roughness will be assessed under various machining circumstances. The obtained data will then be assessed, initially using the L9 algorithm array of the Taguchi technique, and subsequently using the genetic algorithm.

### Material:

In the manufacturing industry, various types of metals and their alloys are widely used. Alloys are made in combination with some more essential materials with the original materials. Alloys can do operations that no pure material can. One of the most popular forms of material alloy is Aluminum alloy. Its lightweight is one of the reasons for its widespread use. Other materials are added in different proportions. Aluminum alloys are classified into seven primary varieties that are utilized in manufacturing. Aluminum Alloy 4343 is employed as a workpiece in this research. The alloy 4343 belongs to the 4000-series of aluminum alloys. Silicon is the principal alloying component. It can be easily machined due to its high silicon and low copper content, and the mechanical properties of the product are also good. This is why aluminum 4343-grade materials have been chosen for this study.

**Fig.- 1:** Workpiece (after casting)

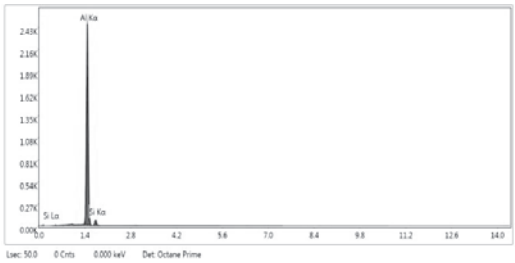

**Fig.- 2:** EDX Report

**Table 1:** Material Composition

| Element | Weight % | Atom % |
|---|---|---|
| AlK | 92.23 | 92.51 |
| SiK | 7.77 | 7.49 |

Figure 1 represents the workpiece condition after casting. Figure 2 ensure3s the components of the workpiece and the component percentages are being given in table 1.

**Experimental setup:**

The experiments have been performed under wet condition. Carbide insert has been used as cutting tool. The experimental setup in HAAS VF-2 CNC milling has been shown in fig. 3.

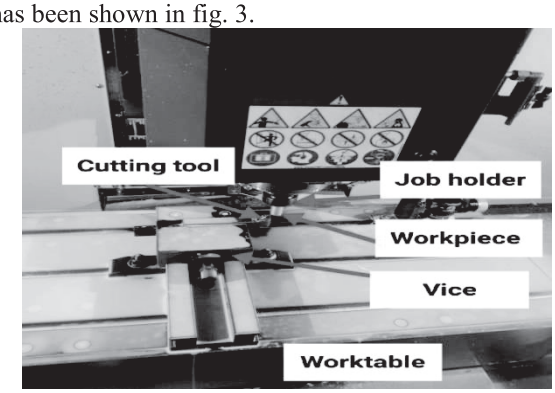


**Fig.- 3:** Experimental Setup

**Experiment Design:**

Table 2 represents the initial cutting levels. Taguchi's L9 orthogonal array has been used. The minitab suggested the experimental combinations (Table 3) which were used for the machining procedures.

**Table 2:** Levels of Input Parameters

| Input Parameters | Levels | | |
|---|---|---|---|
| | 1 | 2 | 3 |
| Feed Rate (mm/min) | 100 | 300 | 500 |
| Depth of Cut (mm) | 0.1 | 0.2 | 0.3 |
| Number of Passes | 1 | 2 | 3 |
| Spindle Speed (RPM) | 3000 | 5000 | 7000 |

**RESULT AND DISCUSSION**

Minitab suggested 9 combinations of cutting parameters for machining. The values of surface roughness have been measured by Phase 2 SRG 4500 profile roughness-tester (Table 3).

In table 4, the maximum value for feed rate is -3.504, and the minimum value is -15.572, resulting in a delta of 12.068. Similarly, the deltas for spindle speed, depth of cut, and number of passes are 9.912, 7.511, and 6.640, respectively. For Rank 1, 2, 3, and 4, these deltas are arranged from a higher value to a lower value.

**Table 3:** Response Table

| SL | $F_r$ (mm/min) | $D_c$ (mm) | P | N (RPM) | $R_a$ (µm) |
|---|---|---|---|---|---|
| 1 | 100 | 0.1 | 3 | 5000 | 1.32 |
| 2 | 100 | 0.2 | 2 | 7000 | 0.399 |
| 3 | 100 | 0.3 | 1 | 3000 | 6.369 |
| 4 | 300 | 0.1 | 2 | 7000 | 4.061 |
| 5 | 300 | 0.2 | 3 | 3000 | 6.479 |
| 6 | 300 | 0.3 | 1 | 5000 | 4.19 |
| 7 | 500 | 0.1 | 1 | 3000 | 7.414 |
| 8 | 500 | 0.2 | 2 | 5000 | 4.748 |
| 9 | 500 | 0.3 | 3 | 7000 | 6.156 |

**Table 4:** Response Table for Signal to Noise Ratios

| Level | $F_r$ | $D_c$ | P | N |
|---|---|---|---|---|
| 1 | -3.504 | -10.662 | -7.288 | -16.571 |
| 2 | -13.616 | -7.260 | -13.928 | -9.462 |
| 3 | -15.572 | -14.771 | -11.476 | -6.659 |
| Delta | 12.068 | 7.511 | 6.640 | 9.912 |
| Rank | 1 | 3 | 4 | 2 |

| Factor | Name | Units | Type | Level 1 | Level 2 | Level 3 |
|---|---|---|---|---|---|---|
| A | Cutting Speed | m/min | Numeric | 75 | 94 | 119 |

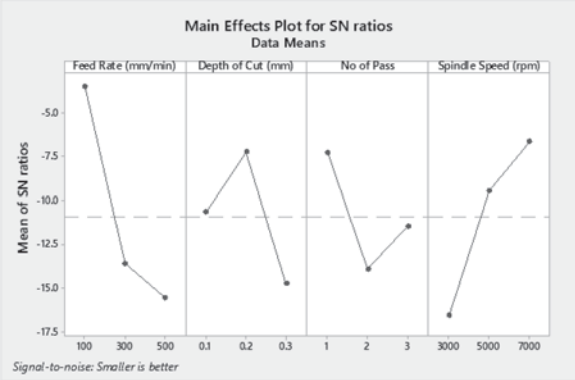


**Fig.- 4:** Graph of Signal to Noise Ratio

Figure 4 explains the main effect plot for SN ratio. The optimum cutting parameters achieved by taguchi analysis are the highest peak points of the graphs which are also shown in table 5.

**Table 5:** Optimum Cutting Conditions

| $F_r$ | $D_c$ | P | N |
|---|---|---|---|
| 100 mm/min | 0.2 mm | 1 | 7000 RPM |

The regression equation (eqn 1) gives us the theoretical value of the surface roughness for taguchi analysis.

$$R_a = 4.07 + 0.00852\,F_r + 6.53\,D_c + 0.325\,P - 0.000804\,N \quad (1)$$

The model summery (Table 6) shows that the $R^2$ value is almost 79%.

**Table 6:** Model Summery

| Std. Dev. | $R^2$ | Adjusted $R^2$ | Predicted $R^2$ |
|---|---|---|---|
| 1.56 | 0.7878 | 0.5757 | -0.0558 |

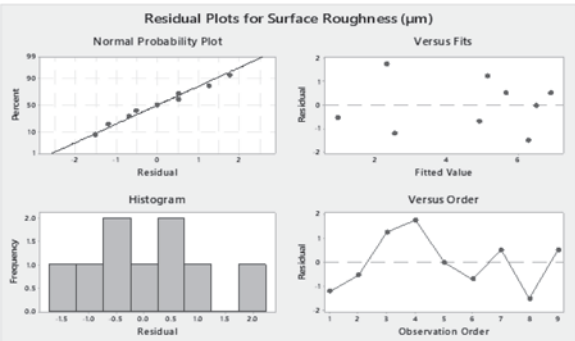


**Fig.- 5:** Residual plots

In table 7, we can see that by using the optimum cutting condition suggested by taguchi analysis, the value of $R_t$ found is 0.925 µm. The actual value has been got 1.1079 µm with an error of 10%.

**Table 7:** Results of Taguchi Analysis

| $R_1$ | $R_2$ | $R_3$ | $R_a$ | $R_t$ | Error % |
|---|---|---|---|---|---|
| 1.0175 | 1.0198 | 1.0165 | 1.0179 | 0.925 | 10.04 |

Equation (1) has been used in Genetic Algorithm (GA) to optimize the cutting parameters. The ranges were the upper and lower bounds of taguchi analysis. The outputs have been given in Fig. 6, table 8 and table 9 respectively.

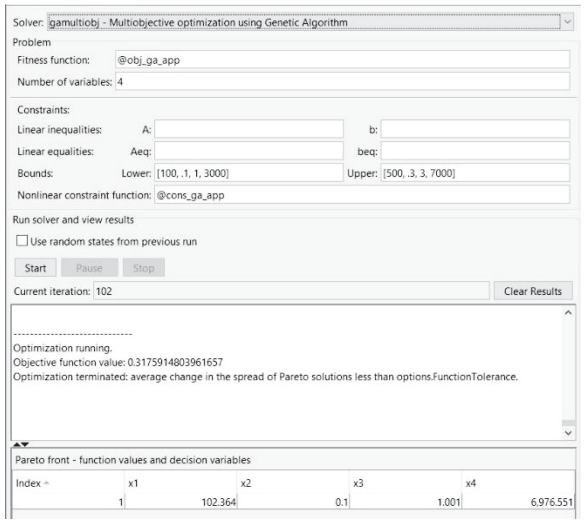


**Fig.- 6:** Simulation window of GA

**Table 8:** Optimum Cutting Conditions

| $F_r$ | $D_c$ | P | N |
|---|---|---|---|
| 102.364 mm/min | 0.1 mm | 1 | 6976.551 RPM |

**Table 9:** Results of GA

| $R_1$ | $R_2$ | $R_3$ | $R_a$ | $R_t$ | Error % |
|---|---|---|---|---|---|
| 0.3398 | 0.3367 | 0.3348 | 0.3367 | 0.3176 | 6.01 |

GA gives the better result than Taguhi Analysis with a percentage of error of 6.01%.

**CONCLUSION:**

Studies have been done on how the number of passes, depth of cut, spindle speed, and feed rate affect the machined surface roughness during turning operations. The experiment was conducted on AA 4343, and the Taguchi technique and Genetic Algorithm were used to analyze the results. It has been noted that a tiny amount of experimenting yields a lot of information from Taguchi's orthogonal array. All four criteria, which primarily influence the response, have been taken into account. Taguchi approach and genetic algorithm have been used to identify the ideal machining parameter combination. The results of the two procedures have been compared, and the best machining parameter

combination setup for the least amount of surface roughness has been recommended. Surface roughness measured using Taguchi technique is 0.925 μm, 10.04% off the anticipated value, whereas surface roughness measured using genetic algorithm is 0.3367 μm, 6.01% off the projected value.

**NOMENCLATURE:**

| | |
|---|---|
| AA | Aluminum Alloy |
| $D_c$ | Depth of Cut |
| $F_r$ | Feed Rate |
| N | Rotational Speed |
| P | Number of Pass |
| $R_a$ | Average Surface Roughness |
| $R_t$ | Theoretical Surface Roughness |

**REFERENCES**


1. Optimization of Process Parameters in Vertical CNC Mill Machines Using Taguchi's Design of Experiments," 4(2), pp. 61–75.
2. Bilga, R. K. P., Singh, S., Sehijpal, 2016, "Optimization of energy consumption response parameters for turning operation using Taguchi method," J. Clean. Prod., 137, pp. 1406–1417.
3. Thamizhmanii, S., Saparudin, S., Hasan, S., 2007, "Analyses of surface roughness by turning process using Taguchi method," J. Achiev. Mater. Manuf. Eng., 20(1–2), pp. 503–505.
4. Abdulkareem, S., Rumah, U. J., Adaokoma, A., 2011,"Optimizing Machining Parameters during Turning Process," Int. J. Integr. Eng. 3(1) pp. 23-27.
5. Saravanakumar, A., Karthikeyan, S., C., Dhamotharan, B., Kumar, V. G., 2018, "Optimization of CNC Turning Parameters on Aluminum Alloy 6063 using Taguchi Robust Design," Mater. Today Proc., 5(2), pp. 8290–8298.
6. Routara, B. C., Sahoo, A. K., Parida, A. K., Padhi, P. C., 2012, "Response surface methodology and the genetic algorithm used to optimize the cutting condition for surface roughness parameters in CNC turning," Procedia Eng., 38, pp. 1893–1904.
7. Radha Krishnan, M. R. B., 2019, "Optimization of machining process parameters in CNC turning process of IS2062 E250 Steel using coated carbide cutting tool," Mater. Today Proc., 21, pp. 346–350.
8. Selvam, M. D., Karuppusami, G., Dawood, A. K. S., 2012, "Optimization of Machining Parameters for Face Milling Operation in a Vertical CNC Milling Machine Using Genetic Algorithm," An Int. J. 2(4), pp. 2250–3498.

# CONCEPT OF SELF-PROPELLED FLOATING CONVENTION CENTER IN BANGLADESH

**Md. Abrar Faiyaz Taseen[1], Md. Shafayat Kabir[1], Md. Mashiur Rahaman[1*] and Md. Moynul Hasan[1]**

[1]Department of Naval Architecture and Marine Engineering, Bangladesh University of Engineering and Technology, Dhaka-1000, Bangladesh

*Corresponding Email: *mashiurrahaman@name.buet.ac.bd*

***Abstract:*** *Convention centers are one of the most pivotal establishments in our society whose vital purpose is hosting weddings in the perspective of Bangladesh. But the existing convention centers are riddled with issues like expensive rental costs, long waiting periods, etc. The survey conducted for this study shows the rental cost of the venues becoming 3-5 Lac BDT during November-February which is difficult to afford. Also, the waiting period becomes quite high, extending up to 1 year. Moreover, with the rise of per capita income, people's wish for new experiences like a unique wedding, corporate gateway, etc. have significantly increased. Reflecting the changing wedding trends, over 80 percent of the responses from the survey participants consider aesthetics and environment to be significant factors in deciding venues. As such, a gap is created between the unfulfilled clients and the unsatisfactory service of the existing convention centers in Bangladesh. Furthermore, the current predicament of cities provides exceptionally low chances of establishing modern convention centers. This study introduces a new concept of convention centers in the form of self-propelled vessels where a ship is specialized for holding such ceremonies. Due to the propulsive nature, scintillating experience aligning with the changing wedding trends, and affordable hiring cost of the self-propelled floating convention center, over 80% of the survey respondents have shown a keen interest. Considering the amenities and backed by the survey results, the prospects of this venture are endless under the current demography of Bangladesh.*

***Keywords:*** *convention center, issues, survey, changing wedding trends, self-propelled, prospects.*

## INTRODUCTION

Convention centers are one of the pivotal establishments of society with multiple purposes. From the perspective of Bangladesh, the main functions that stand out include hosting marriage ceremonies and receptions, hosting seminars and conferences, etc. Although the existing land-based convention halls provide amenities for the above-mentioned functions, there are noticeable gaps. For example, the environment that they provide leaves much to be desired during weddings or seminars. Furthermore, the substantial number of weddings held every year often creates the issue of finding suitable convention halls at suitable times for customers. As such, the market has a situation where there is far more demand than supply. Surprisingly, marine vessels can tap into this market. Through the construction and operation of specialized vessels whose purpose is to host conventions, more options can be provided to potential customers to explore this unique opportunity of hosting their programs in the riverine environment. Although issues like cost, safety, etc. will exist, this niche prospect has its own pros of a scenic environment and unique experience. As such, it is not a pessimistic option when compared to traditional land-based convention centers. This project of self-propelled floating convention vessels has never been explored anywhere else before worldwide. Bangladesh, being a riverine country and for hosting so many conventions and seminars every year is the ideal demography and location for undertaking this project. As such, it is believed that this project has an extraordinarily rich prospect in the context of Bangladesh.

The prospect of self-propelled floating convention vessels can be implemented due to the changing trends of marriage in contemporary periods. That is, previously ideas like destination weddings were not as commonplace as they are nowadays. The evolution of wedding photographs depicts this very fact. Going back a couple of decades, weddings used to emphasize a cohesive blending of the families of the wedding couple in a wholesome environment that did not put much importance on the aesthetic element and experience[1]. A similar scenario was observed during the hosting of seminars. Any traditional convention center that could accommodate the necessary amount of people along with the availability of other amenities would be a worthwhile choice.

An extensive amount of data was collected through various means including comprehensive literature reviews, surveying of potential

stakeholders in the potential venture, route, demography analysis, etc. Stakeholders, namely people who are looking to get married, and their concerned relatives, were approached and a detailed survey was conducted. Furthermore, other primary stakeholders, for instance, various multinational companies, banks, etc. were approached about another survey regarding a potential seminar hosting conference or a picnic spot was also carried out in order to account for primary data. As for secondary data, the market situation around convention halls, marriage, seminar halls, picnic spots, etc. was carried out. Furthermore, information on wedding trends, the importance of the environment in which the seminar or conference is conducted, etc. was taken from the detailed literature review and article review. A professional attitude was ensured in the collection of data through the above-mentioned methods.

## CURRENT SCENARIO of BANGLADESH

In the present state, in the context of venue selection for marriage ceremonies, the clientele looking to book their suitable venues face a grave issue. It is often found that their desired community center is either already booked and there is a long waiting period to get a date there or the cost of booking the venue is so high that they are forced to look elsewhere.

Moreover, as a sign of changing of the times, wedding and other event trends are also changing. As such, the aesthetic element and experience of an immersive environment have become a priority[2]. To provide support to this argument, the evolution of wedding photography again shows that weddings have transformed from being focused on the union of two families to a much more intimate setting between the wedding couple[1]. Thus, to highlight this aspect of weddings, the aesthetic element of the convention hall is a primary aspect of consideration.

In another context, the recent lockdown due to the outbreak of the corona virus left a deep and lasting impact on the people. Health and hygiene issues have become one of the primary concerns among people. In this situation, many of the existing convention centers are losing customers as they are deemed unhygienic. Furthermore, the taste of people in choosing a venue for their special occasions is also changing. The lockdown has really shown the people the importance of fleeting moments. As such, people now wish to experience the uniqueness that will be memorable to them. A wedding between a couple in the scenic environment of a river and the setting sun surely counts as one of them.

Bangladesh is a riverine country with a navigable waterway length of 5968 km (about 3708.34 mi) in monsoon and 3865 km (about 2401.6 mi) in the dry season with a minimum draft of 1.5m, the service of self-propelled floating convention halls can be made available to most of the cities in the country[3]. To take advantage of this aspect and keep pricing in mind, this service should be made available to most of the market. Thus, during customer segmentation, appealing to the middle-class demography instead of the elite class exclusively should be made a priority.

## SCENARIO WORLDWIDE

Looking beyond Bangladesh, diverse types of wedding reception programs are observed. For instance, destination weddings. Besides, cruise weddings are also increasing in popularity. Furthermore, wedding tourism has been an expanding market for the last decade due to multiple reasons including lower cost than a domestic wedding, increased frequency of international flights, and slowly decreasing cost of having weddings abroad[4]. Moreover, seminars are hosted in an environment that provides their participants with an immersive experience of the topic on which the seminar is being held. For instance, seminars on global warming and rising sea levels are held in countries which will be most drastically affected by the changing climate. Such a conference was held on 17$^{th}$ October 2009 in the form of an underwater cabinet meeting between the then President of Maldives and 13 government officials in Girifushi, Maldives[5].

## ANALYSIS of PROSPECTS

To get an initial understanding of the rich prospect of the venture of a Self-propelled floating convention vessel, an extensive survey was conducted to assess the demand. A total of 1238 participants filled out the survey form.

**Fig.-1** represents whether the participants consider the self-propelled floating convention vessel as an alternative to traditional convention centers. It is seen from Figure 1 that about 95.4% of the respondents are positive.

**Fig.-1:** Capability of Self-propelled floating convention vessel as an alternative to traditional convention centers

**Fig.-2** illustrates the perspective on whether the self-propelled convention vessel is a suitable venue for hosting marriage ceremonies. From Figure 2, it is noticed that about 89.1% of the participants respond positively.

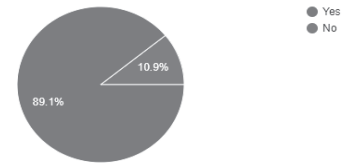


**Fig.-2:** Suitability of self-propelled convention vessel for hosting marriage ceremonies

**Fig.-3** depicts the view on whether the self-propelled convention vessel is a suitable venue for hosting picnics and seminars. It is seen from Figure 3 that about 93% of the participants find it suitable.

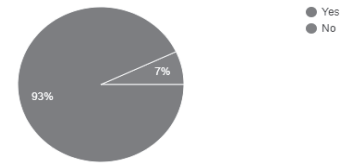


**Fig.-3:** Suitability of self-propelled convention vessel for hosting picnics and seminars

**Fig.-4** shows whether the potential customers are willing to pay an extra amount of money (about 5 ~10 thousand Bangladeshi Taka) to acquire the venue provided by a self-propelled floating Convention Vessel. About 85.8% of the participants are willing to pay additional amount which is shown in Figure 4.

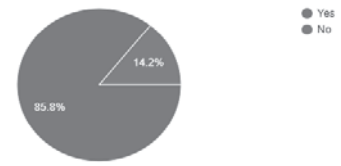


**Fig.-4:** Willingness to pay additional amount of cost for the use of self-propelled convention vessel

From the survey results shown in **Figs.-1~4**, it is noticeably clear that the self-propelled floating convention vessel has garnered interest in the sample space of the surveyed lot. Participants of the survey have also agreed to pay a definite amount greater than what they would pay traditional convention halls of similar capacity provided that the pricing is made affordable.

## CHALLENGES

### Cost:

Congruent to all situations, the cost is a major concern when it comes to making any pivotal decision for the customers. No matter the amenities, the service will never be used if its cost is beyond the budget of the customers. An analogous situation arises in the case of a self-propelled floating convention vessel. Although it will provide a very fulfilling experience, its pricing cannot be positioned as too pricy. Care must be taken so that substantial revenue can be earned that will, on the one hand, offset the incurred cost by the service provider, and on the other hand, it will not be a burden to the customers. In this way, it will eventually become a successful business with a continuous stream of revenue and customers.

### Health and Safety Issues:

Since the events hosted by the self-propelled convention vessels will take place in a water body (mostly rivers), health and safety will always be a concern. If safety cannot be ensured, not only will no customer ever avail themselves of their service, but it will also attract an awfully bad rapport along with severe sanctions from various authorities. The major points that will have to be ensured include stability, a nominal rolling period, minimized vibration, etc. Nevertheless, a small margin of the market can never be accessed by this venture due to a fear of water and seasickness among some of the potential customers. This service will have to maximize its revenue keeping this issue in mind.

### Miscellaneous:

Some other barriers remain with the venture. For example, during the hosting of a marriage ceremony, time restriction positions itself as a concern in a different manner compared to land-based traditional convention centers. As the vessel will have to depart the port, all the guests will have to embark on the vessel within the given time. Ensuring this promptness is quite difficult from the perspective of customers. Furthermore, if a fresh lunch or dinner is to be served at the event, then cooking of the required volume will have to be carried out aboard the vessel. Thus, the general arrangement of the vessel will have to be adapted properly.

## PRELIMINARY CONCEPT DESIGN of VESSEL

The next predominant barrier to the realization of this venture is the actual design of a vessel that is well-equipped with the amenities required for the service demanded by the customers. That is, as far as the general arrangement of the vessel is concerned, she must be able to accommodate several people as per demand, host the event for an amount of time, provide enough space for the event to take place, and have the required kitchen space for the required amount of food preparation and other necessary things as per event demand. Furthermore, the vessel must also meet the stability criterion of International Maritime Organization (IMO) and vibration guidelines of international classification society in order to ensure the safety and comfort of the people aboard the ship. Keeping all these aspects in mind a preliminary General Arrangement (GA) Plan of the vessel is developed, which is shown in **Fig.-5**. **Table-1** shows the principal particulars of the vessel.

**Table-1:** Principal particulars of the Vessel

| Item | Symbol | Value | Unit |
|---|---|---|---|
| Length Overall | $L_{OA}$ | 56.03 | [meter] |
| Length Between Perpendiculars | $L_{BP}$ | 51.00 | [meter] |
| Breadth Moulded | $B_{MLD}$ | 11.10 | [meter] |
| Depth Moulded | $D_{MLD}$ | 3.40 | [meter] |
| Draft Design | T | 2.20 | [meter] |
| Block co-efficient | $C_B$ | 0.61 | -- |

## CONCLUSION

Self-propelled floating convention vessels are an ingenuine alternative to land-based traditional convention centers. While there remain some concerns about the realization of the project and safety involved, the prospect of a floating convention vessel undeniably has a unique appeal to her potential customers with its unique experience. And since the venture has garnered a huge positive response initially through extensive surveys, it can conclude that the project is not without prospects. As such, as per recommendations, advancement should be made in order to financially determine the profitability of the venture.

## RECOMMENDATION

After the detailed design of the vessel, the entire business venture must be analyzed rigorously from economical and financial standpoint.

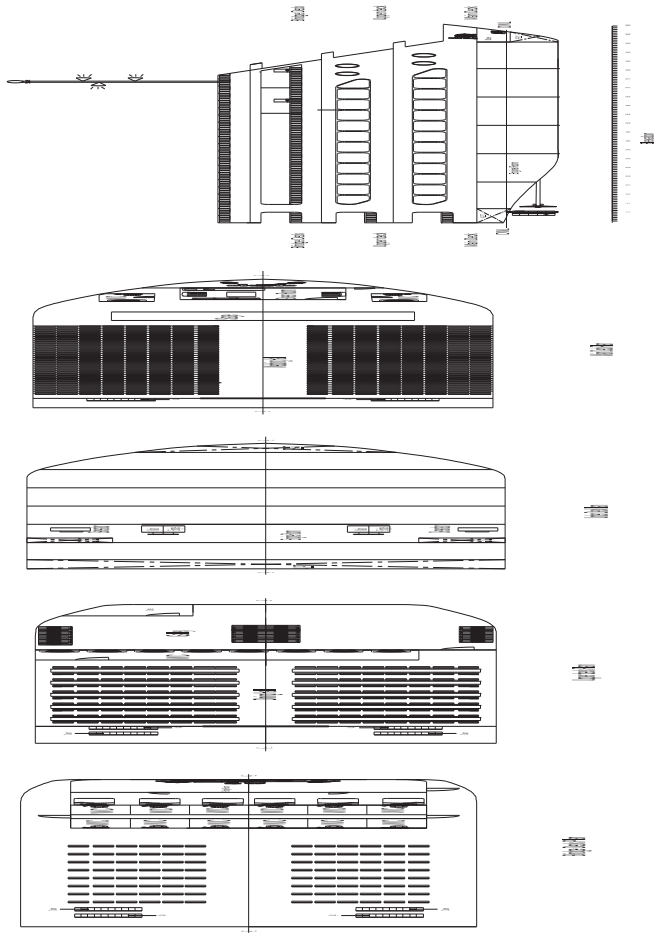

**Fig.-5:** Concept General Arrangement Plan of the Vessel

## REFERENCES

1. Mosharrof Hossain, "Changing Patterns of Wedding Photography in Bangladesh" *International Conference on "Visual South Asis: Anthropological Explorations of Media and Culture", 2017.*
2. Prisciani Blesy Umbas, "The environmental stimuli of the wedding decoration towards customer satisfaction", Journal *Berkala Ilmiah Efisiensi,* Volume 15, No. 05 Tahun 2015
3. BIWTA, "Bangladesh Waterways Assessment"
4. Jaclyn Breg, "Now and Forever: Growth, Impacts and Future Evolution of Wedding Tourism", *The Atrium, University of Guelph*.
5. Christina Garcia, "Underwater Cabinet Meeting in the Republic of the Maldives", *Environment and Society Portal*

# Waste to Energy: Utilization of Leather-Trimmed Wastage as Solid Fuel from Footwear and Leather Products Industries

Benu Chakraborty[1*], Raju Kumar Das[1,3], Uttam Kumer Roy[1], Sujit Kumer Banik[2], Mohammad Sarwar Morshed[3]

[1]Institute of Leather Engineering and Technology, University of Dhaka, Dhaka-1209, Bangladesh
[2]Institute of Fuel Research and Development, Bangladesh Council of Scientific and Industrial Research, Dhaka-1205, Bangladesh
[3] Ahsanullah University of Science and Technology (AUST), Tejgaon Industrial Area, Bangladesh
*Corresponding Email: benu.ilet.du.ac.bd@gmail.com

***Abstract:*** *This research focuses on the utilization of solid leather waste as energy which was derived from different footwear and leather products industries in Bangladesh. The fundamental goal is to achieve green energy as better performance through solid leather waste management. The coal industry may utilize leather waste as a partial coal substitute since it has the potential to provide overall heating benefits similar to high-grade coal. In this research, the ratio between 40%-50% leather waste and 50%-60% coal sample indicate that the maximum energy would be generated. Leather waste is partly used as a partial replacement for coal, so coal demand and its operating expenses can be considerably decreased. Increasing the utilization of solid leather waste as a partial substitute of coal would positively improve the economy and save our environment by reducing the leather waste management cost and space.*

***Keywords:*** *Green Energy, Coal, Renewable Energy, Solid Waste Management, Calorific Value*

## INTRODUCTION

The leather and footwear industry is the largest industry in the world, based mainly on a by-product. The byproduct of the slaughterhouses is used as the raw resource in the manufacturing of leather [1]. The process of converting raw hides and skins into leather involves several steps, including pre-tanning, tanning, and post-tanning [2] [3]. The produced leather is then utilized as a raw material by the footwear and leather goods industries which are approximately 60-65% and more than 21 billion pairs of shoes are produced annually over the world [4]. This production process generates huge amounts of wastage from the leather products and footwear industries. The types of waste generated each day mostly depend on the production process, the ingredients, and the techniques employed in the production of footwear and leather goods. Solid wastes are generated during the production of leather items, particularly footwear and leather goods, and they account for 15-20% of the raw materials used [5]. Although the leather goods and footwear industries are commercially significant, the amount of solid waste it generates has a detrimental effect on the environment. The majority of the waste is produced in the leather products and footwear industry during the production stage and primarily is disposed of in landfills [4].

Any undesired material in our environment or from everyday products that is neither liquid nor gas is referred to as solid waste that consists of trash or refuses, sewage treatment plant sludge, and other waste products from commercial, industrial, mining, and agricultural operations as well as residential activities [6]. When solid waste is not properly disposed of, it may have a variety of negative effects on the environment, including soil, water, and air pollution as well as the spread of illnesses including dengue, yellow fever, and dysentery [7]. The leather solid waste is generated from footwear and leather goods industries contain different heavy metal used in the leather processing period like chromium, zinc, aluminum, etc. which may cause several serious health diseases and harmful for our environment [3]. In addition, solid waste that contains chromium is difficult to manage and unsafe to use. Existing solid waste management practices are inadequate, and the resulting waste has a harmful result on public health, the economy, and the environment [7]. By developing effective technology (thermal conversions, Biochemical conversion, etc.) solid waste can be used to produce sustainable energy which protects the environment by reducing the impact of solid waste as well as generating valuable energy [8]. Waste-to-energy (WtE) is the process of turning waste into energy, either in the form of heat or electricity [9].

The cutting process is primarily responsible for the solid waste produced during the manufacture of shoes and footwear and this is dependent on the type of footwear being produced [5]. Natural leather has grown irregularly causing animal skin not to have an ideal geometrical shape [10].]. In footwear and leather goods industry, the majority of waste is produced from leather. According to accepted statistics, the amount of waste produced by leather typically ranges from 20 to 45 percent, depending on the type and quality of leather used as well as the cutting skill, and an average of 30% of waste is produced altogether [5]. That's why small or broken pieces of leather will not be utilized in manufacturing another product. The leather-cutting waste decreases with the size and quality of the animal skin surface. In essence, each pair wastes 30% of the leather's two square feet, which has a thickness of 0.8 grams per cubic centimeter (gm/cm$^3$) and around 90 gm of leather waste is produced for every pair on average [4]. Annually, over 4600 million pairs of footwear are produced utilizing around 6300 million square feet of leather sheets, resulting in approximately 0.5 million tons of waste [4].

This research aims to a new process to utilize the huge amount of leather waste as a fuel with the combination of coal. Generating energy from waste provided multiple benefits to the environment by reducing the dumping problem and its consequent health-related issues as well as to the economy by reducing the overall solid waste management cost [11][12].

## METHODOLOGY

### SAMPLE COLLECTION:

Waste leather samples were collected from renowned industries in Bangladesh i.e; Apex Footwear Limited (Gazipur, Bangladesh), Footbed Footwear Limited (Gazipur, Bangladesh), and Bengal Leather complex limited (Hazaribagh). A huge number of raw materials were used in the footwear and Leather Products Industries like leather [13][14], synthetic, textiles, foam, rubber, plastic, adhesive, thread, etc. Samples were collected during the production phase of those industries and after collection samples were conditioned by following standard norm [15]. Then samples were cut into small sizes by hand with a scissor.

### DETERMINATION OF MOISTURE CONTENT:

The moisture content in the material is to be resolved to utilize a straightforward test. Took the waste leather sample and weighed for which the moisture content was to be found. Further measured the weight of the sample after oven-dried. The moisture content was determined by following the standard method [16].

Mathematical calculation to determine the moisture content: $W= (W_d/W_m)\times100\%$

Here, the term W is the moisture content of the sample, $W_m$ is the most weight of the example and $W_d$ is the oven-dried weight.

### DETERMINATION OF ASH CONTENT:

The Ash content measurement needed a known quantity of samples and the weighed sample was put in a dry / pre-weighted silica crucible. 6 gm of the sample was taken for this test. Before taking the weight of the sample and crucible both were needed to put in the oven for removing moisture content. Then the waste leather sample was put into the furnace and burned away in the air at temperatures above 800°c for 2 hours. After the complete burning sample was weighed after cooling in a desiccator at 25-degree temperature. By using the initial and final weight of the sample within a simple equation ash content was calculated.

Mathematical calculation:

$$\text{Percentage (\%) of Ash} = (W_a/W_s)\times100\%$$

Where; $W_a$= weight of ash, $W_s$= weight of the sample

### DETERMINATION OF CALORIFIC VALUE:

All of the samples were properly cut into small pieces to complete this test and those were weighed separately. The calorific value had been determined for four samples. These samples were mainly wastages that were collected from different footwear and leather product industry. Each of the samples was kept for 10 days before the calorific value measurement test was performed in the laboratory at 25-degree temperature.

The heat that an ignitable solid-liquid substance emanates is measured by Bomb Calorimeters following the standard method [17]. This was achieved by calculating the exacted quantity of the sample material in a crucible, placing the crucible inside a "bomb" (a sealed metal holder called a bowl), filling the oxygen pipe, and contacting the material. In controlled settings, a Bomb-Calorimeter is used to

measure the warmth of a specimen ingested in a vessel encircled by water in an oxygen climate. The results of the calculation are called the Combustion, Calorific, and BTU estimates [18].

Mathematical Calculation Of Calorific Value:

Heat liberated by the fuel = Heat taken up by the calorimeter

$$X \times C = (W+w)\times(t_2 - t_1)$$
$$C= \{(W+w)\times(t_2- t_1)\}/X$$

$$\text{i.e., } H.C.V = \{(W+w)\times(t_2 - t_1)\}/X$$

Where,
C= calorific value of the fuel
X= mass in kg of the fuel sample
W= mass of water in the calorimeter
w= water equivalent of the calorimeter, stirrer, thermometer, bomb, etc. in the gm unit
$t_1$= Initial temp of the water in the calorimeter
$t_2$= Final temp of the water in the calorimeter

## RESULT AND DISCUSSION

### DETERMINATION OF MOISTURE CONTENT OF WASTAGE LEATHER SAMPLES:

The moisture content of the collected leather samples with standard deviation is exposed in "Figure 1". All hides and skins have a comparable creation. The moisture content of the hide is 12-14% ideal in the finished leather [19]. Most of the leather samples contained an average moisture range of 11-15%. Among the three leather samples, the skiving dust of the shoe upper leather (SDSUL) contained maximum moisture of about 14.74% and the lowest moisture gained by oil pull-up leather (OPL) is about 11.56 % [Figure 1]. The shoe upper leather (SUL) showed nearly the high value of 13.6% [Fig-1].

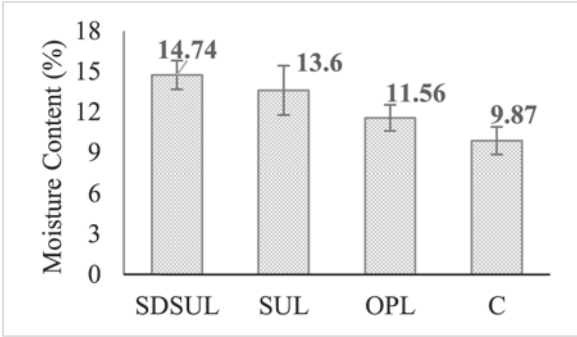


**Figure 1:** Moisture content of the different samples and coal

The coal (C) contained moisture of about 9.87% which was used for the comparison with leather to find out the heat produced by the wastage leather samples. In all of the leather samples, only oil pull-up leather was near the moisture content of coal. The increased heating value of materials is influenced favorably by their moisture content and the sample that has lower moisture content provides maximum heat value than the sample that has higher moisture content [20].

### DETERMINATION OF ASH CONTENT OF THE WASTAGE LEATHER SAMPLES

The composition of ash reflects the residual incombustible portion after burning the leather sample. In general, ash content is poor in a substance. The residue that remains in the air at particularly high temperatures after sample combustion is known as the inorganic residue. The ash content was determined by following a standard method [16]. The ash content of the collected leather samples with standard deviation is illustrated in "Figure 2". For better accuracy, the ash content determination test was performed three times and the result is shown with standard deviation. After burning the sample, the composition of ash represents the remaining incombustible component. The content of ash in a product is usually low. The inorganic residue is defined as the residue that persists in the air following sample combustion at, particularly high temperatures. Three waste leather samples are experiments to find out the ash content.

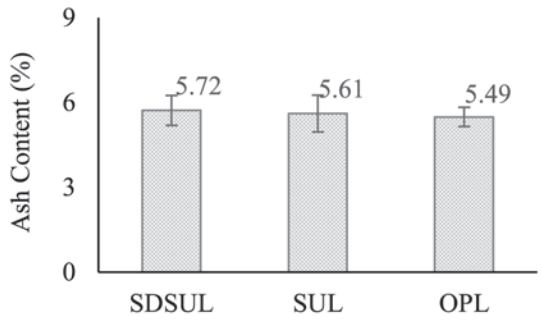


**Figure 2:** Determination of Ash content of the wastage leather sample

The highest ash content from above those samples is 5.72% which showed the skiving dust of shoe upper leather (SDSUL) and the lowest ash content is 5.49% in oil pull-up leather (OPL) [Figure 2]. The shoe upper leather (SUL) showed a moderate result of 5.61%. On average, the all-leather sample contains approximately 5.50% ash content after burning at 800°A for 2 hours.

## DETERMINATION OF CALORIFIC VALUE OF WASTAGE LEATHER SAMPLES:

Calorific value is characterized as the number of calories produced when a unit measure of substance is oxidized and is resolved to utilize the bomb calorimeter. Calorific value (likewise called heat worth or warming worth) is the absolute warmth delivered from the total burning of any substance [21]. The calorific value of the collected leather samples with standard deviation are shown in "Table 1". The calorific value determination test was performed three times and the result is shown with standard deviation in table 1. The heat of ignition of a natural compound was intently equivalent to the burning of the components in it, increased by their percent content in the compound.

**Table 1:** Calorific value of the different leather sample

| SAMPLE MATERIAL | CALORIC VALUE(Kcal/kg) | GRADE |
|---|---|---|
| SDSUL | 5902.91±77.53 | B |
| SUL | 5096.21±79.87 | C |
| OPL | 6225.68±82.24 | A |
| Coal (A Grade) | 6482.21±20.13 | A |
| 50% Coal + 50% SDSUL | 6253.22± 78.33 | A |
| 50% Coal + 50% SUL | 5691.39 ±81.47 | B |
| 50% Coal + 50% OPL | 6442.95±83.77 | A |

From the three leather samples, oil pull-up leather has the maximum calorific value of 6225.68 kcal/kg and shoe upper leather has the lowest calorific value of 3994.84 kcal/kg [Table 1]. According to the coal grade, the oil pull-up leather and shoe upper leather refer to garde-A and grade-C respectively [Table 2] [22]. The range of the calorific value of leather samples was nearly as same as the range of high-grade coal. The combination of 50% coal and 50**%** skiving dust of shoe upper leather provided a calorific value of 6253.22 kcal/kg which is equal to coal grade A. After mixing the 50% skiving dust shoe upper leather, having a calorific value of 5902.91 kcal/kg (grade B) with 50% high-quality coal (grade A) having a calorific value of 6482.21 kcal/kg produced a heat value nearly the same as (grade A) high-grade coal. In the other case, mixing between 50% coal and 50% shoe upper leather generates a heat value of 5691.39 kcal/kg which is equal to coal grade B [Table 1].

Though the 50% oil-pullup leather samples were used as the substitute for 50% coal, the level of heat value remain nearly the same as the heat value of 100% coal. It was noticed that mixing wastage leather with coal in a specific portion can have the ability to produce the same level of heat value which will reduce the nearly 50% of coal consumption.

**Table 2:** Calorific value of different coal grades [22]

| COAL GRADE | CALORIFIC VALUE (kcal/kg) |
|---|---|
| A | Above 6200 |
| B | 5600-6200 |
| C | 4940-5600 |
| D | 4200-4960 |
| E | 3360-4200 |

## CONCLUSION

The core outcome of this research is to discover the huge opportunity in the utilization of solid leather waste in the field of energy. The study finds that leather has the ability to provide an average heat value like upper-grade coal, so it can be used as a partial substitute for coal in the coal-based industry. It is suggested that the ratio between 40%–50% leather waste and 50%–60% coal sample provides the maximum energy. Solid leather waste can be used with coal as a partial substitute, which can greatly reduce coal consumption and its expenditures in a production field. Reducing coal consumption by using waste leather will greatly help our economy as well as save our environment through waste and solid waste management costs.

## REFERENCES


[1] K. Joseph and N. Nithya, "Material flows in the life cycle of leather," *J. Clean. Prod.*, vol. 17, no. 7, pp. 676–682, 2009, doi: 10.1016/j.jclepro.2008.11.018.

[2] R. K. DAS, A. MIZAN, F.- ZOHRA, B. BAŞARAN, and S. AHMED, "Application of Indigenous Plant-Based Vegetable Tanning Agent Extracted from Xylocarpus granatum in Semi-Chrome and Chrome Retanned Leather Production," *TEKSTİL VeKonfeksiyon*, vol. 32, no. 3, pp. 258–264, 2022, doi: 10.32710/tekstilvekonfeksiyon.1066811.

[3] R. K. Das, A. Mizan, F. T. Zohra, S. Ahmed, K. S. Ahmed, and H. Hossain, "Extraction of a novel tanning agent from indigenous plant bark and its application in leather processing," *J. Leather Sci. Eng.*, vol. 4, no. 1, 2022, doi: 10.1186/s42825-022-00092-5.

[4] N. C. Jadhav and A. C. Jadhav, *Waste and 3R's in Footwear and Leather Sectors*, no. August. Springer Singapore, 2020. doi: 10.1007/978-981-15-6296-9_10.

[5] N. M. Sivaram and D. Barik, *Toxic waste from leather industries*. Elsevier Ltd., 2018. doi: 10.1016/B978-0-08-102528-4.00005-5.

[6] R. Agarwal Professor, M. Chaudhary Associate Professor, and J. Singh, "Waste Management Initiatives in India for Human Well Being," *Eur. Sci. Journal, ESJ*, vol. 7881, no. June, pp. 1857–7881, 2015, [Online]. Available: https://eujournal.org/index.php/esj/article/view/5715

[7] M. Kumar and V. Prakash, "A Review on Solid Waste: Its Impact on Air and Water Quality," *J. Pollut. Eff. Control*, vol. 8, no. 4, pp. 1–3, 2020, doi: 10.35248/2375-4397.20.8.252.Copyright.

[8] R. P. Singh, V. V. Tyagi, T. Allen, M. H. Ibrahim, and R. Kothari, "An overview for exploring the possibilities of energy generation from municipal solid waste (MSW) in Indian scenario," *Renew. Sustain. Energy Rev.*, vol. 15, no. 9, pp. 4797–4808, 2011, doi: 10.1016/j.rser.2011.07.071.

[9] L. Sun, W. Liu, M. Fujii, Z. Li, J. Ren, and Y. Dou, *An overview of waste-to-energy: feedstocks, technologies and implementations*. INC, 2020. doi: 10.1016/b978-0-12-816394-8.00001-x.

[10] D. R. Jones, "A fully general, exact algorithm for nesting irregular shapes," *J. Glob. Optim.*, vol. 59, no. 2–3, pp. 367–404, 2014, doi: 10.1007/s10898-013-0129-z.

[11] C. S. Psomopoulos, A. Bourka, and N. J. Themelis, "Waste-to-energy: A review of the status and benefits in USA," *Waste Manag.*, vol. 29, no. 5, pp. 1718–1724, 2009, doi: 10.1016/j.wasman.2008.11.020.

[12] J. Portugal-Pereira and L. Lee, "Economic and environmental benefits of waste-to-energy technologies for debris recovery in disaster-hit Northeast Japan," *J. Clean. Prod.*, vol. 112, no. May 2015, pp. 4419–4429, 2016, doi: 10.1016/j.jclepro.2015.05.083.

[13] M. A. Moktadir, T. Rahman, S. M. Ali, N. Nahar, and S. K. Paul, *Examining barriers to reverse logistics practices in the leather footwear industry*, vol. 293, no. 2. Springer US, 2020. doi: 10.1007/s10479-019-03449-y.

[14] C. García and M. A. Prieto, "Bacterial cellulose as a potential bioleather substitute for the footwear industry," *Microb. Biotechnol.*, vol. 12, no. 4, pp. 582–585, 2019, doi: 10.1111/1751-7915.13306.

[15] T. S. Preview, "INTERNATIONAL STANDARD ISO 2419 IULTCS / IUP 1 and iTeh STANDARD PREVIEW iTeh STANDARD PREVIEW," *Iultcs Iup 1/ Iup 3*, vol. 2012, 2012, [Online]. Available: https://standards.iteh.ai/catalog/standards/sist/b17c48ad-7582-49e7-854a-

23c9f344a3a0/iso-2419-2012

[16] F. Analysis, L. M. L. Nollet, N. York, and Y. Park, "Park , Y . W . 1996 . Determination of Moisture and Ash contents of Foods . Title : ( Determination of ) MOISTURE AND ASH CONTENTS OF FOODS Author : Affiliation : Young W . Park , Ph . D . Cooperative Agricultural Research Center Prairie View A & M Univer," no. January 1996, pp. 59–92, 2016.

[17] R.- Derived, "Test Procedures for the Determination of the Gross Calorific Value of Refuse and Conventional Bomb and Large Bomb Calorimetry".

[18] "Precise Measurement of Heat of Combustion With a Bomb Calorimeter".

[19] M. Dereje, M. Urge, G. Animut, and M. Y. Kurtu, "Effect of Dietary Supplementation on Physico-mechanical and Chemical Quality of Hide and Leather of Dromedary Camels," vol. 7522, no. Au 2006, pp. 18–24, 2015.

[20] J. Posom, A. Shrestha, W. Saechua, and P. Sirisomboon, "Rapid non-destructive evaluation of moisture content and higher heating value of Leucaena leucocephala pellets using near infrared spectroscopy," *Energy*, vol. 107, pp. 464–472, 2016, doi: 10.1016/j.energy.2016.04.041.

[21] T. Processes, "Determination of the Calorific Value of Refuse-Derived- Fuels by Large-Bomb Calorimetry Summary of the 1 978 Fiscal Year Results," no. 80, 1980.

[22] A. T. Submitted *et al.*, "PREDICTION OF CALORIFIC VALUE OF INDIAN COALS BY ARTIFICIAL NEURAL NETWORK PREDICTION OF CALORIFIC VALUE OF," 2015.

# FABRICATION & MECHANICAL CHARACTERIZATION OF JUTE, COIR AND BANANA FIBER-REINFORCED HYBRID EPOXY COMPOSITE

**Aquib Rahman*, Mahjabin Rahman, Shadman Sharar Alam, Zahid Hasan Shuvo, Mohammad Morshed, Md. Muntasir Arafat, Tanjil Hossain**
Department of Mechanical and Production Engineering (MPE)
Ahsanullah University of Science and Technology (AUST), Tejgaon Industrial Area, Bangladesh
*Corresponding Email: aquib.rahman.mpe@aust.edu

***Abstract:*** *Natural fibers reinforced epoxy hybrid composite has been the focus of numerous studies in recent years since it has proven to be useful in a variety of fields due to its eco-friendly nature. Jute, banana, and coir fibers have been used in this research to fabricate a hybrid composite reinforcing with epoxy resin. The fibers (jute: banana: coir = 1: 1: 1) are maintained at a fixed ratio during the manufacturing process of the composite. Five various fiber loading (0%, 5%, 10%, 15%, 20%) are considered for the investigation. The composites were manufactured using a hand lay-up technique. Mechanical properties were examined and evaluated in this investigation through various mechanical testing. Tensile, hardness, and flexural properties indicated a decreasing trend. On the other hand, the impact properties showed an increase where the maximum value for impact is found to be 0.163 J/mm for 20% fiber loading. Water absorption percentages climbed as fiber loading increased, with the greatest value recorded at 20% fiber loading. The analysis demonstrates the usefulness of hybrid green composites in a variety of engineering sectors, as well as possible future potential for making the composite more flexible and trustworthy.*

***Keywords:*** *Composite; Natural Fiber; Hybrid Composite; Epoxy; Mechanical Properties.*

## 1. INTRODUCTION

Jute fibers are a form of natural fiber that is easily obtainable, inexpensive and has excellent mechanical properties. Jute fibers are the current and potential raw material for polymer composites, that are used in a variety of sectors such as aerospace, vehicles, accessories, furniture, etc. (Singh et al., 2018). Due to insufficient fiber-matrix bonding, the mechanical properties of jute fiber-reinforced polymer composites increased up to a point and then declined. Chemical treatments of various kinds have indeed been employed to enhance the mechanical properties of jute fiber-reinforced polymer composites, with promising findings like excellent mechanical properties (Gupta et al., 2015). Banana fiber-reinforced composites are environmentally sustainable and can be used to replace toxic plastics in passenger car interiors, decorative components, and furniture uses. The tensile and flexural properties of the banana fiber composite can be raised to great strength by the alkali treatment (Sollapur et al., 2017). The mechanical properties of banana fiber-based epoxy composites are seriously influenced by the hand lay-up process, such as hardness, tensile strength, flexural strength, and impact strength (A REVIEW ON MECHANICAL PERFORMANCE OF BANANA FIBER, 2020). Coir fiber-reinforced polymer composites have already proven their worth as weight-saving materials. Coir fiber is used in a variety of applications, including aerospace, shipping, and decoration sectors. Appropriate surface treatment, reduction of dependency of properties on the volume percentages of fibers, and the quality at the fiber-matrix interface can be improved the composite to a great extent (Bongarde & Khot, 2019). In terms of mechanical characteristics, treated coir fiber composites outperform untreated ones (Yan et al., 2016). Epoxy resins have a varied range of applications including adhesives, automotive, electronic components, and tissue engineering. The nature of epoxy resin, hardener, and curing method used to determine the properties of treated epoxy resins (Jin et al., 2015). When the epoxy resin is reinforced with natural fibers, a tremendous increase in mechanical properties was found in the hybrid composite (Jeyapragash et al., 2019). It can be concluded that by combining jute, banana, and coir fibers with epoxy resin, a natural fiber-reinforced composite can be produced that contributes a high level of strength to the mechanical properties of the composite.

In this research, we have set some objectives that are based on the recent study of hybrid green composites. Our objectives are:

- Fabrication of a hybrid epoxy resin composite with jute, banana, and coir short fiber reinforcement.
- Characterization of mechanical properties such as tensile properties, flexural properties, impact strength, and hardness of the fabricated hybrid composite according to different fiber loading percentages (5%, 10%, 15%, 20%).
- Investigate the biodegradable nature of water absorption of the hybrid reinforced composite.

## 2. LITERATURE REVIEW

Polymer matrix composites made of thermoset polymers such as polyester, vinyl ester, and epoxy can be used in a variety of industrial purposes. According to the researchers, the tensile strength of the polymer composite was increased by 10% by weight when micronized rubber powder was introduced as a filler. If the filler content increases, so does the composite's hardness value (Nagaraja et al., 2020).

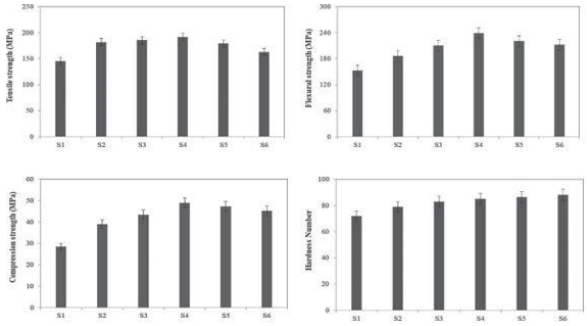

**Fig.-1:** Mechanical properties of polymer-matrix composites (Nagaraja et al., 2020)

Natural fibers are used extensively in aircraft applications, accounting for around 21% of all fibers used by the aircraft industry and 19% of all fibers used by the automotive industry (Shireesha & Nandipati, 2019).

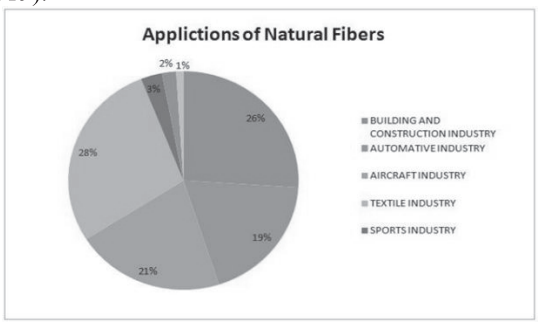


**Fig.-2:** Application of natural fibers (Shireesha & Nandipati, 2019)

**Table 1:** Chemical composition of natural fibers (Kiruthika, 2017) (Ahmad et al., 2014) (Saba et al., 2016)

| Fiber-type | Cellulose [%] | Lignin [%] | Hemicellulose [%] | Pectin [%] | Wax [%] | Ash [%] | Microfibrillar angle [°] |
|---|---|---|---|---|---|---|---|
| Banana | 63–83 | 5 | - | – | 11 | – | 11–12 |
| Coir | 36–43 | 0.15–0.25 | 41–45 | 3–4 | – | – | 30–49 |
| Jute | 61–72 | 12–13 | 18–22 | 0.2 | 0.5 | 0.5–2 | 8 |

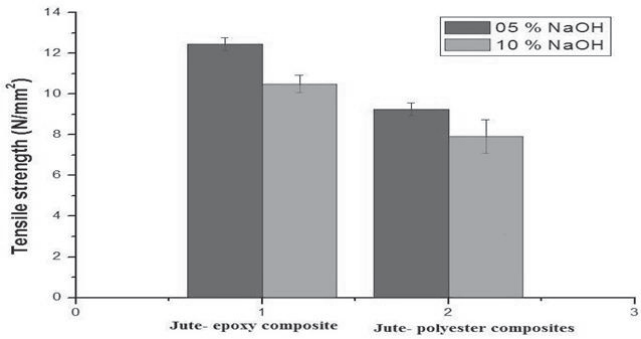


**Fig.-3:** Tensile strength difference in jute reinforced composites treated with 5% and 10% NaOH (Gopinath et al., 2014)

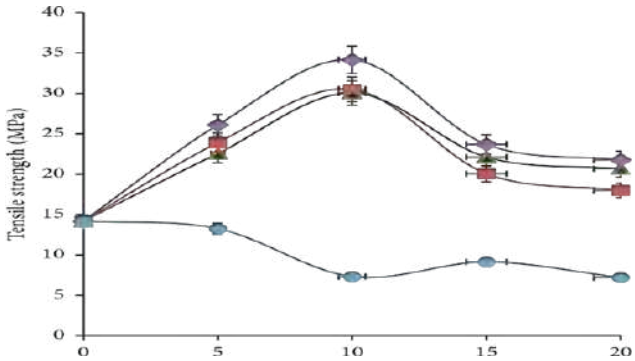


**Fig.-4:** Tensile strength of composite at various fiber loading (Liew et al., 2017)

(Wang et al., 2019) demonstrated that the tensile strength of treated jute fiber composites was discovered to be larger than that of their raw jute fiber counterparts. As treated jute composites have a reduced void fraction and higher volume percentages, they have a higher tensile strength. (Premnath, 2019) observed that tensile strength was higher after the surface treatment is done in case of jute fiber reinforced hybrid composite.

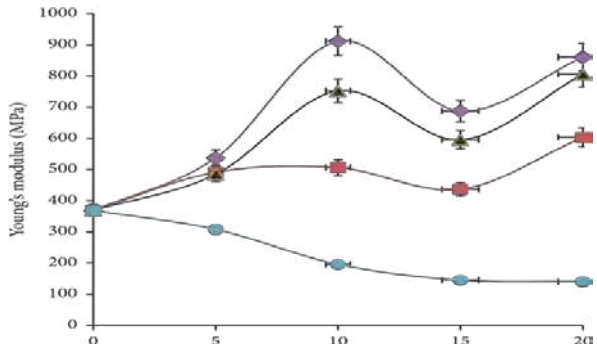


**Fig.-5:** Young's modulus of composite at various fiber loading (Liew et al., 2017)

(Liew et al., 2017) observed that water absorption was substantially lower for all treated cellulose hybrid composites, as compared to untreated hybrid fiber composites.

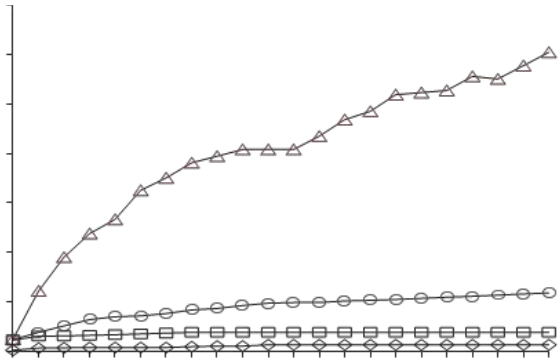

**Fig.-6:** Water absorption rate for 10% fiber loading (Liew et al., 2017)

Banana fiber is currently a byproduct of banana farming, so it can be harvested for industrial purposes at no additional cost (Ramesh et al., 2014) examined that when different percentages of banana fiber and epoxy resin fiber loading were used to determine the tensile strength, the maximum value of tensile strength was reported for 50% banana fiber and 50% epoxy resin. (Bujjibabu et al., 2018) evaluated that the highest tensile strength was found at 15% banana and 5% coir fiber loading.

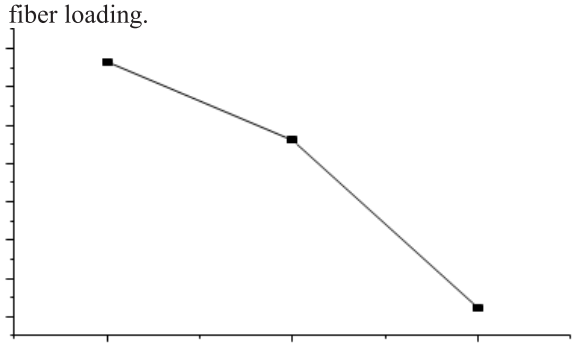

**Fig.-7:** Weight fraction effect on tensile strength variations for banana reinforced composite (Bujjibabu et al., 2018)

(Zhihui Sun et al., 2017) observed that treated coir fiber reinforced composite has a higher tensile modulus compared to the untreated at the same fiber content. Alkali treatment facilitated sufficient stability and permeability between fiber and matrix by removing pectin and lignin from treated coir fiber. (Ac Ce Us Pt, 2018) reported that the tensile strength and modulus of coir and pineapple leaf fiber reinforced composite was massively enhanced when the volume fraction of both the fibers were 50%. (Nagarjun et al., 2020) examined that the tensile properties shown higher in case of coir reinforced hybrid composites compared to the single coir fiber composite. (Sumesh & Kanthavel, 2020) demonstrated that when coir and sisal hybridized as a composite, the tensile properties were increased at 10 wt.% coir fiber loading to 15%.

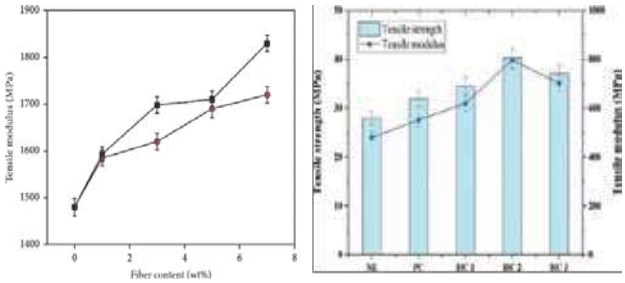


**Fig.-8:** Tensile modulus and tensile strength of coir reinforced hybrid composite (Zhihui Sun et al., 2017) (Nagarjun et al., 2020)

## 3. METHODOLOGY

### 3.1. Materials

The jute, banana, and coir fibers are fabricated in this experiment to form the hybrid composite. The matrix is made of epoxy resin and hardener. The following are three different types of natural fibers that were used: (i) Jute fiber (JF), (ii) Banana fiber (BF), and (iii) Coir fiber (CF). Epoxy resin is used as a matrix material with the hardener.

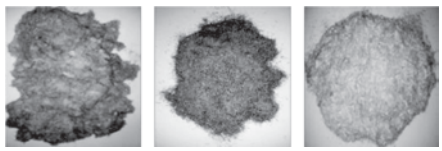

**Fig.-9:** From left Jute Fiber, Coir Fiber & Banana Fiber.

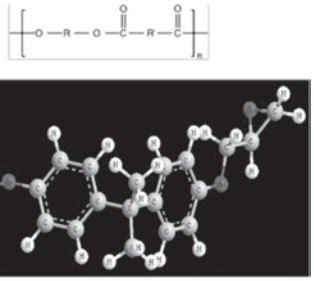

**Fig.-10:** Chemical structure of epoxy resin (Pilato, 2010) (Sathishkumar et al., 2020).

### 3.2. Extraction of Jute Fiber

Fiber extracted from the jute plant is a potential element with a bright future in the composites industry (Indran et al., 2018) (Sajin et al., 2020). Jute takes approximately three months to reach a height of 12–15 feet during the growing season before being harvested, packaged, and soaked for the retting process, which involves separating the inner stem and outer plant and tailoring the outer plant to make a fiber (Ramesh et al., 2014). The stems must be excoriated after harvesting to obtain the fibers. Due to the hot temperature in the locality, this is done by macerating the stems in the river for around 8–10 days, which allows easier decomposition of the stems and subsequent fiber extraction. The fibers are then dried in the sun without chemical additives beneath covers and folded into bundles (Alves et al., 2010).

### 3.3. Extraction of Banana Fiber

Banana fiber belongs Musaceae family of natural fiber that is derived from the pseudo stem of the banana tree. This fiber retains a lot of water and is strong in nutrients (Pandya & Rathod, 2019). During the extraction procedure, the tapering top and broad bottom ends of the pseudostem are removed, and the cylindrical component of the stem is used to extract the fiber. The sheaths are extracted layer by layer from the pseudostem after it has been divided in half. A knife was used to remove the thin sheath margins. Three-quarters of the sheath is then fed into the raspador machine and carefully drawn back. After that, another section has been fed, and the fiber is extracted. The extracted fibers are allowed to dry in the sunlight for 2–3 hrs (Paramasivam et al., 2020).

### 3.4. Extraction of Coir Fiber

Huge quantities of various wastes, including coir shells, are generated during the manufacturing of coconut fruits. Coir fibers can be recovered from these shells, leaving coir shell particles that can be utilized in polymer reinforcements, in addition to the usual usage of coir wastes in heat treatment (Essabir et al., 2016). Before being used in polymer reinforcement, coir fibers can be pulverized and ground into particles, then sliced into various sizes (Essabir et al., 2016) (Morandim-Giannetti et al., 2012). The water retting method can also be used to remove coir fibers from coconut husks (Verma & Gope, 2015) (Deyholos & Potter, 2014) (Sisti et al., 2018). Husks are softened and can be decorticated during the retting process. The fiber is extracted by battering, which is generally done by hand. The fibers are loosened and cleansed after hackling, rinsing, and curing. The extra stem has subsequently pioneered a suitable marketplace as a peat moss substitute in the agricultural sector (Verma & Gope, 2015). Locally produced coconut husks from a nearby farm can also be applied in the pilot plant for pure coir fiber extraction. The coconut husks are stored in tanks loaded with oxygen-free water that is passed through an anaerobic reactor in this process of fiber extraction. The husks are retrieved after just a month of operation and mechanically pounded to extract the fiber from the residuals. The fibers are then allowed to dry (Manilal et al., 2010).

### 3.5. Preparation of Epoxy-Hardener & Fibers Mixture

Fabrication of hybrid composite is mainly done according to different fiber loading percentages (5%, 10%, 15%, 20%). Epoxy and hardener are used in a 10:1 ratio for each sample (For every 10 gm of epoxy 1 gm of hardener is added). Jute, banana, and coir fibers are used in a 1:1:1 proportion. Despite the same ratio, there is variation in each amount of the fibers. It's because the jute, banana, and coir fibers have various densities (1.45gm/cc, 1.25gm/cc, and 1.3gm/cc, respectively).

### 3.6. Fabrication Procedure

A simple hand lay-up technique has been applied. The easiest solution of fabrication process is the hand lay-up technique. This approach has a minimal initial requirement as well. The processes involved in the procedure are straightforward (Abdurohman et al., 2018). Mainly, stacking sequence of different single of fibers is used with the hand lay- up technique. A few years ago, in a study, it was proved that a stacking up different types of single fiber composites produce better results than any particular type of single fiber composite (Potluri et al., 2017). At first, the mold is prepared with a dimension of (30.5mm * 30.5mm * 2.5mm). Thin plastic sheets are initially placed at the top and bottom of the mold surface to produce an outstanding smooth surface (Yogeshwaran et al., 2020). A releasing agent called silicon spray is sprayed on the mold surface to make it easier to remove the composite from the mold after it has cured (Boopalan et al., 2013).

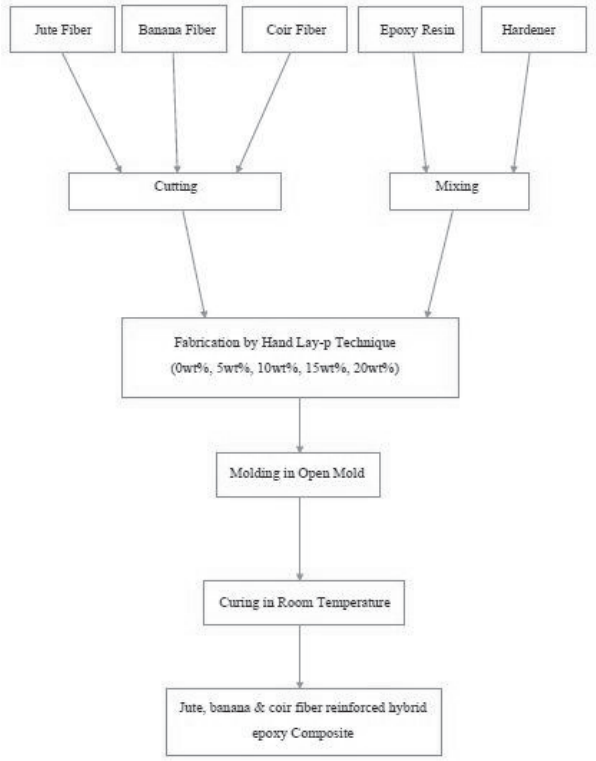


**Fig.-11:** Composite Fabrication Process

The first layer is then formed by putting the matrix into the mold, which has been combined with a certain wt.% hardener. Then, on top of the matrix layer, 3-5 mm of short jute, banana, and coir fibers are randomly combined as a second layer. With the help of a brush, epoxy is then uniformly spread over the prepared mixture once again as a third layer. To take away any air bubbles as well as any overabundance epoxy, a roller is used with light pressure on the composite mixture. Each sample of the composite is fabricated using the same procedure. Special care is maintained to obtain a consistent sample as particles have a proclivity to agglomerate and mess together when melded. A wood cover is placed over the mold, which is also wrapped in plastic sheet, and each cast of the composite is treated for 5-6 hours under a load of about 2.5 kg before being removed from the mold. Following the removal of the cast from the mold, it has been post-cured in the air for another 4-5 hours. For mechanical characterization, acceptable specimens are cut using an angle grinder cutter machine from the samples (Boopalan et al., 2013).

## 4. EVALUATION OF PROPERTIES

### 4.1. Fiber Volume Fraction Calculation

Density of Jute Fiber, $\rho_j$ =1.45 gm/cm$^3$
Density of Banana Fiber, $\rho_b$ =1.35 gm/ cm$^3$
Density of Coir Fiber, $\rho_{co}$ =1.30 gm/ cm$^3$

**For 0% of Fiber Loading:**

Dimension of the die = Dimension of the Composite
= (30.5 × 30.5 × 0.4) cm3 = 372.1 cm$^3$
Total volume of the Epoxy matrix, $V_m$ = 372.1 cm$^3$

**For 5% of Fiber Loading:**

Dimension of the die = Dimension of the Composite
= (30.5 × 30.5 × 0.4) cm3 = 372.1 cm$^3$
Mass of Jute Fiber, $M_j$ = 9.0 gm
Mass of Banana Fiber, $M_b$ = 8.7 gm
Mass of Coir Fiber, $M_{co}$ = 8.0 gm
Volume of Jute Fiber, $V_j = \frac{9.0}{1.45}$ cm$^3$ = 6.2 cm$^3$
Volume of Banana Fiber, $V_b = \frac{8.7}{1.35}$ cm$^3$ = 6.2 cm$^3$
Volume of Coir Fiber, $V_{co} = \frac{8.0}{1.30}$ cm$^3$ = 6.2 cm$^3$
Total Volume of fiber, $V_f = V_j + V_b + V_{co}$ = (6.2 + 6.2 + 6.2) = 18.6 cm$^3$
So, Volume fraction of Fiber = $\frac{V_f}{V_c} = \frac{18.6}{372.1} \approx 0.050 \approx$ 5.0%
Therefore, Volume fraction of Epoxy matrix, $V_m$ = (100−5.0) = 95.0%

**For 10% of Fiber Loading:**

Dimension of the die = Dimension of the Composite
= (30.5 × 30.5 × 0.4) cm3 = 372.1 cm$^3$
Mass of Jute Fiber, $M_j$ = 18.0 gm
Mass of Banana Fiber, $M_b$ = 16.7 gm
Mass of Coir Fiber, $M_{co}$ = 16.1 gm
Volume of Jute Fiber, $V_j = \frac{18.0}{1.45}$ cm$^3$ = 12.4 cm$^3$
Volume of Banana Fiber, $V_b = \frac{16.7}{1.35}$ cm$^3$ = 12.4 cm$^3$
Volume of Coir Fiber, $V_{co} = \frac{16.1}{1.30}$ cm$^3$ = 12.4 cm$^3$
Total Volume of fiber, $V_f = V_j + V_b + V_{co}$ = (12.4 + 12.4 + 12.4) = 37.2 cm$^3$
So, Volume fraction of Fiber = $\frac{V_f}{V_c} = \frac{37.2}{372.1} \approx 0.10 \approx$ 10.0%
Therefore, Volume fraction of Epoxy matrix, $V_m$ = (100−10.0) = 90.0%

**For 15% of Fiber Loading:**

Dimension of the die = Dimension of the Composite
= (30.5 × 30.5 × 0.4) cm3 = 372.1 cm$^3$
Mass of Jute Fiber, $M_j$ = 27.0 gm
Mass of Banana Fiber, $M_b$ = 25.1 gm
Mass of Coir Fiber, $M_{co}$ = 24.1 gm
Volume of Jute Fiber, $V_j = \frac{27.0}{1.45}$ cm$^3$ = 18.6 cm$^3$
Volume of Banana Fiber, $V_b = \frac{25.1}{1.35}$ cm$^3$ = 18.6 cm$^3$
Volume of Coir Fiber, $V_{co} = \frac{24.1}{1.30}$ cm$^3$ = 18.6 cm$^3$
Total Volume of fiber, $V_f = V_j + V_b + V_{co}$ = (18.6 + 18.6 + 18.6) = 55.8 cm$^3$
So, Volume fraction of Fiber = $\frac{V_f}{V_c} = \frac{55.8}{372.1} \approx 0.15 \approx$ 15.0%

Therefore, Volume fraction of Epoxy matrix, $V_m$ = (100−15.0) = 85.0%

**For 20% of Fiber Loading:**

Dimension of the die = Dimension of the Composite = (30.5 × 30.5 × 0.4) cm3 = 372.1 $cm^3$

Mass of Jute Fiber, $M_j$ = 36.0 gm

Mass of Banana Fiber, $M_b$ = 33.5 gm

Mass of Coir Fiber, $M_{co}$ = 32.3 gm

Volume of Jute Fiber, $V_j = \frac{36.0}{1.45}$ $cm^3$ = 24.8 $cm^3$

Volume of Banana Fiber, $V_b = \frac{33.5}{1.35}$ $cm^3$ = 24.8 $cm^3$

Volume of Coir Fiber, $V_{co} = \frac{32.3}{1.30}$ $cm^3$ = 24.8 $cm^3$

Total Volume of fiber, $V_f = V_j + V_b + V_{co}$ = (24.8 + 24.8 + 24.8) = 74.4 $cm^3$

So, Volume fraction of Fiber = $\frac{V_f}{V_c} = \frac{74.4}{372.1} \approx 0.20 \approx$ 20.0%

Therefore, Volume fraction of Epoxy matrix, $V_m$ = (100−20.0) = 80.0%

### 4.2. Mechanical Characterization of Composites

#### 4.2.1 Tensile Test

Five separate specimens are taken for testing, each with a distinct weight ratio. A hand cutter is used to cut the specimens to the desired dimensions, and the surfaces are shined with salt paper. They've been created in compliance with ASTM D638-14 standard.

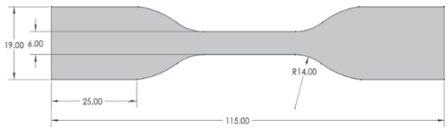


**Fig.-12:** Tensile Test Specimen

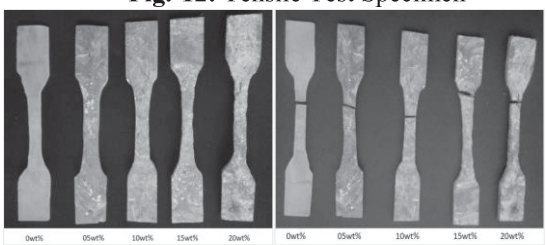


**Fig.-13:** Tensile Test Specimens: Before Test and After Test

The ASTM D638- 14 standard guides the selection of dimensions, gauge length, and cross head speeds. The tensile test is carried out using the Universal Testing Machine (Ramesh et al., 2014). During the experiment, the load has been gradually applied to the specimen with a traveling crosshead until it is being fractured. The load strength is determined by the load measurement instrument. An extensometer is also used to measure the strain (Yogeshwaran et al., 2020).

#### 4.2.2 Flexural Test

Flexural test has been done on the five different specimens. The stiffness of a material when inclination occurs is reflected by the ratio of stress to strain in flexural distortion, or the propensity for a substance to stretch (Rachchh & Trivedi, 2018) (Pandya & Rathod, 2019). A three-point bending test on a flexural testing machine is used to calculate the flexural characteristics. The dimension of the specimen is 128 * 16* 4 mm and the ASTM D790 standard is followed in this purpose.


**Fig.-14:** Flexural Test Specimen

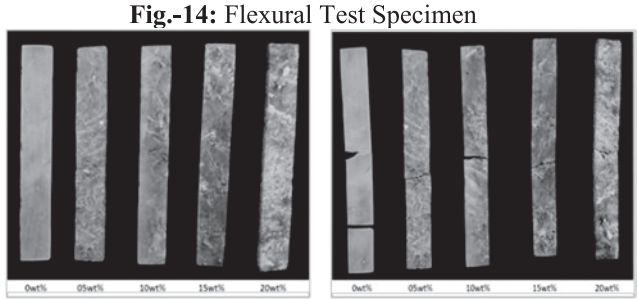


**Fig.-15:** Flexural Test Specimens: Before Test and After Test

The following formula is used to calculate flexural strength:

Flexural Strength = M/Z = 3WL / $2bd^2$ (Premnath, 2019)

Here,

W = flexural load

L = length of the support span

B = width of specimen

D = depth of specimen

#### 4.2.3 Impact Test

Following the ASTM 4812 standard, five impact test specimens are built according to the appropriate dimension. The dimension of the specimen is 64 * 12.7 * 4mm. The specimen should be inserted into the testing equipment, which then enables the pendulum to swing before it cracks or splits. The Izod impact testing machine is used to assess the impact strength of the specimens. During the test, the highest amount of energy that can be stored to shatter the specimen is recorded for the whole specimen so that the data may be analyzed (Ramesh et al., 2014) (Pandya & Rathod, 2019).

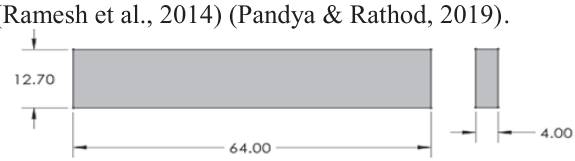


**Fig.-16:** Impact Test Specimen

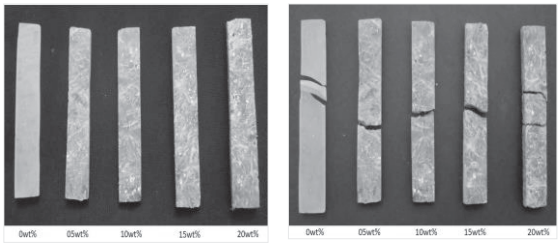


**Fig.-17:** Impact Test Specimens: Before Test and After Test

#### 4.2.4 Hardness Test

The hardness test has been done by portable leeb hardness tester. The dimension of the specimen is 15 * 15 * 4mm. A spring-loaded impact mechanism propels an impact item in the Leeb hardness test. There are three phases to the velocity of the impact item. During the approach phase, the spring force accelerates the impact object towards to the test surface. During the impact phase, the impact object and the specimen are in close proximity. The specimen becomes dynamically and plastically twisted as a result, and the impact object comes to a halt. The impact object recovers due to the elastic spring-back of the impact object and specimen. The impact object is propelled out of the impact phase with the residual energy during the rebound phase.

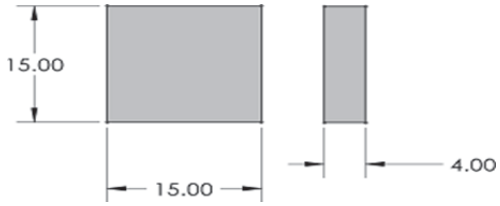


**Fig.-17:** Hardness Test Specimen

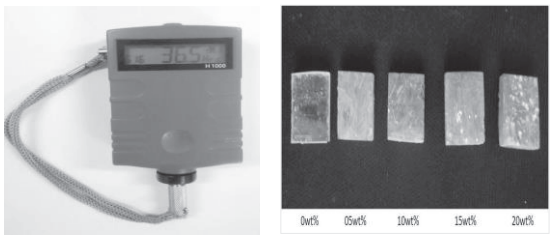


**Fig.-18:** Leeb Hardness Tester & Hardness test specimens

### 4.3. Characterization of Physical Property

#### 4.3.1 Water Absorption Test

Five specimens have been taken to measure the percentages of the water absorption. The dimension of the specimen is 15 × 15 × 4mm. The experiment is carried out in accordance with ASTM D 570-98. The specimens are initially weighted without being bathed in clean water at room temperature for varying amounts of time. The specimens are separated from the water after 24 hours and then all surface water has been cleaned with a washcloth before the specimens are reweighted. The specimens are immersed for 28 days and the percentages of water absorption are measured on a daily basis per day interval (Huzaifah et al., 2019) (Munshi et al., 2020).

$$\% \text{ Water absorption} = [(\text{weight wet} - \text{weight dry})/\text{weight dry}] \times 100$$

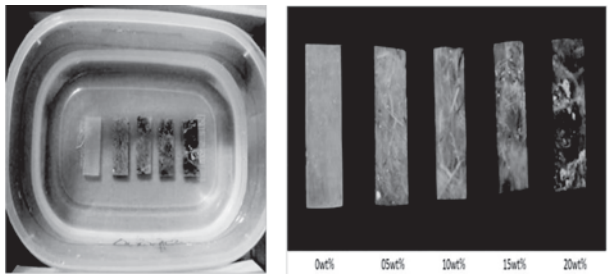


**Fig.-19:** Water Absorption Test

## 5. RESULTS ANALYSIS AND DISCUSSION

### 5.1. Tensile Properties

In this section, tensile properties of jute-banana-coir fiber reinforced epoxy hybrid composite containing the fiber loading of 0wt%, 05wt%, 10wt%, 15%wt and 20wt% has been analyzed.

From the figure 20 & 21, it can be said that the tensile strength and tensile modulus are reduced from 0wt% percent to 05wt%, then a higher value is abruptly displayed in 10wt%, and then the value is reduced from 15wt% to 20wt %. So, it can be concluded that, the tensile strength and the tensile modulus are followed a decreasing trend except the 10wt% fiber loading. The most significant factor affecting the tensile characteristics of natural fiber composites is the interfacial bonding between the resin and the fibers (Mathur, 2021) (Ku et al., 2011). The fiber volume fraction in the resin matrix has a significant impact on the tensile characteristics of natural fiber composites. Many researchers observed that, as the fiber volume fraction falls below an optimum level, the load is dispersed over a larger number of fibers, and the matrix may sustain the applied stress after the fibers rupture. This may result in a composite with a higher tensile strength (Ku et al., 2011). That's the reason, we have seen in case of 5wt% to 10wt% fiber loading. After the optimum amount of fiber volume fraction, brittle fracture develops in the fibers, and the matrix is unable to support the increased load from the fibers. Under these conditions, the lower tensile strength of the composite eventually ends to the fractures (Gholampour, 2019). The trend shows in case of 15wt% to 20% fiber loading in this experiment. When the fiber volume fraction of banana-coir reinforced is increased after an optimum percentage, tensile strength and modulus are also reduced (Bujjibabu et al., 2018). In a study, it has been observed that when jute and banana fiber are reinforced with the epoxy, the tensile modulus shows a great deceased compared to the coir reinforced

epoxy composite (Khan et al., 2018). Due to a lack of epoxy resin matrix, the tensile properties are also degraded. Several causes may generate inconsistent and erratic tensile property tendencies, such fiber- matrix incompatibilities, fiber deterioration, and improper production procedures (Ku et al., 2011).

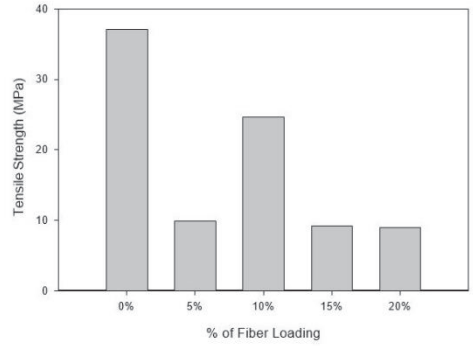


**Fig.-20:** Variation of tensile strength with different fiber loadings

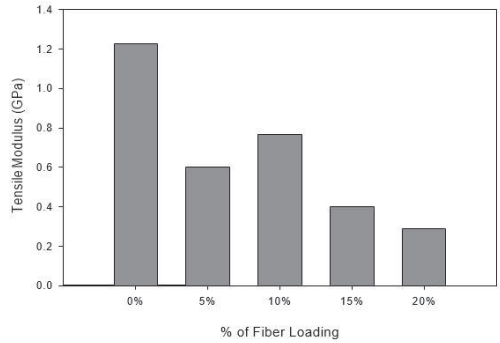


**Fig.-21:** Variation of tensile modulus with different fiber loadings

**Elongation Percentage at break:**

Elongation percentage at break is also calculated for manufactured composites. From the figure 22, it can be seen that when the fiber loading is increased, the elongation percentage at break decrease in a great extent. This may occur as a result of fiber dispersal in the matrix. The composite is more solid in the end as its interaction between fiber and matrix is much greater and tougher. It has increased matrix rigidity and reduced matrix deformation. It has resulted in the composites' flexibility being reduced (Barkoula et al., 2008) (Munshi et al., 2020) (Premalal et al., 2002) (Haque et al., 2021).

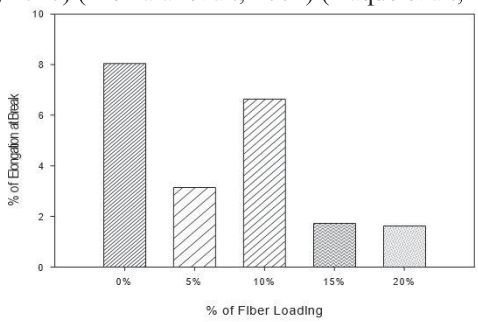


**Fig.-22:** Variation of elongation percentage at with different fiber loadings

**5.2. Flexural Properties**

From the figure 23 & 24, it has been observed that the flexural strength and flexural modulus decrease from 0wt% to 05wt% and 15%wt to 20%wt, a higher value is attained at 10wt% that is similar to the tensile properties pattern. Almost, the flexural properties are followed the decreasing pattern except the 10wt%. It seems to be possible that poor surface adherence between fibers and matrix, as well as the existence of bubbles during the fabrication process, must be responsible for the decreased result (Huzaifah et al., 2019). One of the most essential parameters for identifying a composite's resistance to bending distortion is its flexural stiffness.

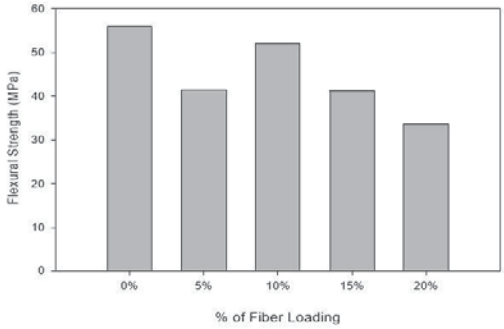


**Fig.-23:** Variation of flexural strength at with different fiber loadings

In an experiment, it has been examined that after reaching an optimum level of fiber concentration, subsequent increases in fiber content lower the flexural strength, due to flaws in fiber wetting that can cause stress concentration areas in the composites (Faruk et al., 2012) (Gholampour, 2019). At 10wt% loading, the tensile strength is suddenly increased because of the due to well impregnation of epoxy in to the natural fibers. On the other hand, the matrix couldn't bind well the higher fiber completely. As a result, a massive decline is case of 0wt% to 10wt% and 15wt% to 20wt% fiber loading gradually (Chai Hua & Norkhairunnisa, 2017) (Nor et al., 2018).

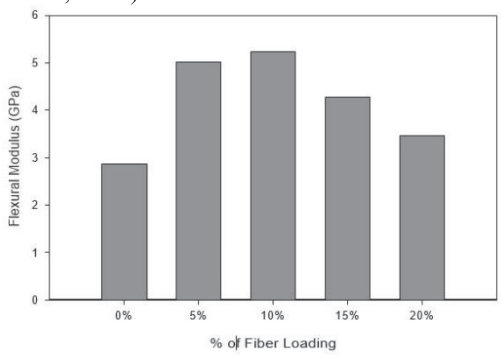


**Fig.-24:** Variation of flexural modulus at with different fiber loadings

**5.3. Impact strength**

The impact strength of composites comprising 0wt%, 5wt%, 10wt%, 15wt%, and 20wt% is investigated. From the figure 25, it has been found that with the increase of fiber loading, the impact strength is also increased in case of 0wt% to 5wt% and 15wt% to 20wt% fiber loading, but a sudden decrease shown in 10wt% fiber content. So, it can be said that, an increasing pattern is followed by the impact specimens.

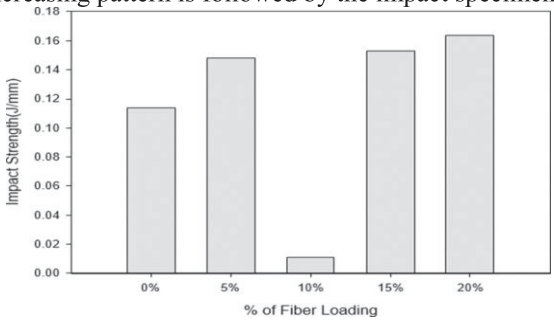


**Fig.-25:** Variation of impact strength at with different fiber loadings

The impact strength of natural fiber reinforced polymer composites is heavily reliant on fiber-matrix adhesion as well as the composition of the fiber and polymer matrix (Mir et al., 2013). Due to the extreme high interfacial interaction between fibers and matrix, impact strength is gradually increased. Fiber pull out might cause impact fracture of a composite. Pulling out fibers needs more force as fiber loading increases, resulting in higher impact strength (Siddika et al., 2014). In case of 10wt% fiber content, the interaction between the fibers and the matrix becomes considerably harder and stronger, resulting in a more stiff composite. Thus, the dynamism of the matrix material is hampered and the impact strength is greatly reduced. However, minor flaws in specimen machining, as well as in the testing apparatus, can be another reason of decreased result (Premalal et al., 2002) (Munshi et al., 2020) (Ismail et al., 2019).

### 5.4. Hardness

The hardness properties of the composite containing 0wt%, 5wt%, 10wt%, 15wt% and 20wt% are also measured. From the figure 26, it can be seen that, the hardness decreases from 0wt% to 05wt% and 15wt% to 20wt% fiber loading, but sudden increase is observed in 10wt% fiber content.

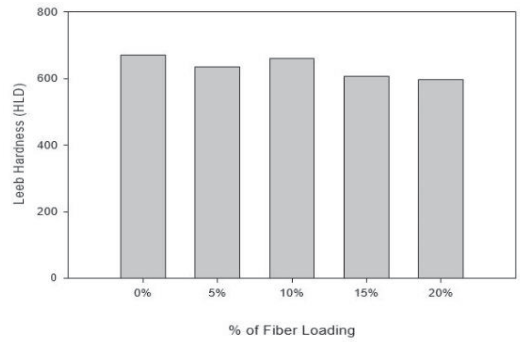


**Fig.-26:** Variation of hardness at with different fiber loadings

It can be said that, hardness is followed a decreasing pattern. As the elongation percentage increased with the increment of the fiber loading, the hardness of the composite also decreased in a great extent. The incorporation of a more pliable matrix typically results in composites with a lower hardness. The epoxy matrix reinforced composite shows a more ductile nature in this experiment. But, in case of 10wt%, the adhesion between the matrix and fibers becomes solid. That's why, the composite is showed a brittle nature and the hardness was maximum in that case (Siddika et al., 2014) (Munshi et al., 2020).

### 5.5. Water Absorption

For each fiber loading, an average value of water absorption was calculated for the five specimens. From the figure 27, it has observed that the rate of water absorption is continuously increased for 0wt% to 20wt% fiber loading. The polar hydroxyl group in the fibre molecular structure increases as the fibre content in the composites increases, allowing it to establish hydrogen bonds with water molecules. The creation of hydrogen bonds will increase the likelihood of water being consumed as a result of this event. Usually, the inclusion of cellulose, hemicelluloses, and lignin in natural fiber causes it to absorb water. Attributed to the prevalence of voids, natural fiber reinforced polymer composites that have not been chemically treated typically have a higher water absorption rate. However, in the case of 10wt % fiber loading, an unusual pattern emerges. It could be due to a lack of fibers and matrix in the composites (Muñoz-Vélez et al., 2018) (Barkoula et al., 2008) (Mir et al., 2013) (Munshi et al., 2020) (Huzaifah et al., 2019).

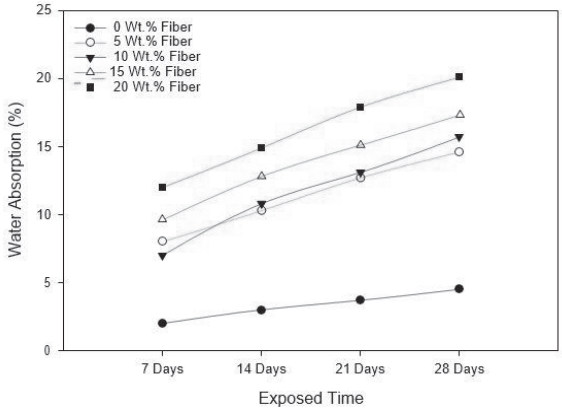


**Fig.-27:** Variation of Water Absorption (%) at Different Fiber Loading with respect to Exposed Days

## 6. CONCLUSION

In this study, mechanical characterization of jute-banana-coir fiber reinforced epoxy matrix at various

fiber loading (0wt%, 5wt%, 10wt%, 15wt% and 20wt%) through hand-lay-up technique has been investigated. Based on the experimental result and evaluation, the following conclusion has been provided.

(1). Tensile properties are decreased with the increase of the fiber loading. Highest tensile strength and modulus values are observed to be 24.69 MPa and 0.769 GPa for 10% fiber loading. The highest value of the elongation percentage at break is 6.64%.

(2). Flexural properties are also followed the same trend as tensile properties. The highest value of the flexural strength and modulus are obtained to be 52.2 MPa and 5.238 GPa for 10% fiber loading.

(3). Impact strength properties are increased with the increase of fiber loading. The highest value is found to be 0.163 J/mm for 20% fiber loading.

(4). The Hardness is decreased with increment of fiber loading. The highest value is obtained to be 662 for 10% fiber loading.

(5). The water absorption rate is increased with the increment of fiber loading. The highest value is obtained at 20% fiber loading.

**ACKNOWLEDGEMENT**

The authors would like to acknowledge the Department of Mechanical and Production Engineering, Ahsanullah University of Science and Technology (AUST), for its helpful recommendations.

**LIST OF ABBREVIATIONS**

| | |
|---|---|
| ASTM | American Society of Test and Materials |
| NFRPC | Natural Fibers Reinforced Polymer Composite |
| SFRPC | Synthetic Fibers Reinforced Polymer Composite |
| JF | Jute Fiber |
| BF | Banana Fiber |
| CF | Coir Fiber |

**LIST OF NOTATIONS**

| | |
|---|---|
| W | Flexural Load |
| L | Length of the Support Span |
| B | Width of Specimen |
| D | Depth of Specimen |
| % | Percentage |

**GREEK SYSMBOLS**

| | |
|---|---|
| ρ | Density of the fiber |

**REFERENCES**

1. Singh, H., Inder, J., Singh, P., Singh, S., Dhawan, V., & Tiwari, S. K. (2018). ScienceDirect. Materials Today: Proceedings, 5(14), 28427–28437.
2. Gupta, M. K., Srivastava, R. K., & Bisaria, H. (2015). Potential of Jute Fibre Reinforced Polymer Composites : A review ISSN 2277-7156 Review Article Potential of Jute Fibre Reinforced Polymer Composites : A Review. September.
3. Sollapur, S., Technical, S., & Society, E. (2017). Review on Mechanical Properties of Banana Fiber. October.
4. A REVIEW ON MECHANICAL PERFORMANCE OF BANANA FIBER. (2020). 4(12), 112– 114.
5. Bongarde, U. S., & Khot, B. K. (2019). A Review on Coir Fiber Reinforced Polymer Composite. 793–795.
6. Yan, L., Chouw, N., Huang, L., & Kasal, B. (2016). Effect of alkali treatment on microstructure and mechanical properties of coir fibres , coir fibre reinforced-polymer composites and reinforced-cementitious composites. CONSTRUCTION & BUILDING MATERIALS, 112, 168–182. https://doi.org/10.1016/j.conbuildmat.2016.02.182
7. Jin, F., Li, X., & Park, S. (2015). Journal of Industrial and Engineering Chemistry Synthesis and application of epoxy resins : A review. Journal of Industrial and Engineering Chemistry, 29, 1–11. https://doi.org/10.1016/j.jiec.2015.03.026
8. Jeyapragash, R., Srinivasan, V., & Sathiyamurthy, S. (2019). Materials Today : Proceedings Mechanical properties of natural fiber / particulate reinforced epoxy composites – A review of the literature. Materials Today: Proceedings, xxxx. https://doi.org/10.1016/j.matpr.2019.12.146
9. Nagaraja, K. C., Rajanna, S., Prakash, G. S., & Rajeshkumar, G. (2020). Materials Today : Proceedings Mechanical properties of polymer matrix composites : Effect of hybridization. Materials Today: Proceedings, xxxx, 2019–2021. https://doi.org/10.1016/j.matpr.2020.03.108
10. Shireesha, Y., & Nandipati, G. (2019). State of art review on natural fibers. Materials Today: Proceedings, 18, 15–240. https://doi.org/10.1016/j.matpr.2019.06.272
11. Kiruthika, A. V. (2017). A review on physico-mechanical properties of bast fi bre reinforced polymer composites. Journal of Building Engineering, 9(December 2016), 91–99. https://doi.org/10.1016/j.jobe.2016.12.003
12. Ahmad, F., Choi, H. S., & Park, M. K. (2014). A Review : Natural Fiber Composites Selection in View of Mechanical , Light Weight , and Economic Properties. 1–15. https://doi.org/10.1002/mame.201400089
13. Saba, N., Paridah, M. T., Abdan, K., & Ibrahim, N. A. (2016). Dynamic mechanical properties of oil palm nano filler / kenaf / epoxy hybrid nanocomposites. Construction and Building

Materials, 124, 133–138. https://doi.org/10.1016/j.conbuildmat.2016.07.059

14. Gopinath, A., Senthil Kumar, M., & Elayaperumal, A. (2014). Experimental investigations on mechanical properties of jute fiber reinforced composites with polyester and epoxy resin matrices. Procedia Engineering, 97, 2052–2063. https://doi.org/10.1016/j.proeng.2014.12.448
15. Liew, F. K., Hamdan, S., Rahman, M. R., & Rusop, M. (2017). Thermomechanical Properties of Jute/Bamboo Cellulose Composite and Its Hybrid Composites: The Effects of Treatment and Fiber Loading. Advances in Materials Science and Engineering, 2017. https://doi.org/10.1155/2017/8630749
16. Wang, H., Memon, H., Hassan, E. A. M., Miah, M. S., & Ali, M. A. (2019). Effect of jute fiber modification on mechanical properties of jute fiber composite. Materials, 12(8). https://doi.org/10.3390/ma12081226
17. Premnath, A. A. (2019). Impact of surface treatment on the mechanical properties of sisal and jute reinforced with epoxy resin natural fiber hybrid composites. Journal of Natural Fibers, 16(5), 718–728. https://doi.org/10.1080/15440478.2018.1432002
18. Ramesh, M., Sri Ananda Atreya, T., Aswin, U. S., Eashwar, H., & Deepa, C. (2014). Processing and mechanical property evaluation of banana fiber reinforced polymer composites. Procedia Engineering, 97, 563–572. https://doi.org/10.1016/j.proeng.2014.12.284
19. Bujjibabu, G., Das, V. C., Ramakrishna, M., & Nagarjuna, K. (2018). Mechanical and Water Absorption Behavior of Natural Fibers Reinforced Polypropylene Hybrid Composites. Materials Today: Proceedings, 5(5), 12249–12256. https://doi.org/10.1016/j.matpr.2018.02.202
20. Sun, Zhihui, Zhang, L., Liang, D., Xiao, W., & Lin, J. (2017). Mechanical and Thermal Properties of PLA Biocomposites Reinforced by Coir Fibers. International Journal of Polymer Science, 2017, 1–9. https://doi.org/10.1155/2017/2178329
21. Nagarjun, J., Kanchana, J., & Rajesh Kumar, G. (2020). Improvement of Mechanical Properties of Coir/Epoxy Composites through Hybridization with Sisal and Palmyra Palm Fibers. Journal of Natural Fibers, 00(00), 1–10. https://doi.org/10.1080/15440478.2020.1745126
22. Sumesh, K. R., & Kanthavel, K. (2020). The influence of reinforcement, alkali treatment, compression pressure and temperature in fabrication of sisal/coir/epoxy composites: GRA and ANN prediction. Polymer Bulletin, 77(9), 4609–4629. https://doi.org/10.1007/s00289-019-02988-5
23. Pilato, L. (2010). Phenolic resins: A century of progress. In Phenolic Resins: A Century of Progress. https://doi.org/10.1007/978-3-642-04714-5
24. Sathishkumar, G. K., Ibrahim, M., Mohamed Akheel, M., Rajkumar, G., Gopinath, B., Karpagam, R., Karthik, P., Martin Charles, M., Gautham, G., & Gowri Shankar, G. (2020). Synthesis and Mechanical Properties of Natural Fiber Reinforced Epoxy/Polyester/Polypropylene Composites: A Review. Journal of Natural Fibers, 00(00), 1–24. https://doi.org/10.1080/15440478.2020.1848723
25. Indran, S., Edwin Raj, R. D., Daniel, B. S. S., & Binoj, J. S. (2018). Comprehensive Characterization of Natural Cissus quadrangularis Stem Fiber Composites as an Alternate for Conventional FRP Composites. Journal of Bionic Engineering, 15(5), 914–923. https://doi.org/10.1007/s42235-018-0078-9
26. Sajin, J. B., Babu Aurtherson, P., Binoj, J. S., Manikandan, N., Senthil Saravanan, M. S., & Haarison, T. M. (2020). Influence of fiber length on mechanical properties and microstructural analysis of jute fiber reinforced polymer composites. Materials Today: Proceedings, 39(xxxx), 398–402. https://doi.org/10.1016/j.matpr.2020.07.623
27. Alves, C., Ferrão, P. M. C., Silva, A. J., Reis, L. G., Freitas, M., Rodrigues, L. B., & Alves, D. E. (2010). Ecodesign of automotive components making use of natural jute fiber composites. Journal of Cleaner Production, 18(4), 313–327. https://doi.org/10.1016/j.jclepro.2009.10.022
28. Pandya, V. J., & Rathod, P. P. (2019). Fabrication and Mechanical Properties Evaluation of Banana and Coir Fiber Reinforced Green Composites. A Journal of Composition Theory, XII(206), 206–215.
29. Paramasivam, S. K., Panneerselvam, D., Sundaram, D., Shiva, K. N., & Subbaraya, U. (2020). Extraction, Characterization and Enzymatic Degumming of Banana Fiber. Journal of Natural Fibers, 00(00), 1–10. https://doi.org/10.1080/15440478.2020.1764456
30. Essabir, H., Bensalah, M. O., Rodrigue, D., Bouhfid, R., & Qaiss, A. (2016). Structural, mechanical and thermal properties of bio-based hybrid composites from waste coir residues: Fibers and shell particles. Mechanics of Materials, 93, 134–144. https://doi.org/10.1016/j.mechmat.2015.10.018
31. Morandim-Giannetti, A. A., Agnelli, J. A. M., Lanças, B. Z., Magnabosco, R., Casarin, S. A., & Bettini, S. H. P. (2012). Lignin as additive in

polypropylene/coir composites: Thermal, mechanical and morphological properties. Carbohydrate Polymers, 87(4), 2563–2568. https://doi.org/10.1016/j.carbpol.2011.11.041

32. Verma, D., & Gope, P. C. (2015). The use of coir/coconut fibers as reinforcements in composites. In Biofiber Reinforcements in Composite Materials. https://doi.org/10.1533/9781782421276.3.285
33. Deyholos, M. K., & Potter, S. (2014). Engineering bast fiber feedstocks for use in composite materials. Biocatalysis and Agricultural Biotechnology, 3(1), 53–57. https://doi.org/10.1016/j.bcab.2013.09.001
34. Sisti, L., Totaro, G., Vannini, M., & Celli, A. (2018). Retting Process as a Pretreatment of Natural Fibers for the Development of Polymer Composites. https://doi.org/10.1007/978- 3-319-68696-7_2.
35. Manilal, V. B., Ajayan, M. S., & Sreelekshmi, S. V. (2010). Characterization of surface-treated coir fiber obtained from environmental friendly bioextraction. Journal of Natural Fibers, 7(4), 324–333. https://doi.org/10.1080/15440478.2010.529312
36. Abdurohman, K., Satrio, T., Muzayadah, N. L., & Teten. (2018). A comparison process between hand lay-up, vacuum infusion and vacuum bagging method toward e-glass EW 185/lycal composites. Journal of Physics: Conference Series, 1130(1). https://doi.org/10.1088/1742-6596/1130/1/012018 Ac ce us pt. (2018).
37. Dixit, S., Goel, R., Dubey, A., Shivhare, P. R., & Bhalavi, T. (2017). Natural Fibre Reinforced Polymer Composite Materials - A Review. 8(2), 71–78. https://doi.org/10.1177/204124791700800203
38. Yogeshwaran, S., Natrayan, L., Rajaraman, S., Parthasarathi, S., & Nestro, S. (2020). Experimental investigation on mechanical properties of Epoxy/graphene/fish scale and fermented spinach hybrid bio composite by hand lay-up technique. Materials Today: Proceedings, 37(Part 2), 1578–1583. https://doi.org/10.1016/j.matpr.2020.07.160
39. Boopalan, M., Niranjanaa, M., & Umapathy, M. J. (2013). Study on the mechanical properties and thermal properties of jute and banana fiber reinforced epoxy hybrid composites. Composites Part B: Engineering, 51, 54–57. https://doi.org/10.1016/j.compositesb.2013.02.033
40. Rachchh, N. V., & Trivedi, D. N. (2018). Mechanical Characterization and Vibration Analysis of Hybrid E-glass/Bagasse Fiber Polyester Composites. Materials Today: Proceedings, 5(2), 7692–7700. https://doi.org/10.1016/j.matpr.2017.11.445
41. Huzaifah, M. R. M., Sapuan, S. M., Leman, Z., & Ishak, M. R. (2019). Effect of Fibre Loading on the Physical, Mechanical and Thermal Properties of Sugar Palm Fibre Reinforced Vinyl Ester Composites. Fibers and Polymers, 20(5), 1077–1084. https://doi.org/10.1007/s12221-019-1040-0
42. Munshi, M. R., Alam, S. S., Haque, M. M., Shufian, A., Rejaul Haque, M., Gafur, M. A., Rahman, F., & Hasan, M. (2020). An Experimental Study of Physical, Mechanical, and Thermal Properties of Rattan-Bamboo Fiber Reinforced Hybrid Polyester Laminated Composite. Journal of Natural Fibers, 00(00), 1–15. https://doi.org/10.1080/15440478.2020.1818354
43. Mathur, M. (2021). Natural fiber composites. In Man-Made Textiles in India (Vol. 49, Issue 2). https://doi.org/10.1201/9781351050944-1
44. Ku, H., Wang, H., Pattarachaiyakoop, N., & Trada, M. (2011). A review on the tensile properties of natural fiber reinforced polymer composites. Composites Part B: Engineering, 42(4), 856–873. https://doi.org/10.1016/j.compositesb.2011.01.010
45. Gholampour, A. (2019). Review A review of natural fiber composites : properties , modification and processing techniques , characterization , applications. In Journal of Materials Science. Springer US. https://doi.org/10.1007/s10853-019-03990-y
46. Khan, M. Z. R., Srivastava, S. K., & Gupta, M. K. (2018). Tensile and flexural properties of natural fiber reinforced polymer composites : A review. https://doi.org/10.1177/0731684418799528
47. Barkoula, N. M., Alcock, B., Cabrera, N. O., & Peijs, T. (2008). Flame-Retardancy Properties of Intumescent Ammonium Poly(Phosphate) and Mineral Filler Magnesium Hydroxide in Combination with Graphene. Polymers and Polymer Composites, 16(2), 101–113. https://doi.org/10.1002/pc
48. Premalal, H. G. B., Ismail, H., & Baharin, A. (2002). Comparison of the mechanical properties of rice husk powder filled polypropylene composites with talc filled polypropylene composites. Polymer Testing, 21(7), 833–839. https://doi.org/10.1016/S0142-9418(02)00018-1
49. Haque, M. M., Rejaul Haque, M., Munshi, M. R., Alam, S. S., Hasan, M., Gafur, M. A., Rahman, F., Firdaus, M., & Ahmod, S. (2021). Physico-mechanical properties investigation of sponge-gourd and betel nut reinforced hybrid polyester composites. Advances in Materials and Processing Technologies, 7(2), 304–316. https://doi.org/10.1080/2374068X.2020.1766298
50. Faruk, O., Bledzki, A. K., Fink, H. P., & Sain, M. (2012). Biocomposites reinforced with natural

fibers: 2000-2010. Progress in Polymer Science, 37(11), 1552–1596. https://doi.org/10.1016/j.progpolymsci.2012.04.003

51. Chai Hua, T., & Norkhairunnisa, M. (2017). Investigation on the flexural properties and glass transition temperature of Kenaf/Epoxy composite filled with mesoporous silica for wind turbine applications. Pertanika Journal of Science and Technology, 25(4), 1261–1274.
52. Nor, A. F. M., Sultan, M. T. H., Jawaid, M., Abu Talib, A. R., Azmi, A. M. R., Harmaen, A. S., & Asa'ari, A. Z. M. (2018). The effects of multi-walled CNT in Bamboo/Glass fibre hybrid composites: Tensile and flexural properties. BioResources, 13(2), 4404–4415. https://doi.org/10.15376/biores.13.2.4404-4415
53. Mir, S. S., Nafsin, N., Hasan, M., Hasan, N., & Hassan, A. (2013). Improvement of physico-mechanical properties of coir-polypropylene biocomposites by fiber chemical treatment. Materials and Design, 52, 251–257. https://doi.org/10.1016/j.matdes.2013.05.062
54. Siddika, S., Mansura, F., Hasan, M., & Hassan, A. (2014). Effect of reinforcement and chemical treatment of fiber on The Properties of jute-coir fiber reinforced hybrid polypropylene composites. Fibers and Polymers, 15(5), 1023–1028. https://doi.org/10.1007/s12221-014-1023-0 https://doi.org/10.1016/j.matpr.2018.10.129
55. Ismail, K. I., Sultan, M. T. H., Shah, A. U. M., Jawaid, M., & Safri, S. N. A. (2019). Low velocity impact and compression after impact properties of hybrid bio-composites modified with multi-walled carbon nanotubes. Composites Part B: Engineering, 163(January), 455–463. https://doi.org/10.1016/j.compositesb.2019.01.026
56. Muñoz-Vélez, M. F., Hidalgo-Salazar, M. A., & Mina-Hernández, J. H. (2018). Effect of content and surface modification of fique fibers on the properties of a low-density polyethylene (LDPE)-Al/fique composite. Polymers, 10(10), 1–14. https://doi.org/10.3390/polym10101050

# EXPERIMENTAL INVESTIGATION ON THE PERFORMANCES OF DIFFERENT PAD MATERIALS USED IN A SUSTAINABLE ECO-FRIENDLY REFRIGERATOR

**Mahbubul Muttakin[1], Md Shahnewaz Bhuiyan[1], Md Kharshiduzzaman[1], Rafat Ahmed[1], Md Mahedi Kabir[1], Julfiqar Ali[1], Muhommad Azizur Rahman*[1,2]**

[1]Department of Mechanical and Production Engineering, Ahsanullah University of Science and Technology, Tejgaon, Dhaka 1208, Bangladesh

[2]Department of Mechanical Engineering, McMaster University, Ontario, Canada

*Corresponding Email: rahmm19@mcmaster.ca

***Abstract:*** *Due to lack of storage facilities, millions of tons of food get wasted every year. The number is even higher in developing countries like Bangladesh and India. Food preservation in cold storages requires electricity, which is scarce in many rural parts of Bangladesh where the fruits and vegetables grow. Hence, in this study, an attempt has been made to develop a zero-electricity low-cost eco-friendly refrigerator (EFR) known as 'pot in pot cooler'. It is made of two different sized clay pots, where one pot is inserted into the other and a pad material is placed between the two. Evaporative cooling of the pad materials keeps the EFR cooler than the environment. The selection and optimization of the pad material is critical in order to enhance the performance of the EFR. In the present study, the performances of four different pad materials, namely, river sand, fill sand, charcoal and coconut fiber, are analyzed. The experimental results show that the river sand is the most suitable pad material among the four considered in this study. It is capable of lowering the temperature of the storage by 2.8 ~ 3.3 °C from an ambient temperature of 30.0 ~ 33.4 °C.*

***Keywords:*** *Evaporative Cooling; Sustainable Development; Food Waste; Zero Electricity.*

## INTRODUCTION

Despite being a very small country Bangladesh is the world's eighth-most populated nation with about 161.4 million inhabitants. Agricultural land accounts for 65% of the total geographical area of Bangladesh. Crops, livestock, and fisheries are the three major sub-sectors of Bangladesh agriculture. Vegetables and fruits are cultivated massively in Bangladesh and more than 60 types of vegetables and 56 varieties of fruits are grown in this country. About 70% of Bangladesh's total population and 77% of its workers live in villages. About half of the population of this country and two-third of the population of the rural areas are primarily dependent on agriculture. Due to the highly perishable nature, almost 30% of the total production of fruits and about 35% of all production of vegetables and fruits go to waste through different phases of the post-harvest process. Lack of cold storage facilities and high cost of storage space are the main causes of such huge wastage. Frequent interruption in the supply of electricity forces the storage owners to use diesel generators, which makes the storages even more expensive. In the recent COVID-19 pandemic in Bangladesh, production of agricultural products such as vegetables, fruits, eggs, broiler meat, and milk was hampered, primarily due to the obstacles in their marketing and distribution. Other reasons were decreasing customer demand and lower affordability due to the pandemic (Hossain, 2020). The break in the food supply chain results in agricultural food wastage. The only solution to such an unwanted situation is increasing the food storage capacity. As post-harvest household food storage deficit in the rural area is one of the major causes of food waste in Bangladesh, an evaporative cold storage can play a vital role in enhancing the food security of Bangladesh.

'Pot in pot' is a simple evaporative cold storage device that utilizes two slightly different-sized pots made of natural resources, invented by a Nigerian teacher named Mohammed Bah Abba in the 1990s. The small container is positioned inside the large container and the gap between the two containers was filled with wet sand. When wind blows on the outer pot, water evaporates from the damp sand through the porous clay container and the food is cooled inside the small container. The higher the evaporation rate, the better the performance of the cooler. Fruits and vegetables of about 12 kg can easily be preserved inside a pot in pot storage. Evaporative coolers are available in several different types. 'Evaptainer' is a new invention which is actually an evaporative portable refrigerator. This portable evaporative refrigerator has a convenient way to preserve food using only a bottle of water (Kim et al.,

2019). But it is expensive and not friendly for large-scale food storage applications.

A Tin in Pot (TIP) model was proposed by Salaudeen et al., in 2013, where, instead of clay, they used tin as the wall material. The results obtained from the study showed that TIP is a very reliable storage system, but it is not suitable for storing food items for an extended period. Because tin is more likely to conduct chemical reactions with fruit. The main benefit of evaporative cold storage of the TIP model is that it retains the fruit's freshness better than the clay model. Another attempt was made to develop an evaporative cold storage system with sand and clay as the wall and pad material, respectively, by Ishaque et al., in 2019. A temperature reduction of 5 ~ 9 °C was reported by them in their study. But the relative humidity inside the system was raised to 90% from an ambient condition of 60% RH. Abhinav et al. developed an evaporative cooling-based Eco-friendly refrigerator (EFR) which can be used as an alternative to traditional refrigerators and rural cold storage. They stated that Eco-Refrigerator can provide efficient cooling with low investment and can be used conveniently in rural areas to preserve food, farm produce, and poultry farm products. It operates more effectively in regions with strong winds and where there is a high amount of moisture present in the air. But the air receiver unit needs a 12 V lithium-ion battery.

An attempt was made to improve the efficiency of pot in pot or Zeer pot refrigerator by including a solar dryer attached to the refrigerator by Gustafsson & Simson in 2016. Since simulations have only been conducted once for each configuration, the findings cannot be analyzed theoretically. With the inclusion of a solar dryer, it is obvious that the flow of air will be increased to enhance the cooling power of the Zeer pot. A comparison between different pad materials in terms of the efficiency of a pot-in-pot refrigerator was conducted by Yahaya & Akande in 2018. The system's average efficiencies for the different pad materials were found to be 66%, 58%, and 75% for sand, sawdust, and charcoal, respectively which shows that charcoal is the best pad material to run the pot in a pot refrigerator made of clay pot. An experiment was conducted with the cooling rate of a clay pot-in-pot refrigerator by varying the height of water in the gap of the inner and outer pots (Gowda, 2014). Their experimental result stated that the cooling rate is highest when the amount of water is 1.5 liters and lowest when the amount is 5.5 liters. An experiment was demonstrated on the effect of storing foods such as vegetables and fruits in the pot-in-pot refrigerator named Earthen pot cool chamber (EPCC-2) by Murugan et al. in 2012. The purpose of their study was to investigate the quality of the stored food. The weight loss of the stored food was measured. Some other parameters such as organoleptic changes (taste and aroma), heterotrophic microbial population (responsible for food decomposition), the shelf lifetime (time till the food is consumable), etc. were also observed. A comparison of all these quality indicators was done between naturally stored fruit and vegetables and the same stored in the pot-in-pot cooler. The results showed that the stored fruits and vegetables remain fresh inside the earthen pot cool chamber with negligible or little change in weight loss and other biochemical characteristics.

Dutt proposed a modified design of EFR in which water was stored in an upper chamber. The result showed that the cooling rate and efficiency were actually better in the conventional pot in the pot cooler when compared with the modified one. Investigation was carried out on the quality of leafy amaranth vegetables preserved in an evaporative cooling system at the post-harvest stage (Ambuko et al., 2017). The results showed that in comparison with ambient room conditions, storing the vegetable samples inside an evaporative cooler using charcoal as pad material was more effective. The food quality was better maintained in the evaporative cooler. An experiment was also conducted to study the alternatives of sand in the pot in the pot refrigerator (Dutt & Gowda, 2015). The authors investigated the performance of charcoal and gunny cloth as two different pad materials. The sand in between the two pots was replaced with Charcoal and gunny cloth. Three different loading conditions were considered. The final results indicated that the cooling rate was better when the gunny cloth was used as pad material compared to sand and charcoal.

The present paper aims to develop an efficient non-electric evaporative refrigeration system for poor rural small-scale farmers and households by using common materials available in rural areas such as Clay, Sand, Coconut Fiber (Coir), and water. The refrigerator uses the simple evaporative cooling principle. The main focus is to compare the performance of four types of pad materials, namely, river sand, fill sand, coal, and coconut fiber (coir) in terms of enthalpy change, temperature reduction from the ambient, and efficiency. For experimental investigation a rural area in Dinajpur, Bangladesh is chosen in this study, as the temperature and humidity are particularly high in that region. The purpose of the study is to offer a low-cost alternative to conventional refrigerators and create a more effective eco-friendly evaporative cooler to minimize food wastage in agro-based countries like Bangladesh.

## WORKING PRINCIPLE OF AN EFR

In an EFR, the evaporative cooling technology is employed to keep the inside chamber cooler than the ambient. External energy such as ambient heat acts as an input to the system. Due to ambient heat, the kinetic energy of water particles starts increasing. Consequently, the internal temperature of water particles increases, which ignites the evaporation of the

water particles that contain the maximum kinetic energy. This results in a decrease in temperature of the remaining water, as the energy required for evaporation is provided by this remaining water. A significant change in temperature reduction can be perceived when the water quantity is low. Thus the inner pot, which is in contact with the filler material that contains the water, gets cooled and this also cools the refrigerated space.

EFR is a concept of pot in a pot refrigerator. From **Fig.-1**, the energy flow for the evaporation inside a pot in a pot refrigerator or, EFR can be identified. Due to the evaporation of water from the wet pad material, the inside small pot achieves a lower temperature zone or cold zone. Airflow can eventually increase the cooling rate of the EFR.

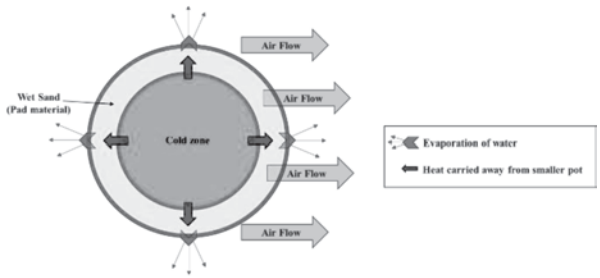


**Fig.-1:** Energy flow in evaporative cooling.

An EFR consists of two different sized pots and a pad material is placed in the gap between the two pots. The pad material is dampened by water to facilitate evaporative cooling. A damp cloth is used as a cover at the top of the EFR. The pad material and the outer pot have conductive heat flow as shown in **Fig.-2**. The damp cloth on the upper portion has all heat flows including conductive with the pad material and the smaller pot.

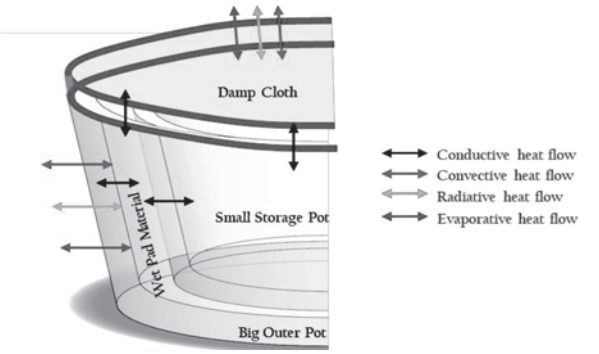


**Fig.-2:** Heat flow in different directions of EFR.

The efficiency of an EFR can be calculated by measuring the temperature reduction and using equation (1),

$$h = \frac{T_{a,db} - T_{i,db}}{T_{a,db} - T_{a,wb}} \qquad (1)$$

where, $T_{a,db}$ and $T_{a,wb}$ are the dry bulb and wet bulb temperatures of the ambient air respectively, and $T_{i,db}$ is the dry bulb temperature of the air inside the pot-in-pot refrigerator.

## EXPERIMENTAL APPROACH

In this research, four types of pad material were investigated. River Sand, Fill Sand, Charcoal, and Coconut Fiber (Coir) were selected as pad materials due to their abundant availability in the rural areas of Bangladesh. A simple pot in pot EFR was first designed in this study and then built by a local potter in Dinajpur, Bangladesh, as shown in **Fig.-3 (a)**, **(b)**, and **(c)**. The smaller pot is stacked inside the bigger pot. The values of the physical parameters of the two pots are stated in **Table 1**.

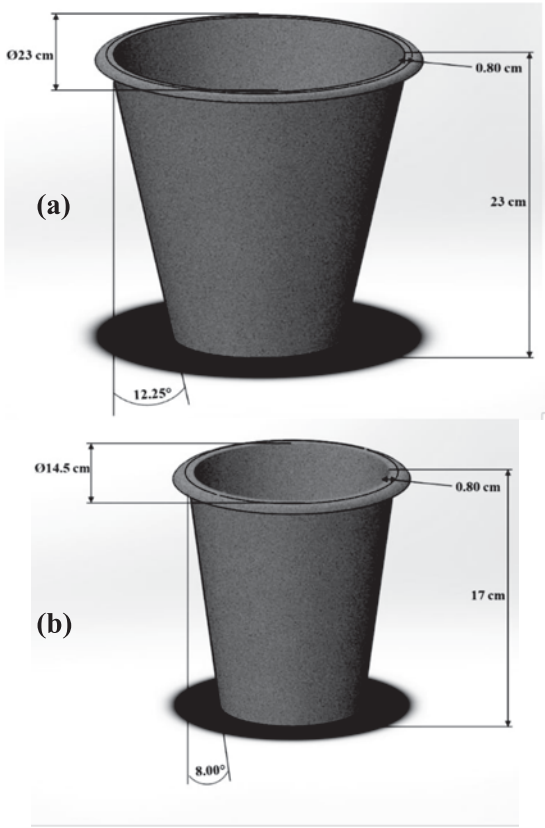

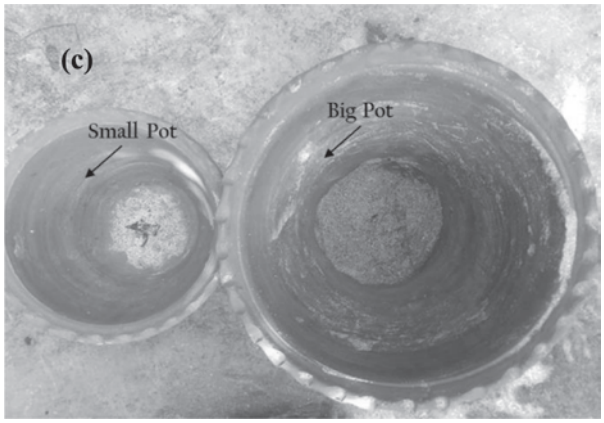


**Fig.-3:** Design and prototype of EFR; **(a)** shows the dimensions of a bigger pot, **(b)** shows the dimensions of a smaller pot, **(c)** shows the actual pots built by a local potter.

**Table 1**: Values of physical parameters of the pots

| Parameters | Bigger outer pot (cm) | Smaller inner pot (cm) |
|---|---|---|
| **Height** | 23 | 17 |
| **Thickness** | 0.80 | 0.80 |
| **Outer Diameter** | 23.80 | 15.30 |
| **Inner Diameter** | 23.00 | 14.50 |
| **Bottom Thickness** | 1.00 | 1.00 |

The hollow space between the two pots was filled with different pad materials as shown in **Fig.-4 (a)**, **(b)**, **(c)**, and **(d)**. The pad materials were dampened with water. A dampen cloth was used to cover the EFR to provide better evaporation. Then different parameters such as ambient temperature and humidity, temperature and humidity inside the inner pot, and stored food weight were measured.


**(a)** **(b)** **(c)** **(d)**

**Fig.-4:** Pot in pot EFR with different pad materials: **(a)** River Sand, **(b)** Fill Sand, **(c)** Charcoal, **(d)** Coconut Fiber (Coir)

## RESULTS AND DISCUSSION

The temperature and humidity values of ambient air and air inside the EFR are measured for four different pad materials on four different days. The results are tabulated as shown in **Table 2**. The average of the four days' data are graphically presented in **Fig-5** and in **Fig-6**.

**Table 2**: Temperature and humidity readings with four types of pad materials

| Pad Material | Day | Ambient Humidity | Ambient temperature (°C) | Ambient Enthalpy, ΔH (kJ/kg) | Inside Humidity | Inside temperature (°C) | Inside Enthalpy, ΔH (kJ/kg) | Temperature reduction (°C) | Enthalpy change, ΔH (kJ/kg) |
|---|---|---|---|---|---|---|---|---|---|
| **River Sand** | 1 | 76% | 33.40 | 92 | 70% | 30.10 | 73 | 3.3 | 19 |
| | 2 | 82% | 32.80 | 96 | 76% | 30.30 | 78 | 2.5 | 18 |
| | 3 | 76% | 30.00 | 78 | 70% | 27.20 | 62 | 2.8 | 16 |
| | 4 | 76% | 32.50 | 89 | 69% | 29.30 | 68 | 3.2 | 21 |
| **Fill Sand** | 1 | 76% | 33.40 | 92 | 71% | 30.80 | 77 | 2.6 | 15 |
| | 2 | 82% | 32.80 | 96 | 76% | 30.50 | 79 | 2.3 | 17 |
| | 3 | 76% | 30.00 | 78 | 71% | 28.60 | 68 | 1.4 | 10 |
| | 4 | 76% | 32.50 | 89 | 71% | 29.50 | 72 | 3.0 | 17 |
| **Char coal** | 1 | 76% | 33.40 | 92 | 72% | 30.90 | 77 | 2.5 | 15 |
| | 2 | 82% | 32.80 | 96 | 78% | 31.30 | 86 | 1.5 | 10 |
| | 3 | 76% | 30.00 | 78 | 71% | 27.70 | 65 | 2.3 | 13 |
| | 4 | 76% | 32.50 | 89 | 72% | 29.80 | 74 | 2.7 | 15 |
| **Coco nut Fiber (Coir )** | 1 | 76% | 33.40 | 92 | 68% | 30.30 | 71 | 3.1 | 21 |
| | 2 | 82% | 32.80 | 96 | 77% | 30.50 | 81 | 2.3 | 15 |
| | 3 | 76% | 30.00 | 78 | 71% | 27.30 | 63 | 2.7 | 15 |
| | 4 | 76% | 32.50 | 89 | 72% | 30.40 | 77 | 2.1 | 12 |

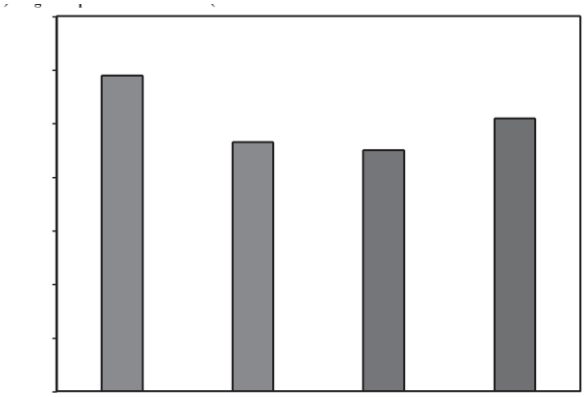

**Fig.-5:** Average temperature reduction with different pad materials.

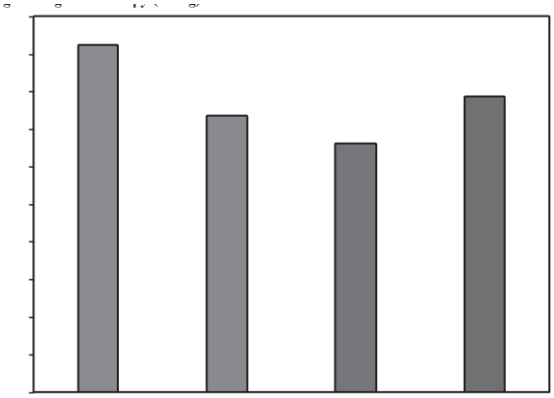

**Fig.-6:** Average change in enthalpy with different pad materials.

Finally, the efficiencies of the EFRs in four different days are calculated using equation (1) and the average efficiencies are plotted in **Fig-7**.

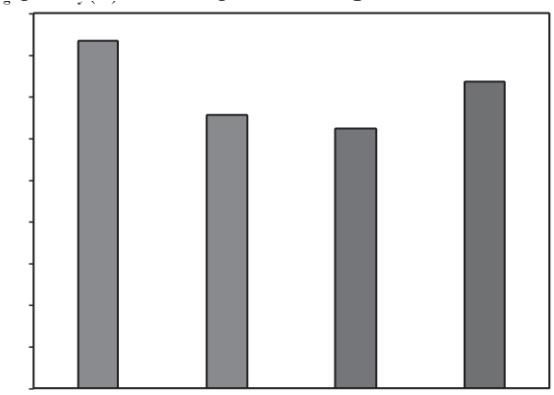

**Fig.-7:** Average efficiencies of the EFRs with different pad materials.

It is evident from **Fig-5**, **Fig-6** and **Fig-7**, that the EFR, with river sand as the pad material, performs the best in comparison to the same with other pad materials. This may be due to the higher water retention capability of river sand when compared to the others. Due to the porous structure, river sand can facilitate higher evaporation rate as well.

The physical properties of the pad materials, as obtained from the literature (Ajao et al., 2018; Ashby, 2013), are presented in **Table 3**.

**Table 3**: Different properties of pad materials

| Properties | River Sand | Fill Sand | Charcoal | Coconut Fiber (Coir) |
|---|---|---|---|---|
| **Grain size (mm)** | 0.0841 | 2.9 – 3.2 | ~20 | <5.00 |
| **Bulk density (kg/m³)** | 1301 | 1519 | 208 | 80 |
| **Specific gravity** | 2.67 | 2.51 | 1.29 | - |

It is observed that the river sand possesses the finer grains as compared to others. The effect of grain size on the water absorption rate was investigated by Hudec in 1989. The results are shown in **Fig-8**.

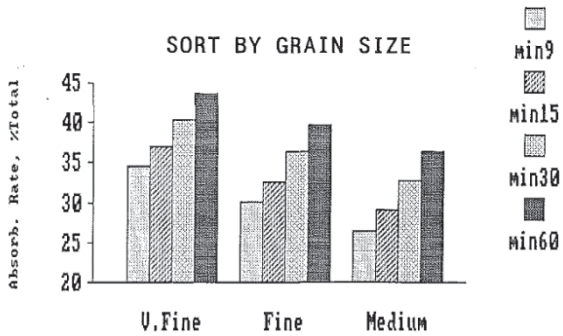


**Fig.-8:** Effect of grain size on rate of absorption at 9, 15, 30, and 60 minute intervals. Rate is expressed as percent of total absorption (Hudec, 1989)

In that study the author opined that the water absorption rate in different carbonate rocks and sands does not depend on the water holding capacity. In **Fig-8**, it is observed that the rate is controlled by the grain structure and pore size. The finer grain can retain water approximately twice of coarse grain, particularly in the initial few minutes after contact with water. River Sand has high water retention and evaporation capabilities due to the small grain structure. Hence, it performs better in terms of evaporation rate and reduction of inside temperature.

In the case of coconut fiber (coir), the setup creates an intense stench after 2 days. Because coconut fiber (coir) itself is a perishable material and water speeds up its decomposition. Hence, using coconut fiber (coir) as pad material in EFR in households is not very favorable.

## CONCLUSION

The study shows that the temperature in EFR has decreased by a maximum of 3.3 °C when river sand was used as the pad material. Comparison among river sand, fill sand, charcoal, and coconut fiber (coir) indicates that the highest average temperature reduction and efficiency were obtained with river sand. The average efficiency of the EFR was found to be 83.54% with river sand being used as the pad material. The smaller grain size of the river sand contributes to its higher water retention and evaporation capabilities, which in turn results in higher efficiency of the EFR.

## NOMENCLATURE

| | |
|---|---|
| *H* | Enthalpy |
| *T* | Temperature |

## SUBSCRIPTS

| | |
|---|---|
| *a* | Ambient |
| *db* | Dry bulb |
| *i* | Inside |
| *wb* | Wet bulb |

## GREEK SYMBOLS

| | |
|---|---|
| $\eta$ | Efficiency |

## ABBREVIATIONS

| | |
|---|---|
| EFR | Eco-friendly refrigerator |
| EPCC | Earthen pot cool chamber |
| RH | Relative humidity |
| TIP | Tin in pot |

## REFERENCES


1. Abhinav, M., Noida, G., Tiwari, S., & Sarkar, P. (2018). *Eco-Refrigerator - A Sustainable approach towards the problem of Food Insecurity*. *6*(4), 94–98.
2. Ajao, A. M., Ogunbayo, B. F., Ogundipe, K. E., Joshua, O., & Olofinnade, O. M. (2018). Experimental datasets on properties of river sand as an aggregate in replacement of crushed rock for interlocking stones production. *Data in Brief*, *20*, 602–608. https://doi.org/10.1016/j.dib.2018.08.056
3. Ambuko, J., Wanjiru, F., Chemining, G. N., Owino, W. O., & Mwachoni, E. (2017). *Preservation of Postharvest Quality of Leafy Amaranth ( Amaranthus spp . ) Vegetables Using Evaporative Cooling*. *2017*, 1–7.
4. An, N., Tang, C. S., Xu, S. K., Gong, X. P., Shi, B., & Inyang, H. I. (2018). Effects of soil characteristics on moisture evaporation. *Engineering Geology*, *239*, 126–135. https://doi.org/10.1016/j.enggeo.2018.03.028
5. Ashby, M. F. (2013). *Materials and the Environment (Second Edition)* (M. F. Ashby (ed.); Second, pp. 459–595). https://doi.org/https://doi.org/10.1016/B978-0-12-385971-6.00015-4.
6. Dutt, P. S. (2016). Experimental Comparative Analysis of Clay Pot Refrigeration Using Two Different Designs of Pots. *International Journal of Latest Research in Engineering and Technology*, *2*(2), 30–35. www.ijlret.com
7. Dutt, P. S., & Gowda, T. (2015). Experimental Study of Alternatives to Sand in Zeer Pot Refrigeration Technique. *Www.Ijmer.Com*, *5*(1), 1–7.
8. Gowda, Y. T. K. (2014). *Thermal Analysis of Clay Pot*. *3*(10), 320–322.
9. Gustafsson, K., & Simson, H. (2016). An experimental study on an evaporative cooler for hot rural areas. *KTH School of Industrial Engineering and Management*. http://www.diva-portal.org/smash/get/diva2:952001/FULLTEXT01.pdf
10. Hossain, S. T. (2020). Impacts of COVID-19 on the Agri-food Sector: Food Security Policies of Asian Productivity Organization Members. *The Journal of Agricultural Sciences-Sri Lanka*, *15*(2), 116–132. https://doi.org/10.4038/jas.v15i2.8794
11. Hudec, P. P. (1989). Durability of Rock as Function of Grain Size, Pore Size, and Rate of Capillary Absorption of Water. *Journal of Materials in Civil Engineering*, *1*(1), 3–9. https://doi.org/10.1061/(asce)0899-1561(1989)1:1(3)
12. Ishaque, F., Hossain, M. A., Sarker, M. A. R., Mia, M. Y., Dhrubo, A. S., Uddin, G. T., & Rahman, M. H. (2019). A Study on Low Cost Post Harvest Storage Techniques to Extend the Shelf Life of Citrus Fruits and Vegetables. *Journal of Engineering Research and Reports*, *9*(1), 1–17. https://doi.org/10.9734/jerr/2019/v9i117009
13. Kim, C., Joshi, S., & Cauwenberghs, G. (2019). *Patent Application Publication: US 2019 / 0253069 A1*. *1*.
14. Murugan, A. M., Chinnathambi, A., Wainwright, M., Shanthi, S., Rajapandian, K., Zayed, M. E., Alharbi, S. A., & Aloufi, A. S. (2012). A study on a cost effective and eco friendly earthen pot cool chamber (EPCC-2) system for rural population to store post harvest vegetables. *Biosciences Biotechnology Research Asia*, *9*(1), 85–96. https://doi.org/10.13005/bbra/969
15. Salaudeen, K. O., Uzoma, A., F.F, O., & E.F, A. (2013). Effect of NSPRI tin-in-pot compared with pot-in-pot evaporative cooler on the stored fruits. *International Journal of Engineering & Technology*, *2*(1), 63. https://doi.org/10.14419/ijet.v2i1.573
16. Yahaya, S. A., & Akande, K. A. (2018). *Development and Performance Evaluation of Pot-in-pot Cooling Device for Ilorin and its Environ Development and Performance Evaluation of Pot-in-pot Cooling Device for Ilorin and its*. *15*(July),2045–2060


**MECHANICAL ENGINEERING DIVISION**

**THE INSTITUTION OF ENGINEERS, BANGLADESH**

Headquarters : Ramna, Dhaka-1000, Bangladesh

Tel : 880-2-9573343, 9556112, 9559485, Fax : 880-2-9562447

E-mail : info@iebbd.org, info.iebhq@gmail.com



Design & printed by Vivid 01819298544